Università Degli Studi Di Napoli

"Federico II"

Physics Department

PhD Thesis in

Novel Technologies for Materials, Sensors and Imaging

Hybrid metamaterial-LC based structures with large tunability range from the microwave to the terahertz region

by

Nassim Chikhi

Advisor:

Prof. A. Andreone

... To

My Parents ...

Preface

This work is submitted for a Doctor of Philosophy degree (PhD), in "Novel Technologies for Materials, Sensors and Imaging" TIMSI. The work was performed under Prof. A. Andreone supervision, at the microwave lab, physical department of Università Degli Studi Di Napoli "Federico II". The metamaterial structure operation in the microwave region was fabricated at the Licryl Lab, University of Calabria. While the terahertz structure was fabricated in Istituto di Cibernetica 'E.Caianiello' (ICIB) of Consiglio Nazionale delle Ricerche (CNR), Pozzuoli, (Napoli) Italy.

Abstract

Following the pioneer works on metamaterials, there has been considerable interest in the practical realizations of this type of materials which were typically comprised of periodic arrays of sub-wavelength metallic resonators within or on a dielectric or semi conducting substrate. The use of metamaterials, on an appropriate form such as Split Ring Resonators (SRR), could find applications for the development of novel devices operating in various frequency regions and aimed at filtering, modulating, and switching the electromagnetic signal. Since the first extensive studies on metamaterials, the attention of most researchers has been focused on the linear properties of these composite structures. Having a controllable device is always of interest, as it makes its response more adaptive to the range of applications they are made for and more interactive with its environment. For that, and in order to achieve the full potential of the unique characteristics of metamaterials, the ability to dynamically control the material properties or tune them in real time, through either direct external tuning or nonlinear response is required. For all these reasons, my work aimed to exploit this new class of artificial materials exhibiting unconventional properties, to build new devices for a wild range of applications, starting from the microwave region up to the terahertz regime. We focused on the design and fabrication of metamaterials with unit cells based on split ring resonators SRRs and other type of resonators for the development of tunable negative refractive index metamaterials. The basic idea is to exploit the nematic liquid crystals properties, whose orientation can be magnetically or electrically controlled, to achieve the dynamic frequency modulation of the fabricated metamaterials, in order to build innovative devices for applications from the microwave up to the THz region, where the metal loss can be still maintained at a reasonable level.

Acknowledgments

First and foremost, I would like to deeply thank my thesis supervisor, *Prof. Antonello Andreone,* for supporting this research, for his advice and encouragement, and especially for his patience and trust all along this thesis. Thanks also to him for providing an excellent working environment and maintaining a great atmosphere in the laboratory. Also would like to thank *Dr. Emiliano Di Gennaro* for his presence and assistance all along my work.

A special thank goes to *Dr. Michele Giocondo,* for his assistance in the realization of the metamaterial structure and for accepting to use his liquid crystal lab facilities. Also would like to acknowledge *Dr. Alfredo Pane* for his help and his assistance in Lycril lab.

A great thank to Dr Mikhail Lisitsky for his help and assistance in the realization of the terahertz metamaterial structure. Also I would like to thanks him for his worm welcome in his lab.

I will never thank enough Mr. Guido Celentano for All …… Grazie Mille Guido. Thanks to *Prof Giancarlo Abbate* and Dr. *Volodymyr Tkachenko* for their assistance.

I will never thank enough my mother and father to whom I dedicate this dissertation and to all my family with special acknowledgment to Islam, Mustapha, our new angle Serine and my wife for here support. And above all I thank God for giving me the will and means to achieve what I have achieved so far.

Summary

Chapter II: Basic physics of LHM

Chapter III: Tunable metamaterials for Microwave & terahertz

Chapter IV: Proposed Microwave and terahertz structures

General Introduction

General Introduction

During the last two decades substantial progress has been achieved in the development of THz science and technology. However, there are several restrictions limiting further accomplishments to fulfill fruitful THz applications by covering the full frequency region. One of the main constraints is the so called "THz Gap", which is basically due to the lack of appropriate response at these frequencies for many naturally existing materials. This problem can be solved using artificially structured electromagnetic materials, named "metamaterials", which can be defined as a class of materials with properties that transcend those available in nature, or at least that cannot be readily available in nature. Historically speaking it's impossible to directly link the metamaterials origin to a specific date, since it is a multi disciplinary field involving a lot of physics aspects. However, there is an almost general agreement among the scientific community that the Father of metamaterial is the Russian scientist *Victor Georgievich Veselago*. With his publication in 1967 ""*The Electrodynamics of Substances with Simultaneously Negative Values of* ε *and* μ*",* he was the first to establish the theoretical bases for this type of material, based on a medium supposed to exhibit a negative permittivity and permeability at the same time. So what are exactly these materials? What are really their capabilities? And how they can be exploited?

According to Veselago, this type of materials has exotic properties namely: negative refraction, reversal of Doppler Effect, reversal of Cherenkov radiation, reversal of Goos-Hänchen shift. Sub wavelength focusing and perfect lenses, Superluminal group velocity and negative group velocity…etc. However, there was a big question mark: "*how we are going to exploit these properties, knowing that this type of materials does not exist*". And that was the reason why Veselago's publication remained a dead letter for long time. As with

great power come great responsibilities, also with big challenges come bigger benefits. For this, the scientists never lost hope for more than 30 year trying to exploit the metamaterial concepts, and they had to wait till 1996 when Pendry theorized a practical way to build this type of materials.

Following the pioneer works on metamaterials, there has been considerable interest in the practical realizations of this type of materials which were typically comprised of periodic arrays of sub-wavelength metallic resonators within or on a dielectric or semi conducting substrate. The use of metamaterials, on an appropriate form such as Split Ring Resonators (SRR), could find applications for the development of novel devices operating in various frequency regions and aimed at filtering, modulating, and switching the electromagnetic signal. Since the first extensive studies on metamaterials, the attention of most researchers has been focused on the linear properties of these composite structures. Most of the early electronic devices involved active and, possibly, nonlinear processes, with the word active meaning that some extrinsic, or intrinsic, action is being added to an original passive design. The actions can include an intrinsic energy source, or an interrogation of the device with an external source of energy, such as a laser beam. In addition, many forms of control can be accessed by putting the device under an externally applied influence, such as a constant electric or magnetic fields, by incorporating into the device a feature that permits significant control over its resonant behavior. Having a controllable device is always of interest, as it makes its response more adaptive to the range of applications they are made for and more interactive with its environment. For that, and in order to achieve the full potential of the unique characteristics of metamaterials, the ability to dynamically control the material properties or tune them in real time, through either direct external tuning or nonlinear response is required.

For all these reasons, my work aimed to exploit this new class of artificial materials exhibiting unconventional properties, to build new devices for a wild range of applications, starting from the microwave region up to the terahertz regime. We focused on the design and fabrication of metamaterials with unit cells based on split ring resonators SRRs and other type of resonators for the development of tunable negative refractive index metamaterials. The basic idea is to exploit the nematic liquid crystals properties, whose orientation can be magnetically or electrically controlled, to achieve the dynamic frequency modulation of the fabricated metamaterials, in order to build innovative devices for applications from the microwave up to the THz region, where the metal loss can be still maintained at a reasonable level.

Chapter I:
Basic concepts on metamaterials

I.1 Terminology and Definition

In the last two decades, there has been rapidly growing interest in engineered materials commonly called "metamaterials". Although a universally accepted definition of the term "metamaterial" does not exist. However, within the framework of this thesis we will try to define them with the maximum accuracy. From the semantic point of view we can get an idea on what is about: the word ***Metamaterial*** can be divided in two parts, "Meta" and "material" where the first one is a Greek prefix which means "beyond" or "after" and therefore, we can designate Metamaterials as a class of materials with properties that in some how can be "beyond" the one of materials available in nature. The prefix "meta" also suggests that the resulting properties transcend those available in nature, or at least that they cannot be readily available in nature. More precisely, we speak about a kind of mediums in witch the internal structure interact with an external wave, in a manner to create "effectives" properties witch are generally unusual or even unobserved in natural materials. From our point of view, we mite be more interested to the metamaterials in witch the fundamental electromagnetic properties describing the interaction wave-matter are the electrical permittivity "ε" and the magnetic permeability "μ"; for example, according to the metamaterial structure and the targeted frequency band, the permittivity can reach some extreme values, either unusually too high or too low approaching zero. While the effective permeability can have some non-trivial values in some frequency bands where is naturally equal to the unit, giving birth to the "artificial magnetism". However, the most particular property that renowned the metamaterials remains the possibility to have a simultaneous negative permeability and permittivity at the same frequency.

Other definitions of metamaterials can be found in a various publications depending on the field of interest or the related

background of authors, describing either, the physics behind the observed properties, the mathematic interpretation of the observed properties, the conditions or the way those properties are observed, or the practical way they are engineered or fabricate the material with the actual properties….etc. therefore, we can cote some definitions namely:

- A new class of ordered nanocomposites materials that exhibit exceptional properties not readily observed in nature. These properties arise from qualitatively new response functions that are not observed in the constituent materials and result from inclusion of artificially fabricated, extrinsic. Low dimensional inhomogeneities [1].
- Macroscopic composites having a man-made, three dimensional, periodic cellular architecture designed to produce and optimized combination, not available in nature, of two or more responses to a specific excitation. Each cell contains metaparticles, macroscopic constituents with low dimensionality that allow each component of the excitation to be isolated and separately maximized. With a strategically selected architecture to recombines local quasi-static responses, or to combine or to isolate specific non-local responses [2].
- Electromagnetic metamaterials are composite materials artificially structured that can be engineered to get special desired properties, while keeping the advantageous material properties [3].
- Materials whose permeability and permittivity derive from their structure rather than their intrinsic properties [4].
- Structures composed of macroscopically scattering elements [5].

From this type of definitions and regardless of the field of interest, all of them have a common point that the metamaterials are engineered materials that can exhibit electromagnetic properties:

- Not observed on the constituent materials, and/or
- Not observed in nature.

The variety of the metamaterial definitions is also extended to their synonyms. In the literature, we can find also several names which describe metamaterials, mostly referring to their extraordinary properties, namely:

- Left Handed Materials (LHM) : this term refer to the fundamental property of metamaterial, which is the opposite orientation between the phase velocity and the group velocity.
- Negative refraction index materials: this name describes the 2D and 3D mediums.
- Double negative materials: this appellation is related to the signs of permittivity and permeability of the material.
- Veselago's medium: obviously this name doesn't refer to any physical properties, how ever is used just to honor the scientist, who is considered as the father of metamaterials.
- Backward wave materials: which underline another physical property of metamaterials.

So all over the thesis we may be using one of this appellations, depending on the context.

I.2 History of metamaterials

This section summarizes the pioneer works on MTMs, more particularly of LHM, from the first theoretical speculations to recent experimental results which confirm the physical existence of negative refraction and LHM.

It's quite difficult to define the starting point of "*history of metamaterials*" or LHM which depends on the field of interest.

Therefore, and in order to give all the scientists their merits, we decided to enumerate all the published works related to this field that we were able to put hands on. Starting from 1898, J.C.Bose proposed the first microwave experiment, using the synthetic twisted fibers to change the electromagnetic waves orientation [6]. In 1914, Lindman studied the effect of artificial chiral mediums (constituted by a bunch of small spiral wires randomly oriented in the principal medium) on electromagnetic waves [7]. The negative refraction was studied for the first time on 1944 by L.I Mandelshtam [8]. After that, the concept of artificial dielectric was first introduced by W.E Kock in 1948, with the idea of realizing dielectric lenses using conducting spheres, discs and ribbons, arranged periodically in a matrix [9]. In 1957, Sivukihin studied the relationship between the negativity of the permeability (μ) and permittivity (ε) and the negative refraction [10]. The Doppler Effect and Vavilov Cerenkov radiation in a negative ε and μ mediums were studied in dept by Pafomov in 1959 [11].

"*The Electrodynamics of Substances with Simultaneously Negative Values of* ε *and* μ*",* was the first key paper to the advancement of physics research in electrodynamics. It was published by the Russian physicist Victor Veselago in 1967 (in Russian, and was later translated into English in 1968). In this paper he studied the electromagnetic properties of a hypothetical medium in which both the permittivity and the permeability were simultaneously negative [12]. Till this time, all the related works were describing the theoretical bases of metamaterials and even with the attempts of J.Brown [13] and W. Rotman [14] to study the thin wires to realize artificial dielectric materials, and those of S. Schelkunoff who studied the Split Ring Resonators SRRs, without being able to achieve a concrete realization of this type of material. For that, we had to wait till 1996, where John Pendry, published his investigations on two types of periodic arrays of metallic elements namely: parallel wires and SRRs, both of them working in the

microwave range. Which were considered later on as the first experimental prove of the Metamaterials existence (more precisely the existence of materials with negative μ and ε). Inspired by this work, David Smith proposed to combine parallel wires and SRRs to obtain a composite material which simultaneously exhibits negative permittivity and permeability over a finite frequency band [15]. They have created the first LHM! This first prototype only exhibited a left-handed behavior for one direction of propagation (1D LHM) and for one polarization of the fields. An improved 2D isotropic version of this structure was subsequently proposed in [17], and by April 2001 with his group demonstrated for the first time the phenomenon of negative refraction [18]. They used a 2D isotropic composite LHM working at microwave frequencies similar to that presented in [15]. These experimental results were consistent with Snell's law if a negative refractive index is taken for the LHM.

In parallel to the investigations on SRR-wire LHM, three groups proposed in 2002 almost at the same time a novel kind of MTMs based on a circuit approach: the group of Christophe Caloz and Tatsuo Itoh [19], the group of George V. Eleftheriades [20] and the group of Arthur A. Oliner [21]. The main idea consisted in realizing a TL with a capacitive element in the series branch and an inductive element in the shunt branch, i.e. the dual topology of a conventional TL. Concretely, these novel MTMs were obtained by periodically loading a TL (for the 1D case) or a grid of TLs (for the 2D case) with lumped L-C elements.

Also at that time, Eleftheriades presented clear experimental evidence confirming negative refraction and went even further to demonstrate for the first time focusing of electromagnetic waves from a left-handed lens [22]. The structure used was a 2D periodically L-C loaded TL network (dual TL medium).

March-April 2003: Good news for LHM: Several groups carried out experiments and simulations which confirmed the existence of

negative refraction, and that LHM do not violate basic physical laws like causality:

- In March 2003, Claudio G. Parazzoli at Boeing Phantom Works at Seattle carried out an experiment similar to that made by Smith in [18]. Using a free-space measurement setup, they detected negatively refracted waves at a remarkably long distance from the LHM sample [23], thereby dispelling any doubt concerning the far field nature of these waves. These results, which fully supported the theoretical results of [24, 25], clearly confirmed the existence of negative refraction.

- In April 2003, Andrew A. Houck at MIT Media Laboratory at Cambridge reported measurement results demonstrating that refraction through a 2D LHM obeys Snell's law with a negative index of refraction [26]. He also presented preliminary evidence that a flat rectangular slab of this material could focus power from a point source, as predicted by Pendry in [17].

March 2003: The group of G. V. Eleftheriades presented simulation results showing subwavelength focusing capability of a LHM lens [27]. They used a 2D dual TL medium sandwiched between two 2D conventional TL media (right-handed media). Evidence of growing evanescent waves within the dual TL medium was shown for both infinite and finite length structures. In December 2003, they published further analytical and simulation results on sub wavelength focusing. In particular, they discussed the required criteria for perfect focusing, as well as the restrictions imposed on the resolution by the periodicity of the LHM used.

March 2004: G. V. Eleftheriades presented for the first time experimental results showing sub wavelength focusing with a planar TL-based left handed lens [28]. At a frequency of 1.057 GHz, the resolution was three times better than the one imposed by the diffraction limit. This resolution enhancement was quite small

because of the mismatch at the lens interfaces and the losses in the left-handed lens.

2006: More recent research on MTMs focuses on the new exciting topic of invisibility, also referred to as cloaking [29, 30], which consists in hiding objects by bending the light around them with MTM cloaks. These applications do not directly involve LHM, but rather MTMs with refractive indices varying between 0 and 1.

From 2006 to present: Since the pioneer works mentioned above, many groups worldwide have investigated metamaterials and the number of related papers published has been continuously increasing. In parallel to these developments, some serious concerns have emerged, concerning the pertinence of considering MTMs as a real *new* field of research, or whether these findings can be fully explained in the frame of more traditional areas of research, such as filter theory. These issues are currently being debated (see for instance [31]). In this section, we have reported the most significant milestones in the emergence of MTMs, more particularly of LHM. However, as is often the case with such a fundamental new field of research as MTMs, there exist former works which are to some extent related to these modern concepts. Reference [32] reports some of these "germs" of negative refractive index MTMs. We can also mention the works on artificial dielectrics, a field of research sharing many similarities with the modern concept of MTM. Nevertheless, the contributions reported in this section were indeed the starting point of the systematic study of the physical properties, possible implementations and applications of MTMs.

I.3 Metamaterials pioneers works

As mentioned previously in the history of metamaterials, it's quit difficult to indicate accurately their origins. However, the most significant theoretical and experimental contributions in the development of this field can be attributed to three of a well known

scientist in this field namely: ***Victor Veselago***, ***John Brian Pendry***, and ***David Smith*** Figure I.1**.** The next section will describe their work and contributions to this field.

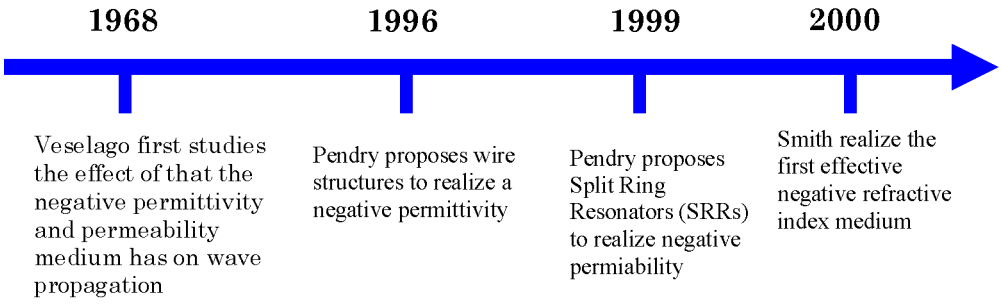

Figure I.1: Metamaterials pioneers works

I.3.1 Veselago's work

The merit of the first idea behind the metamaterials principles goes without a doubt to the Russian physicist *Victor Georgievich Veselago*. All begun from 1964, when he started wondering about the material properties, if its permittivity and permeability were negative in the same frequency region.

For that, he decided to apply Maxwell equations to a plan electromagnetic wave to such type of medium. He noticed that the triad formed by wave vector, magnetic field and electric field is indirect, while is direct in the classical type of medium. Furthermore, Veselago observed that, the triad formed by the Poyting vector, the electric field and the magnetic field remains direct, which means that for such type of medium, the wave vector and Poyting vector have different pointing direction, which is unusual situation. Knowing that the wave vector orientation gives the phase propagation direction, and the Poyting vector one, gives the energy propagation direction, he concludes that in this type of medium the phase and the energy propagate in opposite directions (Figure I.2).

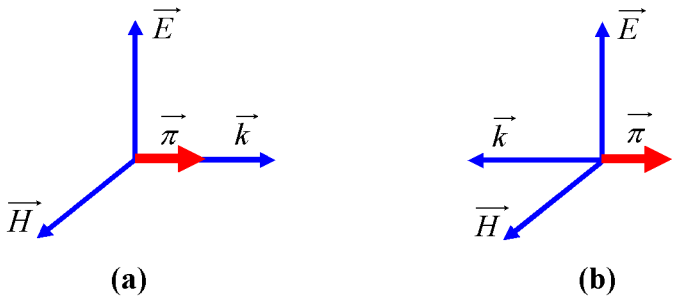

Figure I.2: *$\vec{E}, \vec{H}, \vec{k}$, and $\vec{\pi}$ vectors system for an electromagnetic plan wave in: a) ordinary medium, b) left hand medium.*

Also Veselago, demonstrated using the Snell's refraction theory and the propagation equations between two mediums, that such medium would have a negative refraction index. We will come back to the physics related to Veselago's work in the next chapter.

I.3.2 Pendry's work

In the last part of his famous publication in 1967, Veselago underlined that due to lack of materials with negative permeability, it was impossible at that time, to demonstrate experimentally his results. Therefore, his publication remained a dead letter for long time. We had to wait till 1996 for John Pendry who was the first to theorize a practical way to make a left-handed metamaterial, allowing an electromagnetic wave to convey energy (have a group velocity) in the lode against its phase velocity. Pendry's initial idea was that metallic wires aligned along the direction of propagation could provide a metamaterial with negative permittivity ($\varepsilon < 0$), and proposed the periodic structure which is composed of infinite wires arranged in a simple cubic lattice, joined at the corners of the lattice as shown in Figure I.3. Note however that natural materials (such as ferroelectrics) were already known to exist with negative permittivity.

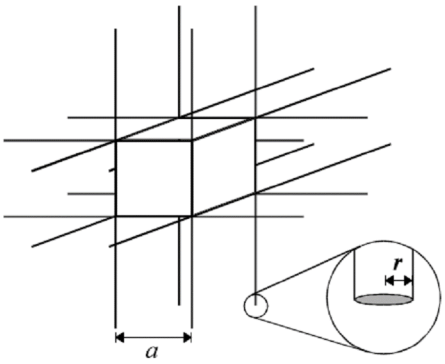

Figure I.3: The wire structure proposed by Pendry to achieve the negative permittivity. The periodic structure is composed of infinite wires arranged in a simple cubic lattice, joined at the corners of the lattice

However, the challenge was to construct a material which also showed negative permeability ($\mu < 0$). In 1999 Pendry demonstrated that a split ring (C shape) with its axis placed along the direction of wave propagation could provide a negative permeability. In the same paper, he showed that a periodic array of wires and ring could give rise to a negative refractive index. A related negative-permeability particle, which was also proposed by Pendry, is the Swiss roll.

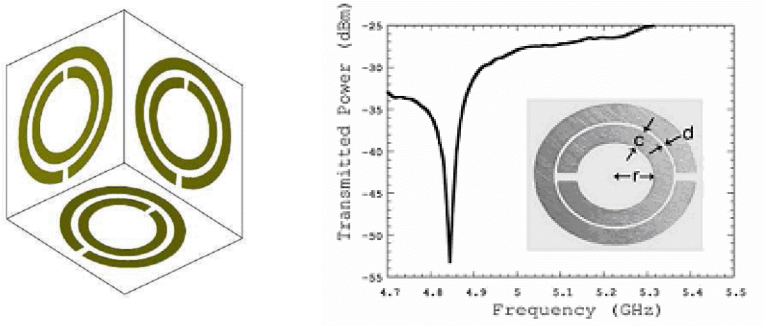

Figure I.4: C split resonator proposed by Pendry to achieve negative permeability, on the left the resonance curve of such SRR

I.3.3 Smith's work

Inspired by the results of Pendry, David Smith proposed the first experimental demonstration of metamaterial with negative

refractive index. His idea was to combine the thin wire and C split resonators already proposed by Pendry to achieve a negative permittivity and negative permiability at the same frequency region.

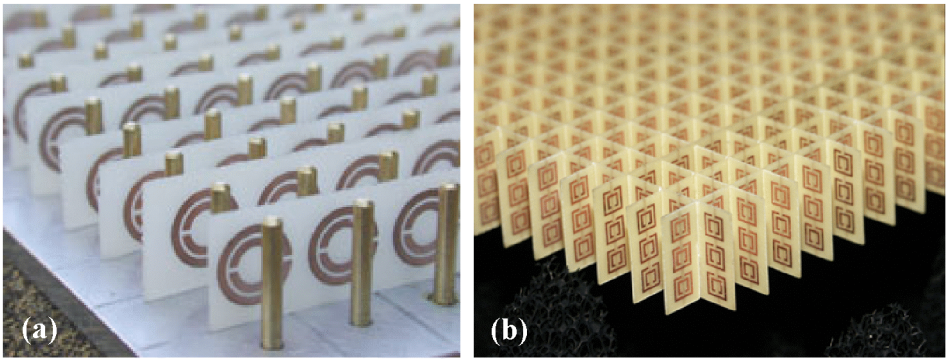

Figure I.5: The first experimental demonstration of an actual metamaterial a)1D metamaterial, b) 2D metamaterial.

The Figure I.5 (a) shows the first uni-axial experimental prototype of an actual metamaterial. The second example shown in Figure I.5 (b), is the bi-dimensional metamaterial proposed and realized by Shelby [18].

I.4 Metamaterial Types

Metamaterials can be classified in different categories, according either to their physical properties, materials, functioning principles or even their operating frequency. In the following section we will give a general description of metamaterial classes operating from microwave to optic region, made of metallic or dielectric structures, we are more interested in SRRs- Wire mediums; so more details about this will be given in the next chapters.

I.4.1 Electromagnetic bandgap materials

As example of this type of metamaterial we have Photonic crystals, which are periodically arranged artificial dielectric or metallo-dielectric nanostructures, with period on the same order of the

wavelength of the working electromagnetic wave. The wave propagation in photonic crystals is determined by the Bragg scattering of the periodic structure, and the photonic band-gaps can be present for a properly designed photonic crystal. Electromagnetic waves with frequencies within the range of the band-gap are suppressed from propagating in the photonic crystal, and with surface defects, a photonic crystal could support surface modes that are localized on the surface of the crystal, with mode frequencies within the band-gap. With line defects, a photonic crystal could allow the propagation of electromagnetic waves along the channels.

Due to the existence of band-gap in properly designed photonic crystals, many interesting applications can be realized to manipulate the flow of electromagnetic waves and light [33]. For example, by introducing point defects in photonic crystals, high-Q cavities can be fabricated. By introducing line defects in photonic crystals, waveguides can be realized, where light is guided along the line defects. The guiding mechanism of photonic crystal waveguides is different from the dielectric planar waveguides.

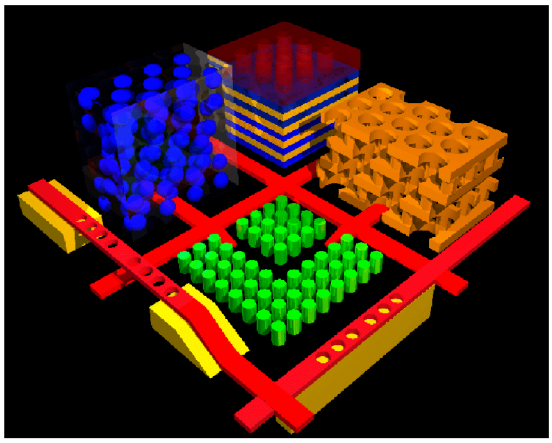

Figure I.6: reference picture of photonic crystals.

The dielectric constant of the waveguide does not have to be larger than the surroundings. Actually, the wave guiding region can be lower-indexed materials including air. This is an important

advantage of photonic crystal waveguides; as the propagation losses can be significantly reduced. Also, photonic crystal waveguides can bend light at sharp angles with lower loss.
The photonic crystal structure can be either of one dimension (1D), tow dimensions (2D) or three dimensions (3D) depending on the function target. In the one-dimensional 1D photonic crystal, layers of different dielectric constant are deposited together to form a band gap in a single direction. And, typical 2D photonic crystals consist of a lattice of parallel rods embedded in a substrate of different dielectric constant. This can be either air pores in a dielectric or dielectric rods in air ordered in a square or hexagonal lattice; such that the dielectric constant is homogeneous in the direction parallel to the rod axis (generally defined as z-direction) and periodic in the (x, y)-plane. However, Three-dimensional (3D) photonic crystals have a complete PBG in all directions, which might allow the complete control of light emission and propagation in devices.

I.4.2 Frequency Selective surfaces

A Frequency Selective Surface (FSS) is any surface construction designed as a 'filter' for plane waves. FSS characteristics are Narrow Band, periodic in two dimensions. FSS has become an alternative to the fixed frequency metamaterial; where static geometries and spacing of unit cells determine the frequency response of a given metamaterial. Since arrayed unit cells maintain static positions throughout operation, a new set of geometrical shapes and spacing would have to be embedded in a recently fabricated material for each different radiated frequency and response. Instead, FSS based metamaterials permit for optional changes of frequencies in a single medium, rather than a restriction to a fixed frequency response. Frequency selective surfaces can be fabricated as planar 2-dimensional periodic arrays of metallic elements with specific geometrical shapes, or can be periodic apertures in a metallic screen. The transmission and reflection coefficients for these surfaces

depend both on the frequency of operation, on the polarization and the angle of the transmitted electromagnetic wave striking the material or angle of incidence. The versatility of these structures is shown when having frequency bands at which a given FSS is completely opaque (stop-bands) and other bands at which the same surface allows wave transmission. FSS was first developed to control the transmission and reflection characteristics of an incident radiation wave. This has resulted in smaller cell size along with increases in bandwidth and the capability to shift frequencies in real time for artificial materials.

I.4.3 Bi-isotropic and bianisotropic metamaterials

Usually metamaterials are classified according to the independent electric and magnetic responses described by the parameters ε and μ. Which is not the case of all the electromagnetic metamaterials where, the presence of an electric field causes magnetic polarization, and the presence of magnetic field induces an electrical polarization, this phenomena is called magneto-electric coupling. In general linear material response, which can be anisotropy and contain magneto-electric coupling at the same time, is called bianisotropic material, and characterized by mean of four dyadic parameters. The constitutive relations relate the electric (**E**) and magnetic (**H**) field strength quantities to the electric (**D**) and magnetic (**B**) flux densities.

$$D = \varepsilon E + (\chi + i\kappa)\sqrt{\mu_0 \varepsilon_0}\, H$$

And

$$B = (\chi - i\kappa)\sqrt{\mu_0 \varepsilon_0}\, E + \mu H$$

Where, the four material parameters are ε, μ, κ and χ or permittivity, permeability, strength of chirality, and the Tellegen

parameter respectively. These parameters do not vary with changes along a rotated coordinate system of measurements, and they are also defined as invariant or scalar parameters [18].

The intrinsic magneto-electric parameters κ and χ affect the phase of the wave. Moreover, the effect of the chirality parameter is to split the refractive index. In a bi-isotropic media when χ assumed to be zero, and κ a non-zero value, different results can be obtained and both a backward wave / a forward wave can occur. Alternatively, two forward waves or two backward waves can occur, depending on the strength of the chirality parameter.

I.4.4 Chiral metamaterial

In metamaterial a chiral medium is composed of particles that cannot be superimposed on their mirror images [3]. A chiral medium has different responses for a left circularly polarized wave and a right circularly polarized wave because of its intrinsic chiral asymmetry. This kind of metamaterial is also characterized by the presence of the cross-coupling between the electric field and magnetic field going through it. A dimensionless chirality parameter κ is used to describe this cross-coupling effect. The refractive index of the left circularly polarized and the right circularly polarized waves become different due to the existence of κ.

Historically the study of chiral media is old enough the start in the early 19th century, where the optical rotation in quartz crystals as well as some liquids and gases had already been discovered by Biot et all [34], and the handedness nature of the molecules in optically active materials was confirmed by Pasteur in the 1840s [3]. 33 years later, in 1873, Lord Kelvin used the word “chirality” for the first time to describe the handedness in his lectures [35]. In the 1910s Lindeman introduced the optical activity phenomenon in visible light to radio waves, using a collection of helical coils serving as artificial

chiral 'molecules' [3], and In 2003, Tretyakov *et al* [36] discussed the possibility of realizing negative refraction by chiral nihility. However, in 2004, Pendry [37] discussed in general the possibility to achieve negative refraction in chiral metamaterials. He showed that the conditions to realize negative refraction in chiral metamaterials are simpler than for regular metamaterials, which require both electric and magnetic resonances to have ε negative and negative μ.

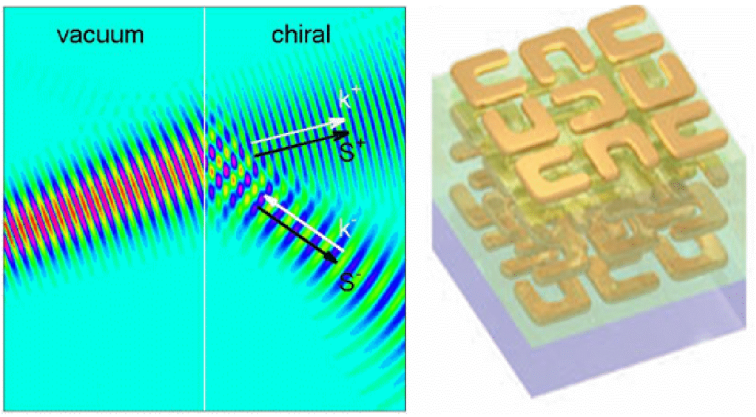

Figure I.7: reference picture of chiral metamaterials

In chiral metamaterials, neither ε nor μ needs to be negative. As long as the chiral parameter κ is large enough, negative refraction can be obtained in chiral metamaterials, and he proposed then a practical model of a chiral metamaterial working in the microwave regime with twisted Swiss rolls as elemental structures.

Actually, the chiral media belongs to a wider range of bi-isotropic media which are characterized by the following constitutive relations:

$$D = \varepsilon E + (\chi + i\kappa)\sqrt{\mu_0 \varepsilon_0}\, H$$

And

$$B = (\chi - i\kappa)\sqrt{\mu_0 \varepsilon_0}\, E + \mu H$$

Where ε is the relative permittivity of the medium, ε_0 is the permittivity of vacuum, μ is the relative permeability of the medium and μ_0 is the permeability of vacuum. The difference between bi-isotropic media and regular isotropic media lies in the extra terms of the constitutive relations, where χ is the dimensionless magneto-electric parameter which describes the reciprocity of the material and when $\chi \neq 0$ the material is non-reciprocal. However, κ is the dimensionless chirality parameter of the material when $\kappa \neq 0$ the material is chiral.

I.4.5 Split Ring Resonators

The first fabricated negative refractive index metamaterials is split ring resonator (SRR) based. Indeed, John Pendry [38] has described SRRs as, "the metamaterial equivalent of a magnetic atom." It is this structure that "interacts with", "responds to" and then "back-reacts" upon the impinging electromagnetic wave, They are based on metallic microstructures, truly sub-wavelength structures with wavelength-to-structure ratio is at least 5:1 [39]. An SRR is composed of two nested copper C-shaped rings. In which, when an electromagnetic wave encounters an SRR, its oscillating magnetic field causes electrons in the SRR to move in sympathy with it, in consequence, enabling an electric current to flow. The gap in the ring component acts like a capacitor, briefly storing a charge before letting it proceed, and this establishes an oscillating electric field that back-reacts upon the impinging electromagnetic wave. The wavelength range over which the magnetic permeability μ is negative, and is controlled by the radius of the inner C-ring as well as the separation between the inner and outer C-rings. The electrical permittivity ε is further determined by an array of straight conducting wires. In this case, the electrical field of the incident wave sets up an oscillating dipole magnet in each wire, and the electrical permittivity is controlled by adjusting the wire spacing and length. It is the combination of the linear wire and SRR arrays along

with their relative size and spacing that determines the wavelength region over which both ε and μ will be negative.

A metamaterial is fabricated by engineering an arrangement of repeated SRRs and vertical wire cells, with the condition that the spacing between each cell and its adjacent should be much smaller than the wavelength of the incident electromagnetic radiation. At that stage the metamaterial will act like a homogeneous material; in a sense that the individual cells within the metamaterial combine to work like a kind of crystal made of artificial atoms (the SRRs). The crystal-like analogy is nicely illustrated by the so-called Boeing Cube (Figure I.8), which was designed by Minas Tanielan and co-workers in 2004 at Boeing Phantom Works in Seattle. Indeed, the Boeing team was working under a $5.6 million DARPA (the Defense Advanced Research Projects Agency) contract, which started in 2001, to study and fabricate metamaterial structures and to investigate their potential application in the aerospace industry.

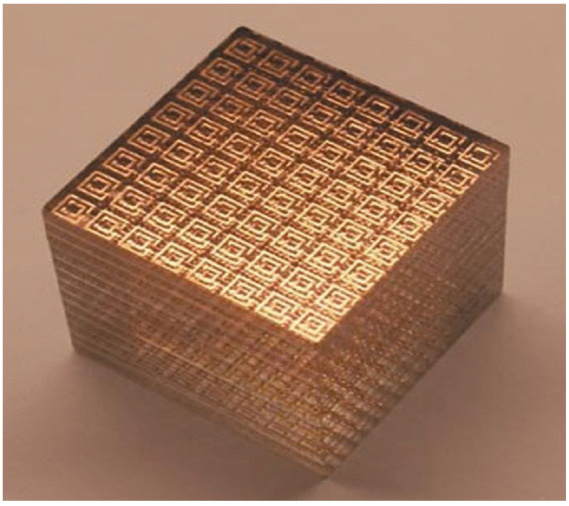

Figure I.8: the Boeing Cube. The component copper SRRs cells and wire array are visible in this metamaterial that has a negative refractive index at microwave/radar wavelengths. The spacing between each lattice cell is 2.68 mm and the entire cube has sides of 2.5 cm (Image courtesy of Boeing Phantom works, Seattle)

The Boeing Cube was designed to work, that is, emulate a negative refractive index medium for incident radiation with wavelengths corresponding to several centimetres – i.e., the radar wavelength range.

To realize negative refraction in metamaterials, both ε and μ need to be negative [12]. The negative ε can be achieved with an array of long and thin metallic wires, serving as electric resonators. Just like the electric plasmonic behavior of metals, the ε of the medium is negative below the effective plasma frequency. By adjusting the geometry of the wires and the distance between wires, the plasma frequency can be scaled down to the microwave region. The negative μ is first realized by the so-called split-ring resonator (SRR) structure, proposed by Pendry *et al* [40]. The SRRs are composed of metallic rings with gaps. Although made of non-magnetic materials, the SRRs are magnetically active and can give strong responses to magnetic fields. By tuning the geometric parameters of SRRs, a band of negative μ can be obtained at the desired frequency range. If designed properly, the combination of these two sets of resonators can give both negative ε and negative μ in the same frequency band. This is realized with microwave experiments by Smith *et al* [15] in 2000. The same group further demonstrated negative refraction by measuring the output signal of EM waves refracted by a metamaterial in a wedge shape [18]. Since then, the SRR and metallic wire structures were studied extensively by research groups all over the world, both theoretically and experimentally. Applications of metamaterials, such as super-lens [39, 41], and invisible cloaks [29, 30], were proposed and studied.

By scaling down the SRR size and simplifying the structure, magnetic metamaterials were fabricated to show magnetic responses from the THz to infrared region [42–45]. However, the scaling rule breaks down beyond 200 THz, due to the fact that metals cannot be considered as perfect conductors anymore [46]. Another disadvantage is that, for the SRR structures, the magnetic field needs to be

perpendicular to the plane to obtain the magnetic resonance. Normal incidence of EM waves to the planar SRR structures does not excite directly the magnetic resonance. Plus, the SRR and wire combination is too complicated to be fabricated in nano-scale, especially when a three-dimensional (3D) medium is needed.

New designs were proposed to achieve negative refraction towards the optical regime [47–50]. Unlike the SRRs, these new designs are typically layered structures, with a dielectric substrate in the middle. The two metal layers on each side of the substrate are identical and composed of short wires, resonances, so that the medium has a higher tolerance to fabrication defects and the loss is smaller than in strongly resonant structures [51, 52]. Moreover, the wire array does not even have to be periodic. Sub-wavelength imaging and negative refraction of the wire medium in infrared and optical frequencies was studied theoretically and numerically. Recently, optical negative refraction has been demonstrated experimentally with silver nanowires [53], metal plates or fishnet-like structures. While the parallel dipole resonance in each metal structure gives negative ε, the negative μ is provided by the anti-parallel resonance in the metal structure pairs separated by the substrate. So, normal incidence of EM waves is supported. Bulk media can be fabricated by stacking the layered structures.

I.5. Characterization techniques and homogenization procedures

A metematerial can be microscopically characterized by employing specific analysis techniques, in order to determine a set of relevant parameters which can be equivalent medium parameters (permittivity and the permeability), refractive index, bianisotropic medium parameters, or equivalent propagation constant and characteristic impedance.

I.5.1 Bloch wave analysis

This technique is called also Bloch theory, is based on the Floquet's Theorem [54, 55], consists in determining the eigen solutions which can exist in the infinite periodic structure in the absence of excitation. Each one of these solutions is usually referred to as a Bloch wave, or Floquet mode. The properties of these waves are usually obtained by solving an eigen-value problem. The resulting eigenvalues represent the possible *Bloch* propagation constants γB, while the associated fields solutions can be regarded as the eigenvectors. The possible values of γB in function of the frequency, the dispersion relation, or band structure, and its graphical representation is the dispersion diagram (Brillouin diagram). Although the information contained in the dispersion relation is sufficient to assess the left-handed or right-handed nature of the considered mode, it does not provide a complete picture of the metamaterial properties. Accordingly, the information contained in the eigenvectors can be further exploited, and possibly combined with the dispersion relation, in order to derive additional macroscopic parameters such as the Bloch impedance, or equivalent medium parameters (permittivity and the permeability). Practically, a single unit cell is considered and periodic boundary conditions (PBC) with variable phase shifts between them are applied to its boundaries. Applying Floquet's theorem to this system allows the obtaining of an Eigen value problem which can be solved analytically or numerically, depending on the complexity of the problem.

I.5.1.1 Circuital representation

The simplest implementation of the Bloch wave analysis, suitable for 1D periodic structure, is based on a two-port circuital representation of the unit cell. The Floquet's Theorem allows a direct determination of the dispersion relation $\gamma_B(\omega)$, provided that the transmission matrix of the unit cell is known, either from a simplified circuit

model, or from full-wave S parameters numerical calculation, and a Bloch impedance Z_B associated to each Bloch wave can be deduced from the corresponding eigenvectors, which are now expressed in terms of voltages and currents. However, this technique can also be extended to 2D or 3D periodic structures in a straightforward manner [56, 57]. Due to its circuital based formulation, this technique has mainly been used for TL-based metamaterials, for which the couple of parameters (γ_B, Z_B) represents the most relevant information in view of practical microwave applications. It should be noted that this approach is accurate provided that the interaction between cells can be accurately described by a single mode of the host guiding structure. Otherwise, a multimode description of the unit cell has to be resorted too.

I.5.1.2 Full-wave approach

For more general formulation, where the non circuital representation based method is employed, the eigen solutions are usually found through some specific numerical computations performed by an "eigenmode solver". Such codes are included in several commercial softwares, like Ansoft HFSS and CST Microwave Studio. However, the dispersion diagram $\gamma_B(\omega)$ directly provided by those softwares is not sufficient for a complete description of the metamaterial properties. To that purpose, several techniques have been proposed to derive macroscopic parameters from the eigen fields and currents in the unit cell (eigenvectors). These techniques are based on various kinds of averaging procedures [58, 69].

I.5.2. Averaging procedures

The averaging strategy used in case of homogenization of artificial dielectrics, consists in performing volume-averages of the fields over a unit cell, and in defining the equivalent medium parameters as those which satisfy the constitutive relations for the macroscopic

(averaged) fields. A well known result obtained with this approach is the Maxwell-Garnett mixing formula [60]. This approach, developed for dielectric inclusions in the static regime, is not easily adapted for the case of metallic inclusions (which can be infinitely thin, like strips) and for the high frequency regime, this is why other averaging strategies have been proposed. In particular, the averaging scheme directly inspired from the topology of Maxwell's equations (in integral form) has been proposed in [59]. Where, the fields **B** and **D** are averaged over the faces of the unit cell, as they are related to flux densities, whereas **E** and **H** are averaged over the edges of the cell, since related to circulations (integration on a path). This averaging scheme is sometimes referred to as the surface/line averaging technique, by comparison to the aforementioned volume/volume approach commonly used for artificial dielectrics. The equivalent medium parameters are those which satisfy the constitutive relations for the macroscopic fields. Some variants of this technique involving the calculation of the wave impedance z from the averaged field quantities, or the calculation of the averaged polarization **P** and magnetization **M** from the currents distribution in the unit cell [58]. Another field averaging procedure, also called the field summation method [61-63], in which a volume/surface averaging scheme applied to the fields numerically calculated for a finite thickness slab under plane wave incidence (scattering parameters analysis) is involved.

I.5.3 Retrieval procedures from scattering parameters

The retrieval procedures from scattering parameters is one of the most used homogenization procedures, to determine equivalent medium parameters for composite structures metamaterials, it consists in the extraction of these parameters from reflection and transmission coefficients (scattering parameters, or Fresnel coefficients) of a slab of finite thickness under plane wave incidence

[64,65]. This technique consists in determining usually the permittivity ε and the permeability μ of the medium of a homogeneous slab exhibiting the same scattering parameters as the real composite periodic structure to study. First, the refractive index n and the normalized wave impedance z are determined from the scattering parameters. Then, the parameters ε and μ are subsequently determined from n and z. As is often the case with such inverse problems, ambiguities are encountered in the determination of n and z. A robust retrieval procedure has been proposed in [66] in order to resolve these ambiguities. With the employment of this method, it has been observed that the parameters extracted exhibit often anomalous behaviours, like incompatibilities with fundamental physical principles such as causality and passivity. In particular, when one of the extracted parameters experiences a resonance, the other exhibits an "antiresonant" behaviour, which is also accompanied with a "wrong" sign of the imaginary part of ε or μ. This problem has been addressed in [67], where this unexpected frequency behaviour has been attributed to the periodic nature of the structure, more precisely to the finite (non zero) size of the unit cell. Moreover, the extracted parameters are sometimes function of the thickness of the metamaterial slab (of the number of cells in the propagation direction, which is a consequence of coupling phenomena occurring between adjacent cells). This issue has challenged the validity of this method since material parameters are expected to be independent from the sample size and shape. Here, it is important to note that the retrieval procedure from scattering parameters has only been developed for normal incidence. So, it only provides the equivalent medium parameters associated to this specific direction of propagation, which is not sufficient to assess the degree of isotropy of 3D complex metamaterial unit cells for example. Moreover, it is often assumed that the material is only described by a permittivity and permeability, whereas other parameters related to magneto-electric coupling (bianisotropy) cannot be easily extracted with this basic

approach. to solve this issue, an improved retrieval procedure also allowing the retrieval of the bianisotropic parameters of metamaterial based on SRRs structures has been reported in [68]. This technique also involves normal plane wave incidence, plus the consideration of several orientations of the unit cell in order to obtain enough equations to deduce all the medium parameters. To avoid the aforementioned anomalies observed on the extracted parameters, an alternative approach has been proposed in [69], which consists in considering the metamaterial as a periodic effective medium, instead of a homogeneous effective medium. Here, the metamaterial is modelled as a succession of homogeneous slabs of unknown parameters ε and μ (to be determined with the method), with layers of vacuum placed in-between. This approach allows distinguishing the resonant behaviour of the parameters from periodicity effects. Actually, the retrieval procedure from scattering parameters is equivalent to the Bloch wave analysis based on a monomode circuital representation, since the latter also involves a description of the unit cell obtained from scattering parameters. As a result, the expressions obtained for n and z are exactly the same.

I.5.4 Quasi-static approaches

Quasi-static techniques, such as the quasi-static Lorentz theory or the Maxwell Garnett model, initially developed for the characterization of conventional and artificial dielectrics [54, 60, 70], are generally used for metamaterials with lattice constant much smaller than the wavelength, to determine effective material parameters. These quasi-static techniques approaches rely on a dipolar representation of the particles forming the metamaterial. More specifically, it is assumed that the response of the particles to an impressed field can be accurately represented by electric and magnetic dipole moments. Those dipole moments are further averaged over the volume of the unit cell, resulting in averaged

polarization and magnetization in the material, from which effective material parameters can be derived.

In the quasi-static Lorentz theory [54,71], it comes out from that effective material parameters can be obtained provided that polarizabilities of the particles are known. These polarizabilities often have to be determined numerically, by calculating the dipole moments from the currents or fields distribution under a specific excitation. It is important to take in account that the quasi-static Lorentz theory is applicable provided that not only the unit cell is small compared to the wavelength, but also the spacing between inclusions, so that the interaction between them can be accurately described by dipole moments.

However, the quasi-static Maxwell Garnett model did not provide reliable results for the effective permittivity and permeability in the resonant bands [72], which considered as one of the limitations of this kind of metamaterial characterization techniques.

I.6 Development of metamaterial field

Starting from Pendry's discovery, metamaterial became a common target for several research groups all over the world. This huge interest, leads to a big development of applications (mainly related to the field of imaging or telecommunication.) and experimental verifications based on metamaterials concepts, extended all over the electromagnetic spectrum. Obviously the most exciting one is the "Cloaking". In this section we will focus on three of the most important application based on metamaterials, that is: Antennas and circuit miniaturization, superlensing, Clocking…

I.6.1 Antennas and circuit miniaturization

Certainly this application is the most concrete one; as already some kind of mobile phones were commercialized with a metamaterials based antenna since 2009. Also, lot of kind of electric and magnetic

resonators developed for the microwave range, have been studied and adapted to fit the telecommunication applications. Due to the simplicity of the fabrication techniques related to that frequency range and the progresses made in the field of artificial magnetism, the characteristics of metamaterials based antennas have been improved, mainly in terms of miniaturization and directivity.

I.6.2 Superlensing

In order to take advantage of the fantastic properties of negative refractive index materials, Pendrey proposed for the first time the "superlens" [73]. His proposal consisted of a metamaterial that compensates for wave decay and reconstructs images in the near field. In addition, both propagating and evanescent waves contribute to the resolution of the image.

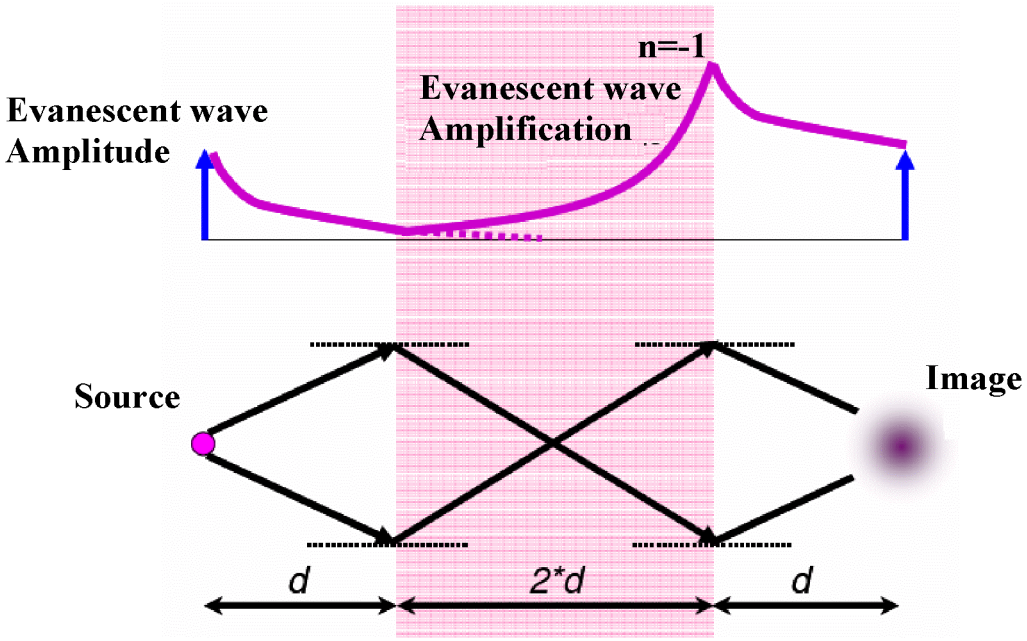

Figure I.9: Pendry's super lens principle

Theory and simulations show that the superlens and hyperlens can work but engineering obstacles need to be overcome.The Figure I.9 shows clearly two light vectors crossing a negative refractive index medium, and how the waves are converged in such medium.

This type of lenses mite be of huge interest to the scientific community However, due to the practical constraint preventing a real exploitation of this lenses, we can not find a big experimental demonstration related to this kind of lensing [74, 75].

I.6.2 Cloaking or invisibility

In order to cope with the constraints preventing the best use of superlenses, the researchers start exploring other aspects of metamaterials and found new applications. The best example is the "cloaking". Again, the merit of this discovery returns to Pendry and Lenhard for their works [76, 77]. In fact, they demonstrate that is possible to realize a sort of invisibility cape using left handed materials.

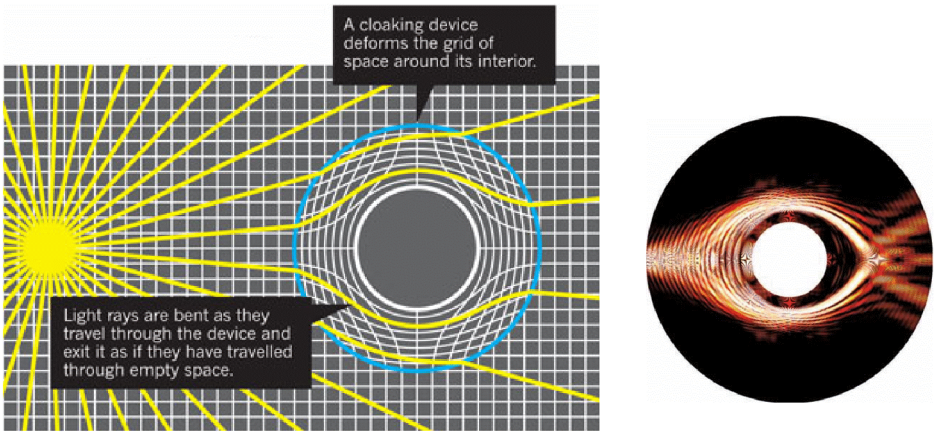

Figure I.10: Cloaking principle as proposed by Pendry,

The idea was based on the use of metamaterials to control the light around the target to be hidden, in a manner that the light after that target would be as it did not cross it. The challenge is to realize a

large band system, mainly with low losses, in order to avoid the blurring effect. This concept is particularly interesting in terms of applications, especially the one related to the defense. The cloaking principle as proposed by Pendry in 2006 is illustrated in the following the Figure I.10.

The cloaking design is essentially based on the transformation of the space coordinate surrounding the object to be hidden. This transformation consists of the definition of the permittivity and permeability tensors that will allow the electromagnetic wave guidance around the target. An actual experimental demonstration of metallic cylinder cloaking has been performed in [78].

I.7 Conclusion

This chapter was devoted to a general introduction in the field of metamaterials, starting from history of metamaterial to the recent development of the field. At first place, we defined the metamaterial and recalled the different works that have been done since the beginning; where a particular attention was given to the pioneers works namely: the theoretical bases of the field set by Veselago, the first theory established by Pendry of a practical way to design them, and finally the first experimental realization of a metamaterial done by Smith. Also, a brief presentation of metamaterials different types was given with an emphasis on the SRRs. Which was followed by a description of a different methods used for their characterization. At the end the most important applications of metamaterial such as Antennas and circuit miniaturization, superlensing, cloaking or invisibility were presented. In the next chapter we will be focusing on the fundamental physical aspects of the metamaterial theory.

Bibliography

[1] Metamaterial home page of the future projects of the Defense Advanced Research Projects Agency's (DARPA) Defense Science Office (DSO).

[2] R.M.Walser, "Electromagneti cmetamaterials. Inaugural lecture, "Proc. Of SPIE (Complex medium II: Beyond Linear Isotropic Dielectric),4467,1-15, 2001.

[3] The web page of Davide Smith, University of California, San Diego, http://physics.ucsd.edu/

[4] J.B.Pendry, "Negative μ, negative ε, negative refractive index, and how to exploit them. Electromagnetic Structure," Euroconference on Electromagnetic Confinement, from Basic research to the Marketplace, St,Andrews, Scotland, 9-14 june 2001.

[5] T.Weiland, R..Schuhman, RP. Greegor, C:G.Parazzoli, A.M.Vetter, D.R.Smith, D.C.Vier, and S.Schultz. "Ab initio numerical simulation of left-handed metamaterials:comparison of calculations and experiments," J of Applied Physics, 90(10), 5419-5424,2001.

[6] J.C. Bose, "On the rotation of plane of polarisation of electric waves by a Twisted structure", proceeding of the Royal Society of London, vol. 63, pp 146-152, 1898

[7] I.V. Lindell, A. H. Sihvola and J. Kurkijarvi, "Karl F. Lindman: The last hertzian, and harbinger of electromagnetic chirality", IEEE Antennas Propagation Magasing, vol. 34, pp 24-30, 1992

[8] I. Mandelshtam, "Lecture on some problems of the theory of oscillations", Complete collection of works, vol. 5, pp 428-467, 1950.

[9] W.E. Kock, "Metallic delay lenses", Bell Sys. Tech. J, vol. 27, pp 58-82, 1948.

[10] D.V. Sivukhin, "The energy of electromagnetic waves in dispersive media", Opt. Spektrosk, vol. 3, pp 308-32, 1957.

[11] V.W. Pafomov, "JETP 33", Soviet Physics, vol. 33, p 1074, 1959.

[12] V.G. Veselago, "The electrodynamics of substances with simultaneously negative values of e and μ ", Soviet Physics uspekhi, vol. 10, N°4, pp 509- 514, February 1968.

[13] J. Brown, "Artificial dielectrics", Progress in dielectrics, vol.2, pp 195-225, 1960.

[14] W. Rotman, "Plasma simulation by artificial and parallel plate media", Antenna and Propagation, IRE Transactions on, vol. 10, pp 82-95, 1962.

[15] D. R. Smith, W. J. Padilla, D. C. Vier, S. C. Nemat-Nasser, and S. Schultz, "Composite medium with simultaneously negative permeability and permittivity," Physical Review Letters, vol. 84, no. 18, pp. 4184–4187, 2000.

[16] R. A. Shelby, D. R. Smith, S. C. Nemat-Nasser, and S. Schultz, "Microwave transmission through a two-dimensional, isotropic, left-handed metamaterial," Applied Physics Letters, vol. 78, no. 4, pp. 489–491, 2001.

[17] J. B. Pendry, "Negative refraction makes a perfect lens," Physical Review Letters, vol. 85, no. 18, pp. 3966–3969, 2000.
[18] R. A. Shelby, D. R. Smith, and S. Schultz, "Experimental verification of a negative index of refraction," Science, vol. 292, pp. 77–79, 2001.
[19] C. Caloz and T. Itoh, "Application of the transmission line theory of left-handed (LH) materials to the realization of a microstrip "LH line"," in IEEE Antennas and Propagation Int. Symp. (AP-S) and USNC/URSI Meeting, vol. 2. San Antonio, TX: IEEE, June 2002, pp. 412–415.
[20] A. K. Iyer and G. V. Eleftheriades, "Negative refractive index metamaterials supporting 2-D waves," in IEEE MTT-S Int. Microwave Symp. Dig., Seattle, WA, June 2002, pp. 1067–1070.
[21] A. A. Oliner, "A periodic-structure negative-refractive-index medium without resonant elements," in IEEE Antennas and Propagation Int. Symp. (AP S) and USNC/URSI Meeting, San Antonio, TX, June 2002, p. 41.
[22] G. V. Eleftheriades, A. K. Iyer, and P. C. Kremer, "Planar negative refractive index media using periodically L-C loaded transmission lines," IEEE Transactions on Microwave Theory and Techniques, vol. 50, no. 12, pp. 2702–2712, 2002.
[23] C. G. Parazzoli, R. B. Greegor, K. Li, B. E. C. Koltenbah, and M. Tanielian, "Experimental verification and simulation of negative index of refraction using snell's law," Physical Review Letters, vol. 90, no. 10, p. 107401, 2003.
[24] D. R. Smith, D. Schurig, and J. B. Pendry, "Negative refraction of modulated electromagnetic waves," Applied Physics Letters, vol. 81, no. 15, pp. 2713–2715, 2002.
[25] J. Pacheco, T. M. Grzegorczyk, B.-I. Wu, Y. Zhang, and J. A. Kong, "Power propagation in homogeneous isotropic frequency-dispersive left-handed media," Physical Review Letters, vol. 89, no. 25, p. 257401, 2002.
[26] A. A. Houck, J. B. Brock, and I. L. Chuang, "Experimental observations of a left handed material that obeys snell's law," Physical Review Letters, vol. 90, no. 13, p. 137401, 2003.
[27] A. Grbic and G. V. Eleftheriades, "Growing evanescent waves in negative-refractive index transmission-line media," Applied Physics Letters, vol. 82, no. 12, pp. 1815–1817, 2003.
[28] ——, "Overcoming the diffraction limit with a planar left-handed transmission-line lens," Physical Review Letters, vol. 92, no. 11, p. 117403, 2004.
[29] J. B. Pendry, D. Schurig, and D. R. Smith, "Controlling electromagnetic fields," Science, vol. 312, pp. 1780–1782, June 2006.
[30] D. Schurig, J. J. Mock, B. J. Justice, S. A. Cummer, J. B. Pendry, A. F. Starr, and D. R. Smith, "Metamaterial electromagnetic cloak at microwave frequencies," Science, vol. 314, pp. 977–980, November 2006.
[31] B. E. Spielman, S. Amari, C. Caloz, G. V. Eleftheriades, T. Itoh, D. R. Jackson, R. Levy, J. D. Rhodes, and R. V. Snyder, "Metamaterials face-off. metamaterials: A rich opportunity for discovery or an overhyped

gravy train [speaker's corner]," IEEE Microwave Magazine, vol. 10, no. 3, pp. 8–42, May 2009.
[32] S. A. Tretyakov, "Research on negative refraction and backward-wave media: A historical perspective," in EPFL Latsis Symposium 2005, Lausanne, Switzerland, February 2005, pp. 30–35.
[33] C. M. Soukoulis, editor. Photonic Band Gap Materials. Springer, 1996.
[34] Applequist J 1987 Optical activity: Biot's bequest Am. Sci. 75 58–68
[35] Barron L D 1982 Molecular Light Scattering and Optical Activity (Cambridge: Cambridge University Press).
[36] Tretyakov S, Nefedov I, Sihvola A, Maslovski S and Simovski C 2003Waves and energy in chiral nihility J. Electromagn. Waves Appl. 17 695–706.
[37] Pendry J B 2004 A chiral route to negative refraction Science 306 1353–5.
[38] Pendry J B, Holden A J, Robbins D J and Stewart W J 1999 Magnetism from conductors and enhanced nonlinear phenomena IEEE Trans. Microw. Theory Tech. 47 2075.
[39] Vassilios Yannopapas and Alexander Moroz, "Negative refractive index metamaterials from inherently non-magnetic materials for deep infrared to terahertz frequency ranges"; JOURNAL OF PHYSICS: CONDENSED MATTER, Matter 17 (2005) 3717–3734; doi:10.1088/0953-8984/17/25/002, 2005.
[40] Pendry J B, Holden A J, Robbins D J and Stewart W J 1999 Magnetism from conductors and enhanced nonlinear phenomena IEEE Trans. Microw. Theory Tech. 47 2075.
[41] Pendry J B 2000 Negative refraction makes a perfect lens Phys. Rev. Lett. 85 3966–9
[42] Yen T J, Padilla W J, Fang N, Vier D C, Smith D R, Pendry J B, Basov D N and Zhang X 2004 Terahertz magnetic response from artificial materials Science 303 1494–6.
[43] Linden S, Enkrich C, Wegener M, Zhou J, Koschny T and Soukoulis C M 2004 Magnetic response of metamaterials at 100 Terahertz Science 306 1351–3
[44] Katsarakis N, Konstantinidis G, Kostopoulos A, Penciu R S, Gundogdu T F, Kafesaki M, Economou E N, Koschny T and Soukoulis C M 2005 Magnetic response of split-ring resonators in the far-infrared frequency regime Opt. Lett. 30 1348–50
[45] Enkrich C, Wegener M, Linden S, Burger S, Zschiedrich L, Schmidt F, Zhou J F, Koschny T and Soukoulis C M 2005, Magnetic metamaterials at telecommunication and visible frequenciesPhys. Rev. Lett. 95 203901
[46] Zhou J, Koschny T, Kafesaki M, Economou E N, Pendry J Band Soukoulis C M 2005 Saturation of the magnetic response of split-ring resonators at optical frequencies Phys. Rev. Lett. 95 223902
[47] Zhang S, Fan W, Panoiu N C, Malloy K J, Osgood R M and Brueck S R J 2005 Experimental demonstration of near-infrared negative-index metamaterials Phys. Rev. Lett. 95 137404

[48] Dolling G, Enkrich C, Wegener M, Zhou J F, Soukoulis C M and Linden S 2005 Cut-wire pairs and plate pairs as magnetic atoms for optical metamaterials Opt. Lett. 30 3198–200
[49] Shalaev V M, Cai W, Chettiar U K, Yuan H, Sarychev A K, Drachev V P and Kildishev A V 2005 Negative index of refraction in optical metamaterials Opt. Lett. 30 3356–8.
[50] Dolling G, Enkrich C, Wegener M, Soukoulis C M and Linden S 2006 Simultaneous negative phase and group velocity of light in a metamaterial Science 312 892–4.
[51] Wangberg R, Elser J, Narimanov E E and Podolskiy V A 2006 Nonmagnetic nanocomposites for optical and infrared negative-refractive-indexmedia J. Opt. Soc. Am. B 23 498–505
[52] Silveirinha M G, Belov P A and Simovski C R 2007 Subwavelength imaging at infrared frequencies using an array of metallic nanorods Phys. Rev. B 75 035108.
[53] Yao J, Liu Z, Liu Y, Wang Y, Sun C, Bartal G, Stacy A M and Zhang X 2008 Optical negative refraction in bulk metamaterials of nanowires Science 321 930
[54] R. E. Collin, Field Theory of Guided Waves, 2nd ed. New York: IEEE Press, 1991.
[55] D. A. Watkins, Topics in Electromagnetic Theory. John Wiley & Sons,
[56] C. Caloz and T. Itoh, Electromagnetic Metamaterials: Transmission Line Theory and Microwave Applications. Wiley-Interscience and IEEE press, 2006.
[57] G.V. Eleftheriades and K. G. Balmain, Negative-Refraction Metamaterials: Fundamental Principles and Applications. Wiley-Interscience and IEEE press, 2005.
[58] D. R. Smith, D. C. Vier, N. Kroll, and S. Schultz, "Direct calculation of permeability and permittivity for a left-handed metamaterial," Applied Physics Letters, vol. 77, no. 14, pp. 2246–2248, October 2000.
[59] D. R. Smith and J. B. Pendry, "Homogenization of metamaterials by field averaging (invited paper)," Journal of the Optical Society of America B, vol. 23, no. 3, pp. 391–403, 2006.
[60] A. Sihvola, Electromagnetic mixing formulas and applications, ser. IEE Electromagnetic Waves Series. London: The Institution of Electrical Engineers, 1999, vol. 47.
[61] J.-M. Lerat, N. Malléjac, and O. Acher, "Determination of the effective parameters of a metamaterial by field summation method," Journal of Applied Physics, vol. 100, p. 084908, 2006.
[62] O. Acher, J.-M. Lerat, and N. Malléjac, "Evaluation and illustration of the properties of metamaterials using field summation," Optics Express, vol. 15, no. 3, pp. 1096–1106, February 2007.
[63] C. Croënne, J.-M. Lerat, N. Malléjac, O. Acher, and D. Lippens, "Retrieval technique by field summation: application to double negative media," in Metamaterials' 2007: First International Congress on Advanced Electromagnetic Materials in Microwave and Optics, Rome, Italy, 22-24 October 2007, pp. 706–709.

[64] D. R. Smith, S. Schultz, P. Markos, and C. M. Soukoulis, "Determination of effective permittivity and permeability of metamaterials from reflection and transmission coefficients," Physical Review B, vol. 65, p. 195104, 2002.
[65] R. W. Ziolkowski, "Design, fabrication, and testing of double negative metamaterials," IEEE Transactions on Antennas and Propagation, vol. 51, no. 7, pp. 1516–1529, 2003.
[66] X. Chen, T. M. Grzegorczyk, B.-I. Wu, J. Pacheco Jr, and J. A. Kong, "Robust method to retrieve the constitutive effective parameters of metamaterials," Physical Review E, vol. 70, p. 016608, 2004.
[67] T. Koschny, P. Markos, D. R. Smith, and C. M. Soukoulis, "Resonant and antiresonant frequency dependence of the effective parameters of metamaterials," Physical Review E, vol. 68, p. 065602, 2003.
[68] X. Chen, B.-I. Wu, J. A. Kong, and T. M. Grzegorczyk, "Retrieval of the effective constitutive parameters of bianisotropic metamaterials," Physical Review E, vol. 71, p. 046610, 2005.
[69] T. Koschny, P. Markos, E. N. Economou, D. R. Smith, D. C. Vier, and C. M. Soukoulis, "Impact of inherent periodic structure on effective medium description of left-handed and related metamaterials," Physical Review B, vol. 71, p. 245105, 2005.
[70] S. A. Tretyakov, Analytical Modeling in Applied Electromagnetics, ser. Artech House electromagnetic analysis series. Norwood: Artech House, 2003.
[71] A. Ishimaru, S. W. Lee, Y. Kuga, and V. Jandhyala, "Generalized constitutive relations for metamaterials based on the quasi-static lorentz theory," IEEE Transactions on Antennas and Propagation, vol. 51, no. 10, pp. 2550–2557, 2003.
[72] C. R. Simovski and S. He, "Frequency range and explicit expressions for negative permittivity and permeability for an isotropic medium formed by a lattice of perfectly conducting omega particles," Physics Letters A, vol. 311, pp. 254–263, 2003.
[73] J.B. Pendry, "Negative refraction makes a perfect lens", Physical review letters, vol. 85, N°18, pp 3966-3969, 2000.
[74] A. Grbic and G.V. Eleftheriades, "Overcoming the diffraction limit with a planar lefthanded transmission-line lens", Physical review letters, vol. 92, N°11, 2004.
[75] A. Koray, B. Irfan and O. Ekmel, "Subwavelength resolution with a negative-index metamaterial superlens", Applied Physical Letters, vol. 90, 2007.
[76] J.B. Pendry, D. Schurig and R. Smith, "Controlling electromagnetic fields", Science, April 2006.
[77] U. Leonhardt, "Optical conformal mapping", Science, vol. 312, pp 1777-1780, June 2006.
[78] D. Schurig, J.J. Justice, S.A. Cummer, J.B. Pendry, A.F. Starr and D.R. Smith, "Metamaterial electromagnetic cloak at microwave frequencies", Science, vol. 314, pp 977- 980, November 2006.

Chapter II:

Basic physics of LHM

II. Basic physics of LHM

II.1 Continuous medium theory for LHM

When we speak about metamaterials or LHM, we generally refer to a kind of mediums in witch the internal structure interacts with an external wave, in a manner to create "effectives" properties witch are generally unusual or even unobserved in natural materials. For that, and in order to understand the physics behind this type of materials, we over flown the fundamental theoretical physics of wave propagation in a continuous LHM. We start with a brief review of Maxwell's equations, which are the fundamental laws that, together with the theory of electromagnetic behavior of matter, explain on a macroscopic scale the properties of the electromagnetic field, the relationships of this field with its sources, and its interaction with matter, followed by an emphasis on the meaning of various terms associated with negative refraction, starting from a basic definition of the involved physical quantities. Also the effective medium approach is adopted, which means that the LHM is considered as an equivalent homogeneous (or continuous) medium characterized by macroscopic parameters.

II.1.1 Review of Maxwell's equations

The general theory of electromagnetic phenomena is based on Maxwell's equations, which constitute a set of four coupled first-order vector partial-differential equations relating the space and time changes of electric and magnetic fields to their scalar source densities (divergence) and vector source densities. Conceptually, Maxwell's equations describe how electric charges and electric currents act as sources for the electric and magnetic fields. Further, it describes how a time varying electric field generates a time varying magnetic field and vice versa. Of the four equations, two of them, Gauss's law and Gauss's law for magnetism, describe how the fields emanate from charges. (For the magnetic field there is no

magnetic charge and therefore magnetic fields lines neither begin nor end anywhere).

Differential form of Maxwell's equations

$$\nabla \cdot \vec{D}(\vec{r},t) = \rho(\vec{r},t) \quad \text{(Gauss' law)} \tag{II.1}$$

$$\nabla \cdot \vec{B}(\vec{r},t) = 0 \quad \text{(Gauss' law for magnetic fields)} \tag{II.2}$$

$$\nabla \times \vec{E}(\vec{r},t) = -\frac{\partial \vec{B}(\vec{r},t)}{\partial t} \quad \text{(Faraday's law)} \tag{II.3}$$

$$\nabla \times \vec{H}(\vec{r},t) = \vec{J}(\vec{r},t) + \frac{\partial \vec{D}(\vec{r},t)}{\partial t} \quad \text{(Generalized Ampere's law)} \tag{II.4}$$

Integral form of Maxwell's equations

$$\oint_S \vec{D}(\vec{r},t) \cdot d\vec{s} = Q_T(t) \quad \text{(Gauss' law)} \tag{II.5}$$

$$\oint_S \vec{B}(\vec{r},t) \cdot d\vec{s} = 0 \quad \text{(Gauss' law for magnetic fields)} \tag{II.6}$$

$$\oint_\Gamma \vec{E}(\vec{r},t) \cdot d\vec{l} = -\int_S \frac{\partial \vec{B}(\vec{r},t)}{\partial t} \cdot d\vec{s} \quad \text{(Faraday's law)} \tag{II.7}$$

$$\oint_\Gamma \vec{H}(\vec{r},t) \cdot d\vec{l} = \int_S (\vec{J}(\vec{r},t) + \frac{\partial \vec{D}(\vec{r},t)}{\partial t}) \cdot d\vec{s} \quad \text{(Generalized Ampere's law).} \tag{II.8}$$

$\vec{B}$ = Magnetic flux density (T or $Wb\ m^{-2}$)

$\vec{D}$ = Electric flux density (coulombs/square meter; $C\ m^{-2}$)

$\vec{H}$ = Magnetic field intensity (amperes/meter; $A\ m^{-2}$)

ρ = Free electric charge density (coulombs/cubic meter; $C\ m^{-3}$)

Q_T = Net free charge, in coulombs (C), inside any closed surface S

$\vec{J}$ = Free electric current density (amperes/square meter; $A\ m^{-2}$).

The other two equations describe how the fields 'circulate' around their respective sources; the magnetic field 'circulates' around electric currents and time varying electric field in Ampère's law with Maxwell's correction, while the electric field 'circulates' around time varying magnetic fields in Faraday's law.

II.1.2 Time harmonic dependence

In linear media if we consider a particular case in which the sources vary sinusoidally in time, the time-harmonic dependence of the sources gives rise to fields which, once having reached the steady state, also vary sinusoidally in time. However, time-harmonic analysis is important not only because many electromagnetic systems operate with signals that are practically harmonic, but also because arbitrary periodic time functions can be expanded into Fourier series of harmonic sinusoidal components while transient non periodic functions can be expressed as Fourier integrals [79]. Thus, since the Maxwell's equations are linear differential equations, the total fields can be synthesized from its Fourier components. Analytically, Maxwell's equations for time-harmonic fields assuming $e^{j\omega t}$ time dependence are given bellow:

$$\nabla \cdot \vec{D} = \rho \text{ (Gauss' law)} \tag{II.9}$$

$$\nabla \cdot \vec{B} = 0 \text{ (Gauss' law for magnetic field)} \tag{II.10}$$

$$\nabla \cdot \vec{E} = -j\omega \vec{B} \text{ (Faraday's law)} \tag{II.11}$$

$$\nabla \cdot \vec{H} = \vec{J} + j\omega \vec{D} \text{ (Generalized Ampère's law)} \tag{II.12}$$

II.1.3 Constitutive relations

Maxwell's equations, involve only macroscopic electromagnetic fields and, explicitly, only macroscopic densities of free-charge, $\rho(\vec{r},t)$, which are free to move within the medium, giving rise to the free-current densities $\vec{J}(\vec{r},t)$. The effect of the macroscopic charges and current densities bound to the medium's molecules is implicitly included in the auxiliary magnitudes $\vec{D}$ and $\vec{H}$ which are related to the electric and magnetic fields, $\vec{E}$ and $\vec{B}$ by the so-called constitutive equations that describe the behavior of the medium. Interactions between matter and electromagnetic fields are described by constitutive relations. If we assume that these interactions can be essentially represented by dipole moments, a linear material can be described by second order tensors (higher order multipoles are neglected). In this case, the constitutive relations take the general form corresponding to a bianisotropic medium, that is, in the Tellegen form [80].

$$D=\overline{\overline{\varepsilon}} \cdot E + \overline{\overline{\xi}} \cdot H \qquad \text{(II.13)}$$

$$B=\overline{\overline{\zeta}} \cdot E + \overline{\overline{\mu}} \cdot H \qquad \text{(II.14)}$$

The tensors $\overline{\overline{\xi}}$ and $\overline{\overline{\zeta}}$ in (II.13) represent magneto-electric coupling. The media considered here are assumed to be homogeneous, thus the medium parameters do not depend on the position r. We do not consider here spatial dispersion, which means that the four tensors $\overline{\overline{\varepsilon}}$, $\overline{\overline{\mu}}$, $\overline{\overline{\xi}}$ and $\overline{\overline{\zeta}}$ do not contain any spatial differential operators. The material is thus characterized by 36 parameters (complex in general), which are not all independent from each other if reciprocity is assumed [80, 81]. Most of the following developments assume that the medium is isotropic and does not present any magneto-electric coupling. In such a case, the medium is completely

characterized by the scalar permittivity ε and permeability μ, and the constitutive relations reduce to

$$D = \varepsilon E \tag{II.15}$$

$$B = \mu H \tag{II.16}$$

A medium characterized by the constitutive relations (II.15) will be referred to here as a simple medium. The permittivity ε and the permeability μ are complex functions of the frequency, whose real and imaginary parts are separated as follows:

$$\varepsilon = \varepsilon' - j\varepsilon'' \tag{II.17}$$

$$\mu = \mu' - j\mu'' \tag{II.18}$$

Relative values of permittivity and permeability are defined as follows:

$$\varepsilon_r = \frac{\varepsilon}{\varepsilon_0} \tag{II.19}$$

$$\mu_r = \frac{\mu}{\mu_0} \tag{II.20}$$

The real and imaginary parts of ε_r and μ_r (ε_r', ε_r'', μ_r' and μ_r'') are defined in a similar way as in (II.17). In the following developments, a clear distinction is made between results applying to general bianisotropic media, and those only applying to simple media.

II.1.4 Energy densities and power consideration

II.1.4.1 Energy densities in simple media

We summarize here the main considerations regarding the electromagnetic energy density stored in passive continuous simple media, and the impact of these considerations on media with negative parameters.

Let us first recall that the time-averaged energy density w (in [J/m^3]) stored in the electric and magnetic fields in a lossless non-dispersive simple medium is given by [83, 84]

$$\omega = \omega_e + \omega_m = \frac{1}{2}\varepsilon|E|^2 + \frac{1}{2}\mu|H|^2 \qquad \text{(II.21)}$$

As a result, a medium with negative values of ε and/or μ cannot be non-dispersive [as assumed in (II.21), since both the electric and magnetic energy densities w_e and w_m must be positive in a passive medium. Therefore, a passive medium with negative parameters is necessarily dispersive. It is known that defining an electromagnetic energy density as a thermodynamical quantity in terms of the macroscopic medium parameters is only possible in the absence of losses [85,86]. Strictly speaking, this means that such a definition of energy density is not possible in dispersive media, since dispersion usually implies dissipation of energy (by causality). However, if losses are small and can be neglected, the energy density can still be defined and formulated in terms of the macroscopic medium parameters. Considering fields with narrow spectrum (compared to the dispersion at the considered frequencies) around a carrier frequency ω, the time-averaged energy density stored in a dispersive medium with negligible losses can be expressed as [84,85, 87]

$$\omega = \omega_e + \omega_m = \frac{1}{2}\frac{d(\omega\varepsilon)}{d\omega}|E|^2 + \frac{1}{2}\frac{d(\omega\mu)}{d\omega}|H|^2 \quad 2.13 \qquad \text{(II.22)}$$

Both the electric and magnetic energy densities w_e and w_m must be positive for a passive medium, which implies that the permittivity and permeability functions must satisfy the following conditions, also called *entropy conditions* [90]:

$$\frac{d(\omega\varepsilon)}{d\omega} \geq 0 \quad \textit{and} \quad \frac{d(\omega\mu)}{d\omega} \geq 0 \tag{II.23}$$

Furthermore, by combining causality requirement and the entropy conditions, it can be shown that the following relations must also be satisfied [85]:

$$\frac{d\varepsilon_r}{d\omega} \geq 0 \qquad \frac{d(\omega\varepsilon_r)}{d\omega} \geq \varepsilon_r$$

$$\frac{d(\omega\varepsilon_r)}{d\omega} \geq 1 \tag{II.24}$$

$$\frac{d\varepsilon_r}{d\omega} \geq \frac{2(1-\varepsilon_r)}{\omega} \qquad \frac{d(\omega\varepsilon_r)}{d\omega} \geq 2-\varepsilon_r$$

and similarly for the relative permeability μ_r. As a result, the requirement for positive energy density does not preclude the possibility that ε and/or μ be negative, provided that the medium is dispersive and satisfy the conditions (II.23) and (II.24). For materials with considerable losses near the frequency of interest, like near a resonance for instance, it is not possible to define the stored energy in terms of the material permittivity and permeability. Nevertheless, it is explained in [86, 87] that such a quantity can still be defined and calculated from the microstructure of the medium, i.e., from the type of mechanism which is the source of its macroscopic properties. Following this idea, several groups have proposed approaches to determine the energy density in lossy dispersive media by considering the microscopic detail of the material [86, 88, and 89]. In

particular, they showed that material responses usually used to provide negative values of ε and/or μ (such as Drude or Lorentz models) always lead to a positive stored energy density, even in the presence of losses and near resonances. Although these methods are general, it is worth mentioning that a specific derivation of the energy density must be carried out for each considered material.

II.1.4.2 Power consideration

In order to speak about the power consideration in such type of medium, we need first to recall Poynting's vector. It's well known that electric and magnetic fields store energy. Thus, energy can also be carried by the electromagnetic waves which consist of both fields. Consider a plane electromagnetic wave passing through a small volume element of area A and thickness dx, as shown in Figure **II.1**

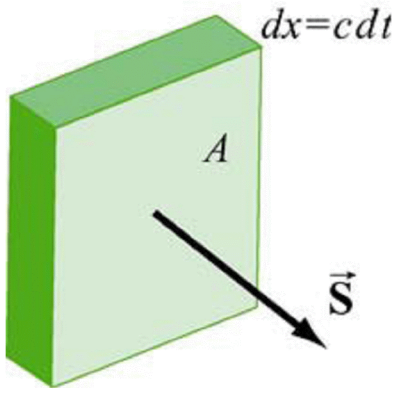

Figure II.1 Electromagnetic wave passing through a volume element

The total energy in the volume element is given by

$$dU = uAdx = \left(u_E + u_B\right)Adx = \frac{1}{2}\left(\varepsilon_0 E^2 + \frac{B^2}{\mu_0}\right)Adx \quad \text{(II.25)}$$

Where

$$u_E = \frac{1}{2}\varepsilon_0 E^2 \qquad , \qquad u_B = \frac{B^2}{2\mu_0}$$

are the energy densities associated with the electric and magnetic fields. Since the electromagnetic wave propagates with the speed of light c, the amount of time it takes for the wave to move through the volume element is dt = dx / c. Thus, one may obtain the rate of change of energy per unit area, denoted with the symbol S, as

$$S = \frac{dU}{Adt} = \frac{c}{2}\left(\varepsilon_0 E^2 + \frac{B^2}{\mu_0}\right) \tag{II.26}$$

Noting that $E = cB$ *and* $c = 1/\sqrt{\mu_0 \varepsilon_0}$, the above expression may be rewritten as

$$S = \frac{c}{2}\left(\varepsilon_0 E^2 + \frac{B^2}{\mu_0}\right) = \frac{cB^2}{\mu_0} = c\varepsilon_0 E^2 = \frac{EB}{\mu_0} \tag{II.27}$$

Where, S is the Poynting vector, which represents the directional energy flux density ($W \cdot m^{-2}$) of an electromagnetic field. It is named after its inventor John Henry Poynting. Mainly, Poynting's vector can be denoted by **S** or **N**, and defined as [91, 92]:

$$\vec{S} = \frac{1}{\mu_0}\vec{E} \times \vec{B} \tag{II.28}$$

II.2. Electrodynamics of Left Handed material

II.2.1. Wave propagation in left-handed media

Over 35 years ago, Veselago [12] suggested that electromagnetic wave propagation in an isotropic medium with negative dielectric permittivity ε and negative magnetic permeability μ can exhibit very unusual properties. Since in such media, the wave vector k, the electric field E, and the magnetic field H of a wave form a left-handed orthogonal set, in contrast to the right-handed orthogonal set in an ordinary medium. Among the many interesting properties of wave propagation in such media are the appearances of a Pointing vector in the direction opposite to the wave vector and a refracted wave on the same side of the surface normal as the incoming wave at a right-handed media/left-handed media interface.

In order to illustrate the unusual and interesting wave propagation in left-handed media, let's first reduce Maxwell equations to the following wave equation [12]:

$$(\nabla^2 - \frac{\eta^2}{C^2}\frac{\partial^2}{\partial t^2})\psi = 0 \qquad \text{(II.29)}$$

Where η is the refractive index, C is the velocity of light in vacuum, and,

$$\frac{\eta^2}{C^2} = \varepsilon\mu \qquad \text{(II.30)}$$

As the squared refractive index η^2 is not affected by a simultaneous change of sign in ε and μ, it is clear that low-loss left-handed media must be transparent. In view of the above equation, we can obtain the impression that solutions to equation (II.29) will remain unchanged after a simultaneous change of the signs of ε and μ.

However, when Maxwell's first-order differential equations are explicitly considered,

$$\nabla \times E = -j\omega\mu H \tag{II.31}$$

$$\nabla \times H = j\omega\varepsilon E \tag{II.32}$$

It is evident that these solutions are quite different. In fact, for plane-wave fields of the type:

$$E = E_0 \exp(-jk \cdot r + j\omega t) \tag{II.33}$$

And

$$H = H_0 \exp(-jk \cdot r + j\omega t) \tag{II.34}$$

The above equations reduce to:

$$k \times E = \omega\mu H \tag{II.35}$$

And

$$k \times H = -\omega\varepsilon E \tag{II.36}$$

Therefore, for positive ε and μ, E, H, and k form a right-handed orthogonal system of vectors. However, if $\varepsilon < 0$ and $\mu < 0$, then the previous equations (II.33) and (II.34) can be rewritten as:

$$k \times E = -\omega|\mu|H \tag{II.37}$$

And

$$k \times H = \omega|\varepsilon|E \tag{II.38}$$

Showing that, E, H, and k can also form a left-handed triplet, as illustrated in Figure II.2. In fact, this is the original reason for the denomination of negative ε and μ media as "left-handed" media.

The main physical implication of the aforementioned analysis is the backward-wave propagation, and the direction of the time-averaged flux of energy, which is determined by the real part of the Poynting vector S,

$$S = \frac{1}{2} E \times H^{*} \qquad \text{(II.39)}$$

Where, the vector S is unaffected by a simultaneous change of the sign of both ε and μ. Thus, E, H, and S still form a right-handed triplet in a left-handed medium. Therefore, in such media, energy and wave-fronts travel in opposite directions. Backward-wave propagation is a well-known phenomenon that may appear in non-uniform waveguides [95, 96]. However, backward-wave propagation in unbounded homogeneous isotropic media seems to be a unique property of left-handed media. And, most of the surprising unique electromagnetic properties of these media arise from this backward propagation property.

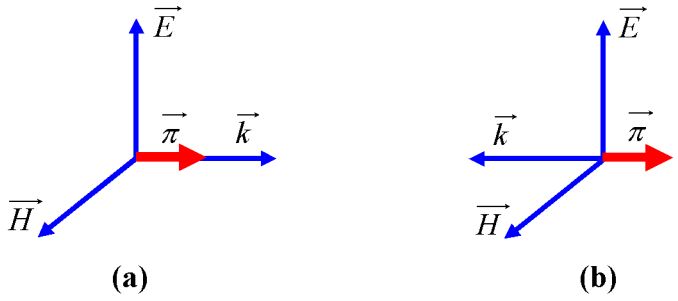

Figure II.2: *$\vec{E}, \vec{H}, \vec{k}$, and $\vec{\pi}$ vectors system for an electromagnetic plan wave in: a) ordinary medium, b) left hand medium.*

So far, we have neglected losses. However, losses are unavoidable in any practical material. The effect of losses in plane-wave propagation will be considered. Let's consider a finite region filled by a homogeneous left-handed medium. In the steady state, and provided

there are no sources inside the region, there must be some power flow into the region in order to compensate for losses. Thus, from the well-known complex Poynting theorem [97],

$$\nabla \cdot \left\{ E \times H^{*} \right\} \;=\; j\omega \left(E \cdot D^{*} - B \cdot H^{*} \right) \qquad \text{(II.40)}$$

It follows that,

$$\mathrm{Re}\left\{ \oint E \times H^{*} \cdot \hat{n}\, dS \right\} \;=\; \omega\, \mathrm{Im}\left\{ \iint \left(\mu \left| H \right|^{2} - \varepsilon^{*} \left| E \right|^{2} \right) dV \right\} < 0. \qquad \text{(II.41)}$$

Where, the integration is carried out over the aforementioned region. As a result,

$$\mathrm{Im}(\varepsilon) < 0 \qquad \text{and} \qquad \mathrm{Im}(\mu) < 0. \qquad \text{(II.42)}$$

We consider now a plane wave with square wave-number $k^2 = \omega^2 \mu\varepsilon$, Propagating in a lossy left-handed medium with $\mathrm{Re}(\varepsilon) < 0$ and $\mathrm{Re}(\mu) < 0$. From expression (1.11), it follows that $\mathrm{Im}(k^2) < 0$. Therefore,

$$\{ \mathrm{Re}(k) > 0 \; \textit{and} \; \mathrm{Im}(k) > 0 \} \;\; \textit{or} \;\; \{ \mathrm{Re}(k) < 0 \; \textit{and} \; \mathrm{Im}(k) < 0 \}. \qquad \text{(II.43)}$$

So, waves grow in the direction of propagation of the wave-fronts. This fact is in agreement with the aforementioned backward-wave propagation.

II.2.2. Energy density and group velocity

If negative values for ε and μ are introduced in the usual expression for the time averaged density of energy in transparent non-dispersive media, U_{nd}, given by:

$$U_{nd} = \frac{1}{4}\left\{\varepsilon|E|^2 + \mu|H|^2\right\} \quad \text{(II.44)}$$

They produce the non-physical result of a negative density of energy. However, as is well known, any physical media other than vacuum must be dispersive [93], equation (II.44) being an approximation only valid for very weakly dispersive media. The correct expression for a quasi-monochromatic wave-packet travelling in a dispersive media is [94].

$$U = \frac{1}{4}\left\{\frac{\partial(\omega\varepsilon)}{\partial\omega}|E|^2 + \frac{\partial(\omega\mu)}{\partial\omega}|H|^2\right\} \quad \text{(II.45)}$$

Here, the derivatives are evaluated at the central frequency of the wave-packet. Thus, the physical requirement of positive energy density implies that

$$\frac{\partial(\omega\varepsilon)}{\partial\omega} > 0 \quad \text{and} \quad \frac{\partial(\omega\mu)}{\partial\omega} > 0. \quad \text{(II.46)}$$

Which are compatible with $\varepsilon < 0$ and $\mu < 0$ provided $\partial\varepsilon/\partial\omega > |\varepsilon|/\omega$ and $\partial\mu/\partial\omega > |\mu|/\omega$. Therefore, physical left-handed media must be highly dispersive. This fact is in agreement with the low-loss Drude–Lorentz model for ε and μ, which predicts negative values for ε and/or μ in the highly dispersive regions just above the resonances [12]. Finally, it must be mentioned that the usual interpretation of the imaginary part of the complex Poynting theorem, which relates the flux of reactive power through a closed surface with the difference between electric and magnetic energies inside this surface [14], is not applicable to highly dispersive media, where equation (II.45) holds instead of (II.44). Thus, this interpretation is also not

valid for left-handed media. Backward-wave propagation implies opposite signs between phase and group velocities. In fact;

$$\frac{\partial k^2}{\partial \omega} = 2k\frac{\partial k}{\partial \omega} \equiv 2\frac{\omega}{\upsilon_p \upsilon_g}. \qquad \text{(II.47)}$$

Where $\upsilon_p = \omega/k$ and $\upsilon_g = \partial\omega/\partial k$ are the phase and group velocities, respectively. In addition, from $k^2 = \omega^2 \varepsilon\mu$ and equation (II.46),

$$\frac{\partial k^2}{\partial \omega} = \omega\varepsilon\frac{\partial(\omega\mu)}{\partial \omega} + \omega\mu\frac{\partial(\omega\varepsilon)}{\partial \omega} < 0. \qquad \text{(II.48)}$$

Finally, from equations (II.47) and (II.48)

$$\upsilon_p \upsilon_g < 0. \qquad \text{(II.49)}$$

This property implies that wave-packets and wave-fronts travel in opposite directions, and can be considered an additional proof of backward-wave propagation in physical left-handed media.

II.2.3. Waves through left-handed slabs

Here, we will analyze the transmission and guidance of electromagnetic waves through left-handed slabs simply by using the transverse transmission matrix technique, which can be applied to the analysis of transmission and guidance of waves through multilayered structures.

II.2 3.1 Transmission and Reflection Coefficients

The transmission matrix for a left-handed slab of width d is obtained by simply cascading the transmission matrices for each interface and for the left-handed medium in between,

$$\begin{pmatrix} E_1^+ \\ E_1^- \end{pmatrix} = \frac{1}{4Z_2 Z_3} \begin{pmatrix} Z_2 + Z_1 & Z_2 - Z_1 \\ Z_2 - Z_1 & Z_2 + Z_1 \end{pmatrix} \cdot \begin{pmatrix} e^{jk_{x,2}d} & 0 \\ 0 & e^{-jk_{x,2}d} \end{pmatrix} \cdot \begin{pmatrix} Z_3 + Z_2 & Z_3 - Z_2 \\ Z_3 - Z_2 & Z_3 + Z_2 \end{pmatrix} \cdot \begin{pmatrix} E_3^+ \\ E_3^- \end{pmatrix} \tag{II.50}$$

Where, we consider the s-polarized waves. In equation (II.50), $k_{x,2} = -\sqrt{\omega^2 \mu_2 \varepsilon_2 - k_z^2} < 0$ is the x-component of the propagation constant for positive waves inside the slab, and subscripts 1, 2, and 3 stand for the left-handed medium (2) and for the media at the left- and the right-hand sides of the slab (1 and 3). Z_i are the wave impedances $Z_i \equiv E_i^+ / H_{z,i}^+ = \omega \mu_i / k_{x,i}$, and electric fields are evaluated just on the left $\left(E_1^{\pm}\right)$ and on the right $\left(E_3^{\pm}\right)$ interfaces of the slab. All waves inside and outside the slab have a common propagation vector, k_z parallel to the slab interface, which determines the angle of incidence $\sin\theta_i = k_z / k_1$.

In the following, media 1 and 3 will be considered identical, so that $Z_3 = Z_1$. In this case, the transmission and reflection coefficients, $t = 2Z_2/(Z_2 + Z_1)$ and $r = (Z_2 - Z_1)/(Z_2 + Z_1)$, which are obtained from equation (II.50) by taking $E_1^+ = 1$, $E_1^- = r$, $E_3^+ = t, E_3^- = 0$. After a straightforward calculation, the following expressions arise:

$$t = \frac{2Z_1 Z_2}{j\left(Z_1^2 + Z_2^2\right)\sin\left(k_{x,2}d\right) + 2Z_1 Z_2 \cos\left(k_{x,2}d\right)} \tag{II.51}$$

And

$$r = \frac{Z_2^2 - Z_1^2}{Z_2^2 + Z_1^2 - 2jZ_1 Z_2 \cot\left(k_{x,2}d\right)} \tag{II.52}$$

With $k_{x,2} < 0$, so the phase advance through the slab is positive for small values of $k_{x,2}d$, which corresponds to the propagation of a backward wave inside the slab.

II.2.3.2 Guided Waves

Waves guided along the slab correspond to the poles of the reflection coefficient (II.52) that may appear for imaginary values of $k_{x,1}$. In such cases, according to the previous definitions, $k_{x,1} = -j\alpha_1$, with $\alpha_1 = \sqrt{k_z^2 - \omega^2 \varepsilon_1 \mu_1} > 0$. so, the surface waves correspond to the solutions of the implicit equation.

$$Z_2^2 + Z_1^2 - 2jZ_1 Z_2 \cot(k_{x,2}d) = 0, \text{ with } Z_1 = j\frac{\omega\mu_1}{\alpha_1} \qquad \text{(II.53)}$$

With the additional condition $k_z > k_1$, so that electromagnetic energy decays at both sides of the slab. Two cases may arise in equation (II.53), depending on whether $k_{x,2}$ is real or imaginary. If $k_z < k_2 = \omega\sqrt{\varepsilon_2 \mu_2}$, $k_{x,2}$ is real and fields inside the slab have a trigonometric dependence, so that they are volume waves. In that case equation (II.53) reduces to

$$\frac{\mu_2 \alpha_1}{\mu_1 k_{x,2}} - \frac{\mu_1 k_{x,2}}{\mu_2 \alpha_1} + 2\cot(k_{x,2}d) = 0 \qquad \text{(II.54)}$$

Taking in account the trigonometric relation $2\cot(2x) = \cot x - \tan x$, the previous equation (II.54), can be written as

$$\left(\frac{\mu_2 \alpha_1}{\mu_1 k_{x,2}} \tan(k_{x,2}d/2) + 1\right)\left(\frac{\mu_1 k_{x,2}}{\mu_2 \alpha_1} \tan(k_{x,2}d/2) - 1\right) = 0 \qquad \text{(II.55)}$$

Equation (II.55) is the implicit dispersion relation for the guided volume wave. In this equation, the two branches, corresponding to symmetric and anti-symmetric modes, are explicitly shown. As can be seen from the above dispersion relations, volume waves in the left-handed slabs do not substantially differ from guided volume waves in ordinary dielectric slabs [105]; waves inside the slab can be seen as the composition of two propagating TEM waves, which suffer total reflection at the slab interfaces. Therefore, energy flow is backward inside the left-handed slab and forward outside the slab, the whole wave being forward or backward depending on the structural parameters of the waveguide.

If $k_z > k_2 = \omega\sqrt{\varepsilon_2 \mu_2}$, the electromagnetic fields show an exponential decay inside the slab, and the guided waves become surface waves. They correspond to the coupling between the surface waves generated at each slab interface. Therefore, when $d \to \infty$, these waves should converge to the surface waves. Where both Z_1 and Z_2 are imaginary for these surface waves, and $\cot(k_{x,2} d)$ becomes a hyperbolic function. Thus, equation (II.53) reduces to

$$\frac{\mu_2 \alpha_1}{\mu_1 \alpha_2} + \frac{\mu_1 \alpha_2}{\mu_2 \alpha_1} + 2\coth(\alpha_2 d) = 0 \qquad \text{(II.56)}$$

By taking in account the following trigonometric relation $2\coth(2x) = \coth x + \tanh x$, this equation can be written as

$$\left(\frac{\mu_2 \alpha_1}{\mu_1 \alpha_2}\tanh(\alpha_2 d/2) + 1\right)\left(\frac{\mu_1 \alpha_2}{\mu_2 \alpha_1}\tanh(\alpha_2 d/2) + 1\right) = 0 \qquad \text{(II.57)}$$

Here, the two branches, corresponding to symmetric and anti-symmetric modes, can be appreciated. The specific dependence of

k_z on frequency will depend on the specific dependence of ε and μ on ω.

II.2.3.3 Backward Leaky and Complex Waves

Is known that, in any open guiding system, most of the electromagnetic modes guided by a left-handed slab leak power to the surrounding space [96,105]. These waves correspond to the poles of the reflection coefficient calculated in (II.52) that may appear for complex values of $k_{x,1}$.

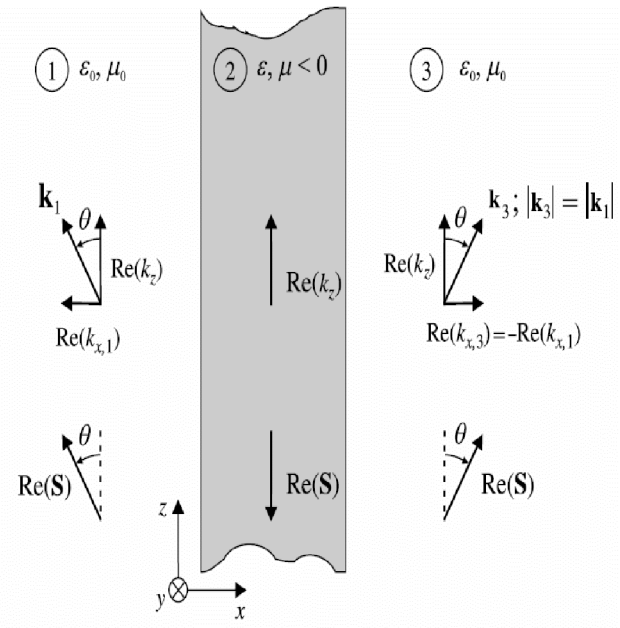

FIGURE II.3: Illustration of the wave-vectors and power flows in a backward leaky mode guided by a left-handed slab. $\mathrm{Re}(k_z)$ ***is the mode phase vector, and Re(S) shows the power flux inside and outside the slab. The angle of leakage is determined by*** $\cos\theta = \mathrm{Re}(k_z)/k_1$ **.**

Now let as consider, without loss of generality, a leaky wave with field dependence $\exp(-jk_z Z + j\omega t)$, and $\mathrm{Re}(k_z) > 0$. The wave-number of such a leaky mode should satisfy $\mathrm{Re}(k_z) < k_1 \equiv \omega\sqrt{\varepsilon_1 \mu_1}$, so that the power leaks at an angle $\cos\theta = \mathrm{Re}(k_z)/k_1$ from the slab (Figure. II.3).

Inside the left-handed slab, power flow is backward, but in the surrounding medium, outside the slab, power flows in the forward direction. Therefore, for the analyzed leaky mode, power always leaks backward with regard to the main stream of guided power, inside the slab. For this reason, such leaky modes have been called backward leaky modes [119].

Physical leaky modes can be excited by sources at the onset of a semi-infinite guiding system. In such a configuration, power is guided along the waveguide, from the source to its end. Considering Figure II.3, this means that the source must be located at the top of the figure. Consequently, it must be that $\mathrm{Im}(k_z) > 0$, so that the leaky wave attenuates towards the lower end of the slab. On both sides of the slab the field dependence must be of the kind $\exp(\mp jk_x x - k_z z + j\omega t)$. On the other hand, boundary conditions impose that $k_z^2 + k_x^2 = k_1^2$, so that, for small attenuating constants,

$$k_1^2 \approx \{\mathrm{Re}(k_z)\}^2 + \{\mathrm{Re}(k_x)\}^2 \qquad \text{(II.58)}$$

$$\mathrm{Re}(k_z)\mathrm{Im}(k_z) + \mathrm{Re}(k_x)\mathrm{Im}(k_x) = 0 \qquad \text{(II.59)}$$

The first equation defines the leakage angle, and the second one determines the sign of $\mathrm{Im}(k_x)$ as follows: at the left-hand side of the slab, power must flow to the left, so that $\mathrm{Re}(k_z) > 0$ and $\mathrm{Re}(k_x) < 0$. Moreover, $\mathrm{Im}(k_x)$>0, as has already been mentioned. Therefore, it must be that $\mathrm{Im}(k_x) > 0$, so that backward leaky waves are attenuated in the transverse direction. This result is somewhat unexpected, as leaky modes in ordinary guiding systems are usually unbounded modes, whose amplitude grows to infinity in the transverse direction [105,120]. This unusual behaviour of leaky modes in left-handed slabs is a direct consequence of the reported backward leakage of power [119], and recalls the behaviour of the

complex modes that may appear in some very inhomogeneous wave-guiding systems [96]. Backward leakage of power in a circuit is analogous to an open left-handed waveguide [121].

II.2.4 Losses in Metamaterials

Even if Metamaterials are enabling an important number of exciting applications, they are exhibiting some limitations due to the occurrence of losses. In present-day metamaterials losses have two primary components: radiation and dissipation, with the first one is far exceeding the second one. Radiation losses [122–124] originate from the part of the incident wave that is temporarily communicated on each meta-atom, but then reradiated or scattered off by the resultant oscillating charges and currents in a direction not necessarily the same as the one followed by the primary wave. This part of the incident wave that is reradiated/scattered away from the primary transmitted wave counts as a source of loss, affecting negatively the loss-behaviour of the metamaterial. However, the dissipative or Ohmic losses arise from intrinsic metallic/dissipative losses, which are associated with photon absorption. Unfortunately, it turns out that for metamaterials, radiation losses are much greater than their ohmic counterparts, even in the optical regime [9]. Furthermore, even when used metamaterial is made of purely dielectric, the obtained magnetic susceptibilities do still have a relatively large imaginary part, leading to "figures-of-merit" that remain at the order of only 1–10 [125] similar to their metallic counterparts.

However, a solution to this problem in a regime where a metamaterial preserves its negative parameters has remained elusive. If such a solution could be found, then up to the THz regime we would be able to harness practically "lossless" in negative-parameters metamaterials with dramatically enhanced figures-of-merit, since metals in these regimes are almost prefect conductors, expelling electromagnetic fields from their interior.

To date, a number of diverse strategies have been proposed toward overcoming the issue of high losses in metamaterials.[126] A first approach relies on the use of stimulated emission to compensate the overall metamaterial losses[127]. This approach is very promising and it has, in fact, been theoretically predicted that it can lead to zero-loss metamaterials, even over a broad yet finite bandwidth [128]. However, it may not always be possible to find a suitable medium to provide the necessary gain at a desired frequency regime. Further, such a strategy is not particularly well suited for confronting the radiation losses of metamaterial that has a geometric/design origin, rather than the Ohmic ones, and if deployed it may result in increasing the radiation losses although the Ohmic or overall losses are, indeed, expected to decrease or be completely eliminated. It is also to be noted that use of stimulated emission for mitigating losses gives invariably rise to amplify spontaneous emission noise, which deteriorates the signal-to-noise ratio (SNR) an extremely important figure-of-merit for optical communication systems, for instance.

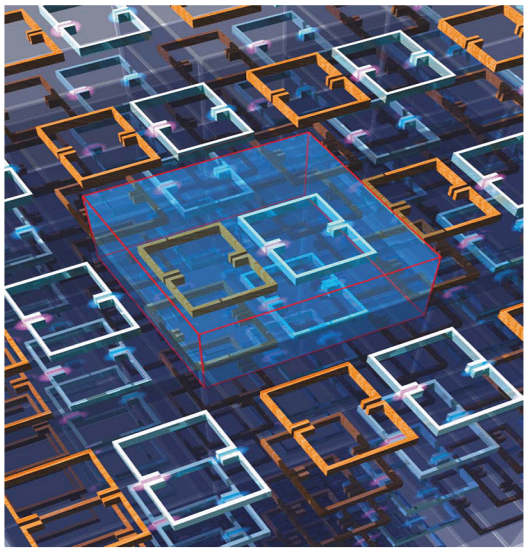

Figure II.4: Obtaining a lossless negative-magnetic metamaterial at GHz frequencies [129]

A second interesting strategy makes use of negatively reflecting/refractive interfaces to reproduce the features of bulk negative-index metamaterials [130]. Upon being negatively refracted at the engineered interfaces, light is allowed to propagate through lossless dielectric materials, such as air, thereby avoiding high-attenuation regions. This scheme relies on the use of nonlinear media and therefore requires intense incident light, which may give rise to nonlinear absorption effects, such as two-photon absorption and amplified spontaneous emission.

More recently, a series of works have deployed concepts Figure 1 such as electromagnetically induced (EIT) or coupled-resonator induced (CRIT) transparency [131] to overcome metamaterial losses.[132]. Unfortunately, even if, with these strategies radiation losses are substantially suppressed, these solutions are only performed in a regime where the metamaterial's effective parameters (permittivity, permeability, refractive index, n) do *not* preserve the negativity in the responses of their real parts [133]. Basically, this is because the adherence of these schemes to a strict EIT/CRIT, results in the radiation losses being reduced [134] in a regime where the real parts of the medium's constitutive parameters are invariably non-negative similarly to EIT or CRIT. Thus, although such diamagnetic metamaterials are expected to find interesting applications in their own right, like in enabling enhanced bio-molecular sensing[135] or diamagnetic levitation, unfortunately they cannot be used in a multitude of exciting and intriguing negative-parameters based metamaterial applications. Note that obtaining low-loss electromagnetic parameters with negative real parts has the important additional advantage that we can also eliminate reflection losses, since with such media one can achieve a perfect impedance matching to, both, positive-index bulk media [136] and waveguides [137].

II.3 Left Handed Material effects

II.3.1 Negative refraction

Index of refraction, or refractive index, is a fundamental constant that describe the interaction between light and material. Index of refraction quantifies, to determine physically how fast light travels in a material and how strongly a material reflects light on its surface, comparing to the vacuum as the reference medium, with unity index of refraction. This index of reflection specific to each material is frequency dependent parameter, it actually results from the interaction electrons and atoms in the material with the electromagnetic field of light, generally all naturally occur ring materials are known to have indexes of refraction that are positive and greater than 1. In 1968, Veselago [12] theorized that a material with negative permittivity and permeability can exist and should have a negative index of refraction; such material should exhibit a reverse Doppler effect, a reverse Cherenkov effect, and reversed focusing properties in lenses. Negative-index materials (NIMs), however, remained as purely theoretical imagination for more than 30 years, until Pendry's [17] seminal paper in 2000 ignited major research activities worldwide. In which he predicted the possibility of the possibility of the realisation of superlens that could focus light to a very small spot. In the present, thanks to the great advances in nanotechnology, it is possible now to design and fabricate artificial structures that can exhibit a negative index of refraction, opening the horizon to a new generation of applications and devices.

Index of refraction n is basically defined as the ratio of the speed of light in a vacuum c to that in the material v:

$$\eta = \frac{C}{\nu} \tag{II.60}$$

Constructing the wave equation from Maxwell's equations, one can relate the index of refraction to the relative permittivity ε and relative permeability μ of the material,

$$\eta^2 = \varepsilon \mu \tag{II.61}$$

Where the relative permittivity ε and relative permeability μ are defined by the constitutive equations,

$$D = \varepsilon \varepsilon_0 E \tag{II.62}$$

And

$$B = \mu \mu_0 H \tag{II.63}$$

Where, **D** is the electric displacement field, **E** is the electric field, **B** is the magnetic field, and **H** is the magnetizing field.

Naturally occurring materials have values of ε and μ that are equal to or greater than 1, so, it is generally assumed that the index of refraction is found by taking the positive root of εμ; that is,

$$\eta = \sqrt{\varepsilon \mu} \tag{II.64}$$

An important exception to this general rule is metals. Because of the large density of free electrons, a metal exhibits negative ε and positive μ in the visible and lower frequency ranges of the electromagnetic spectrum when the frequency is below the metal's characteristic plasma frequency. This results in an imaginary value of *n*, leading to exponentially decaying waves instead of propagating waves. An exponentially decaying wave is called an evanescent wave, and this explains why most metals are highly reflecting, rather than transparent.

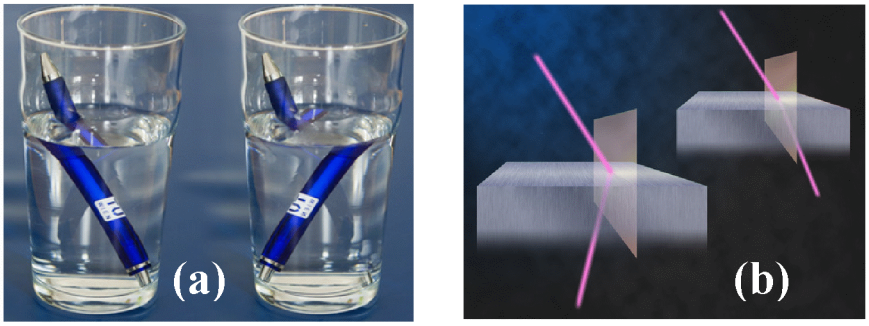

Figure II.5: Bending light the 'wrong' way, a) This is what a liquid with a negative refractive index could look like (right), as opposed to regular water (left). b) The beam of light enters the metal and is refracted into the opposite direction (left) compared to the usual behavior of light in materials (right).

Negative permittivity requires electric resonance in the material, and negative permeability requires strong magnetic resonance when both ε and μ are negative, the index of refraction is real, so that the material should support propagating waves. In nature is easy to find material with negative permittivity like metals at frequencies below their plasma frequencies and materials with strong phonon resonance near their phonon frequencies. However, Negative permeability, which requires a strong magnetic resonance in the material, is much more difficult to find in nature, especially at frequencies greater than the gigahertz range, and thus requires artificial structures that produce a magnetic response at high frequencies.

II.3.2 Double negative index (DNG) material

Mathematically speaking, the simplest way to produce LH behaviour in a medium is to have both $\varepsilon < 0$ and $\mu < 0$, as pointed out by Pafomov [6]. Double negativity, by requiring energy to flow away from the interface and into the medium, also naturally leads to a negative refractive index n, thus facilitating negative refraction at the interface, as discussed by Veselago. However, $\varepsilon < 0$ is only known

to occur near the resonant frequency of a polariton (e.g., plasmon, optical phonon, exciton). Without damping and spatial dispersion, the spectral region of $\varepsilon < 0$ is totally reflective for materials with $\mu > 0$. For $\mu < 0$ known to exist near magnetic resonances, but is not known to occur in the same material and the same frequency region where $\varepsilon < 0$ is found. Indeed, if in the same material for the same spectral region one could simultaneously have $\varepsilon < 0$ and $\mu < 0$ yet without any dissipation, and the material would then turn transparent. In recent years, metamaterials have been developed to extend material response and thus allow effective ε and μ to be negative in an overlapped frequency region. The hybridization of the metamaterials with, respectively, εeff < 0 and μeff < 0 has made it possible to realize double negativity or $n$eff < 0 in a small microwave-frequency window, and to demonstrate negative refraction successfully. However, damping or dissipation near the resonant frequency still remains a major obstacle for practical applications of metamaterials. There is a fundamental challenge to find any natural material with non-unity μ at optical frequencies or higher, because of the ambiguity in defying μ at such frequencies [18,24]. Thus, the double-negativity scheme essentially faces the same challenge that the spatial-dispersion scheme does in realizing the dream of making a perfect lens.

II.3.3 Other effect in left-handed media

Backward-wave propagation in left-handed media also has implications in other well known physical effects correlated to electromagnetic wave propagation. In the following we consider some of them.

II.3.3.1 Inverse Doppler Effect

When a moving receiver detects the radiation coming from a source at rest in a uniform medium, the detected frequency of the radiation depends on the relative velocity of the emitter and the receiver. This

is the well-known Doppler Effect. If this relative velocity is much smaller than the velocity of light, a non-relativistic analysis suffices to describe such an effect. The qualitative analysis is quite simple for ordinary ($n > 0$) media. However, if the receiver moves towards the source, wave-fronts and receiver move in opposite directions. Then, the frequency seen by the receiver will be higher than the frequency measured by an observer at rest. On the other hand, if the medium is a left-handed material, wave propagation is backward, and wave-fronts move towards the source.
Consequently, both the receiver and the wave-fronts move in the same direction, and the frequency measured at the receiver is smaller than the frequency measured by an observer at rest.

A simple calculation shows that the aforementioned frequency shifts are given by

$$\Delta\omega = \pm \omega_0 \frac{\upsilon}{\upsilon_p} \qquad \text{(II.65)}$$

Where ω_0 is the frequency of the radiation emitted by the source, υ is the velocity at which the receiver moves towards the source, υ_p the phase velocity of light in the medium, and the $\pm$ sign applies to ordinary/left-handed media. Equation (II.65) can be written in a more compact form as [6]

$$\Delta\omega = \omega_0 \frac{\eta\upsilon}{C} \qquad \text{(II.66)}$$

Here, η is the refractive index of the medium and C the velocity of light in free pace. In equation (II.66), $\Delta\omega$ is the difference between the frequency detected at the receiver and the frequency of oscillation of the source. For n > 0, the frequency shift becomes negative for positive υ because of the receiver is moving towards the source, as it was qualitatively shown at the beginning of this section.

Interestingly, from equation (II.48), it directly follows that $d|k|/d\omega < 0$ in left-handed media. Consequently, a negative frequency shift results in an increase of $|k|$. And then, a shift towards shorter wavelengths is seen when the receiver approaches the source, both in ordinary and left-handed media.

II.3.3.2 Backward Cherenkov radiation

Cherenkov radiation occurs when a charged particle enters an ordinary medium at a velocity higher than the velocity of light in such a medium. If the deceleration of this particle is not too high, its velocity can be considered approximately constant over many wave periods. Then, as is illustrated in Figure II.6 (a), the spherical wave-fronts radiated by this particle become delayed with regard to the particle motion, thus giving rise to a shock wave, which travels forward, making an angle u with the particle velocity. This angle is given by

$$\cos\theta = \frac{C}{\eta\upsilon} \tag{II.67}$$

In this equation, C/η is the velocity of light in the medium and υ is the velocity of the particle. If the medium has a negative refractive index $\eta < 0$, the wave propagation is backward, and the spherical wave-fronts corresponding to each frequency harmonic of the radiation move inwards to the source, at a velocity $C/|\mu(\omega)|$. Then, each wave-front collapses at the advanced position of the particle shown in Figure II.6 (b).

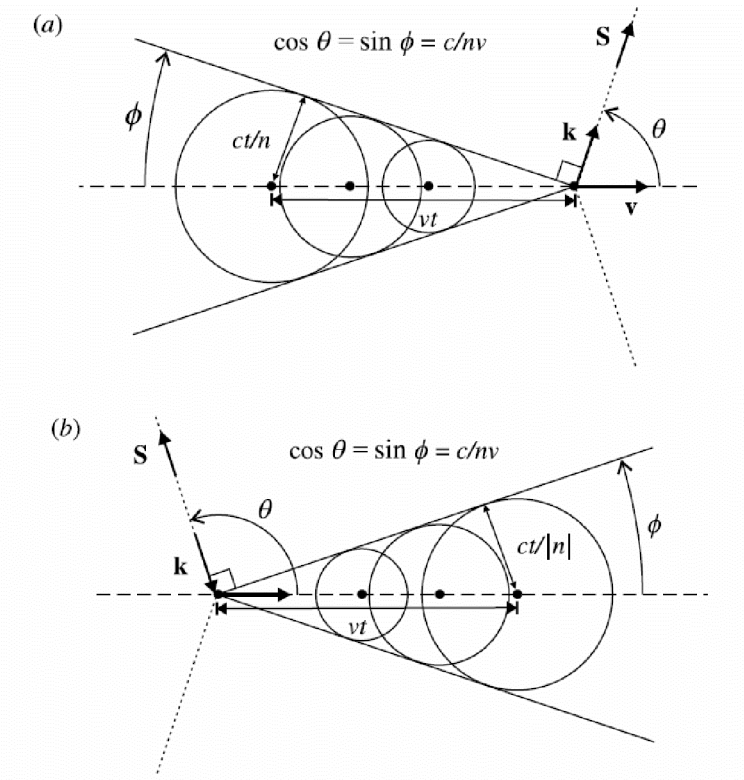

Figure II.6: Illustration of the formation of Cherenkov shock waves: (a) in an ordinary medium, and (b) in a left-handed medium. In (a) the spherical wave-fronts move outwards from the source at a velocity C/η***. In (b) the spherical wave-fronts move inwards to the source at a velocity*** $C/|\eta|$***.***

Therefore, the resulting shock wave travels backward at an obtuse angle from the particle motion. This angle is still given by equation (II.67) [6], as is illustrated in the figure.

In practice, any left-handed medium must be highly dispersive, the left-handed behavior being restricted to some frequency range. Because the particle radiates at all frequencies, the Cerenkov radiation spectra must show wave-fronts moving in both forward and backward directions. In practice, any left-handed medium must be highly dispersive, the left-handed behavior being restricted to some frequency range. Because the particle radiates at all frequencies, the Cerenkov radiation spectra must show wave-fronts moving in both forward and backward directions [98].

II.3.3.3 Negative Goos–Hänchen Shift

When a plane wave is incident from a medium of refractive index $\eta = \eta_1$ onto the plane interface of another medium with $\eta = \eta_2$, where $|\eta_2| < |\eta_1|$ there is a critical angle $\sin\theta = |\eta_2/\eta_1|$, beyond which total reflection onto medium 1 occurs. However, fields penetrate into medium 2 by a small distance, forming a non-uniform plane wave that is evanescent in the direction normal to the interface and propagative along the interface. Power associated with this plane wave flows parallel to the interface in the forward direction for ordinary media and in the backward direction for left-handed media. Thus, when a beam of finite extent is incident from medium 1 to medium 2, the reflected beam experiences a finite lateral shift Δ, as a consequence of the aforementioned energy flow in medium 2. This effect is illustrated in Figure II.7. As energy flow is parallel to wave-front propagation, the Goos–Hänchen shift must be positive in ordinary media. However, if medium 2 is a left-handed medium, energy flow and wave-front propagation are anti-parallel. Therefore, the Goos–Hänchen shift must be negative in such media, as is shown in Figure II.7 (b).

We can calculate the Goos–Hänchen shift Δ by expanding the incident beam in plane waves, and studying the reflection of these waves at the interface. If the angular spectrum of the beam is not too wide, and the angle of incidence is sufficiently away from the critical and grazing angles, the Goos–Hänchen shift is given by [99]

$$\Delta = \frac{\partial \Phi_r}{\partial k_{\parallel}} \tag{II.68}$$

Where Φ_r is the phase of the reflection coefficient and k is the component of the wave-vector parallel to the interface (for lossless left-handed media $|r| = 1$, and $\Phi_r = -j \ln r$). The Goos–Hänchen

effect in left-handed media has been analyzed in detail in [100–103]. In [104], giant Goos–Hänchen shifts due to the excitation of surface waves have been reported for stratified media including left-handed layers. In all these calculations, the sign of the Goos–Hänchen shift agrees with the predictions of Figure II.7.

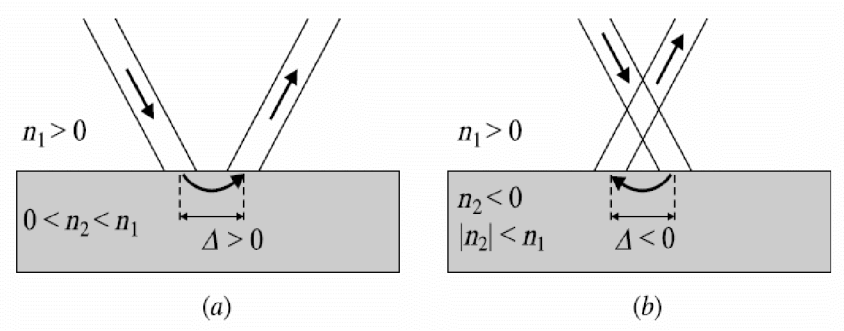

Figure II.7: Illustration of the Goos–Hänchen effect in (a) ordinary media and (b) left-handed media

II.4 Conclusion

This chapter was dedicated to a detailed recall on the physics behind the metamaterial theory. As the metamaterials are a type of mediums in which the internal structure interact with an external wave (electromagnetic wave EM), the first part was about the continuous medium theory which describes this type of interactions. While the second one, was devoted to the electrodynamics of metamaterials, and how the EM waves are affected by type of medium. The last part was a general description of the effects produced by this kind of materials. The next chapter will be consecrated to the practical aspect of metamaterials, with a focus on their tenability systems.

Bibliography

[79] R. Gómez Martín, "electromagnetic field theory for physicists and engineer: fundamentals and application", page 19.
[80] W. S. Weiglhofer, "Constitutive characterization of simple and complex mediums," in Introduction to Complex Mediums for Optics and Electromagnetics, W. S. Weiglhofer and A. Lakhtakia, Eds. Bellingham: SPIE - The International Society for Optical Engineering, 2003, pp. 27–61.
[81] C. M. Krowne, "Electromagnetic theorems for complex anisotropic media," IEEE Transactions on Antennas and Propagation, vol. AP-32, no. 11, pp. 1224–1230, 1984.
[82] A. Lakhtakia and W. S. Weiglhofer, "Constraint on linear, homogeneous, constitutive relations," Physical Review E, vol. 50, no. 6, pp. 5017–5019, 1994.
[83] C. A. Balanis, Advanced Engineering Electromagnetics. John Wiley & Sons, 1989.
[84] J. D. Jackson, Classical Electrodynamics, 3rd ed. New-York: John Wiley & Sons, 1999.
[85] L. Landau and E. Lifchitz, Electrodynamique des milieux continus, ser. Physique theorique. Moscou: Editions MIR, 1969.
[86] S. A. Tretyakov, "Electromganetic field energy density in artificial microwave materials with strong dispersion and loss," physics Letters A, vol. 343, no. 1-3, pp. 231–237, 2005.
[87] A. Tonning, "Energy density in continuous electromagnetic media," IRE Transactions on Antennas and Propagation, vol. 8, no. 4, pp. 428–434, 1960.
[88] T. J. Cui and J. A. Kong, "Time-domain electromagnetic energy in a frequency-dispersive left-handed medium," Physical Review B, vol. 70, p. 205103, 2004.
[89] A. D. Boardman and K. Marinov, "Electromagnetic energy in a dispersive metamaterial," physical Review B, vol. 73, p. 165110, 2006.
[90] C. Caloz and T. Itoh, Electromagnetic Metamaterials: Transmission Line Theory and Microwave Applications. Wiley-Interscience and IEEE press, 2006.
[91] Electromagnetism (2nd Edition), I.S. Grant, W.R. Phillips, Manchester Physics, John Wiley & Sons, 2008, ISBN 978-0471927129
[92] Introduction to Electrodynamics (3rd Edition), D.J. Griffiths, Pearson Education, Dorling Kindersley, 2007, ISBN 81-7758-293-3

[93] J. D. Jackson Classical Electrodynamics. Wiley, New York, 1999 (3rd ed.).
[94] L. D. Landau, E. M. Lifshitz, and L. P. Pitaevskii Electrodynamics of Continuous Media. Pergamon, New York, 1984.

[95] S. Ramo, J. R. Whinnery, and T. Van-Duzer Fields and Waves in Communication Electronics. John Wiley, New York, 1965.
[96] M. Mrozowski Guided Electromagnetic Waves. Properties and Analysis. Research StudiesPress (Taunton, UK) and John Wiley (New York), 1997.
[97] R. F. Harrington "Time-harmonic Electromagnetic Fields". McGraw-Hill, New York, 1961.
[98] J. Lu, T. M. Gregorczyc, Y. Zhang, J. Pacheco, B. Wu, J. A. Kong, and . Chen "Cerenkov radiation in materials with negative permittivity and permeability." Opt. Express, vol. 11, pp. 723–734, 2003.
[99] K. Artmann "Berechnung der Seitenversetzung des totatreflektierten strahles." Ann. Phys. Lpz., vol. 2, pp. 87–102, 1948.
[100] J. A. Kong, B. I. Wu, and Y. Zhang "Lateral displacement of a Gaussian beam reflected from a grounded slab with negative permittivity and permeability." Appl. Phys. Lett., vol. 80 pp. 2084–2086, 2002.
[101]P. R. Bermann "Goos-Ha¨nchen shift in negative refractive media." Phys. Rev. E, vol. 66, paper 067603, 2002.
[102] R.W. Ziolkowski "Pulsed and CW Gaussian beam interactions with double negative metamaterial slabs." Opt. Express, vol. 11, pp. 662–681, 2003.
[103] A. Lakhtakia "On planewave remittances and Goos-Ha¨nchen shifts of planar slabs with negative real permittivity and permeability." Electromagnetics, vol. 23, pp. 71–75, 2002.
[104] I. V. Shadrivov, A. A. Zharov, and Y. S. Kivshar "Giant Goos-Ha¨nchen effect at the refraction from left-handed metamaterials." Appl. Phys. Lett., vol. 83, pp. 2713–2715, 2003.
[105] R. E. Collin Field Theory of Guided Waves. IEEE Press, New York, 1990 (2nd. ed.).
[106] R. Ruppin "Surface polaritons of a left-handed medium." Phys. Lett. A, vol. 277, pp. 61–64, 2000.
[107]S. A. Darmanyan, M. Neviere, and A. A. Zakhidov "Surface modes at the interface of conventional and left-handed media." Opt. Commun., vol. 225, pp. 233–240, 2003.
[108] R. Ruppin "Surface polaritons of a left-handed material slab." J. Phys.: Cond. Matter, vol. 13, pp. 1811–1818, 2001.
[109]A. Alu and N. Engheta "Guided modes in a waveguide filled with a pair of single negative (SNG), double negative (DNG), and/or double positive (DPS) layers." IEEE Trans.Microwave Theory Tech., vol. 52, pp. 199–210, 2004.
[110] H. Coryand A. Burger "Surface-wave propagation along a metamaterial slab." Microwave Opt. Tech. Lett., vol. 38, pp. 392–395, 2003.
[111] B.-I. Wu, T. M. Gregorczyk, Y. Zhang, and J. A. Kong "Guided modes with imaginary transverse wave-number in a slab waveguide with negative permittivity and permeability." J. Appl. Phys., vol. 93, pp. 9386–9388, 2003.

[112] I. W. Shadrivov, A. A. Sukhorukov, and Y. S. Kivshar "Guided waves in negative refractive index waveguides." Phys. Rev. E, vol. 67, paper 057602, 2003.
[113] I. S. Nefedov and S. A. Tretyakov "Waveguide containing a backward-wave slab." Radio Sci., vol. 38, pp. 1101–1109, 2003.
[114] P. Baccarelli, P. Burghignoli, F. Frezza, A. Galli, P. Lampariello, G. Lovat, and S. Paulotto "Fundamental modal properties of surface waves on metamaterial grounded slabs." IEEE Trans. Microwave Theory Tech., vol. 53, pp. 1431–1442, 2005.
[115] R. Ruppin "Extinction properties of a sphere with negative permittivity and permeability." Solid State Commun., vol. 116, pp. 411–415, 2000.
[116] V. Kuzmiak and A. A. Maradudin "Scattering properties of a cylinder fabricated from a left-handed material." Phys. Rev. B, vol. 66, paper 045116, 2002.
[117]R. Ruppin "Surface polaritons and extinction properties of a left-handed material cylinder." J. Phys.: Cond. Matter, vol. 16, pp. 5991–5998, 2004.
[118]N. Engheta and R. W. Ziolkowski "A positive future for double-negative metamaterials." IEEE Trans. Microwave Theory Tech., vol. 53, pp. 1535–1556, 2005.
[119] P. Bacarelli, P. Burghignoli, F. Frezza, A. Galli, P. Lampariello, G. Lovat, and S. Paulotto "Effects of leaky-wave propagation in metamaterial grounded slabs excited by a dipole source." IEEE Trans. Microwave Theory Tech., vol. 53, pp. 32–44, 2005.
[120] T. Tamir and A. A. Oliner "Guided complex waves. Part I: Fileds at an interface. Part II: Relation to radiation patterns." Proc. Inst. Elec. Eng., vol. 110, pp. 310–334, 1963.
[121] A. Grbic and G. Eleftheriades "Experimental verification of backward-wave radiation from a negative refractive index metamaterial." J. Appl. Phys., vol. 92, pp. 5930–5935, 2002.
[122] M. Husnik, M. W. Klein, N. Feth, M. König, J. Niegermann, K. Busch, S. Linden, and M. Wegener, Nat. Photonics 2, 614-2008.
[123] T. P. Meyrath, T. Zentgraf, and H. Giessen, Phys. Rev. B 75, 205102-2007.
[124] B. Sauviac, C. R. Simovski, and S. A. Tretyakov, Electromagnetics 24, 317-2004.
[1125] R.-L. Chern and Y.-T. Chen, Phys. Rev. B 80, 075118-2009.
[126] V. M. Shalaev, Nat. Photonics 1, 41-2007.
[127] S. A. Ramakrishna and J. B. Pendry, Phys. Rev. B 67,201101-2003.
[128]B. Nistad and J. Skaar, Phys. Rev. E 78, 036603-2008.
[129] K. L. Tsakmakidis,1 M. S. Wartak,2,1 J. J. H. Cook,1 J. M. Hamm,1 and O. Hess1, Negative-permeability electromagnetically induced transparent and magnetically active metamaterials, PHYSICAL REVIEW B **81**, 195128 -2010.
[130] J. B. Pendry, Science 322, 71- 2008.

[131] D. D. Smith, H. Chang, K. A. Fuller, A. T. Rosenberger, and R. W. Boyd, Phys. Rev. A 69, 063804-2004.
[132] S. Zhang, D. A. Genov, Y. Wang, M. Liu, and X. Zhang, Phys. Rev. Lett. 101, 047401 _2008_.
[133] N. Papasimakis, V. A. Fedotov, and N. I. Zheludev, Phys. Rev. Lett. 101, 253903 _2008_.
[134] P. Tassin, L. Zhang, Th. Koschny, E. N. Economou, and C. M. Soukoulis, Phys. Rev. Lett. 102, 053901 _2009_.
[135] N. Liu, L. Langguth, Th. Weiss, J. Kästel, M. Fleischhauer, T. Pfau, and H. Giessen, Nat. Mater. 8, 758 _2009_.
[136] J. B. Pendry, Phys. Rev. Lett. 85, 3966-2000.
[137] K. L. Tsakmakidis, A. D. Boardman, and O. Hess, Nature; London, 450, 397-2007.

Chapter III:

Tunable metamaterials for Microwave & terahertz

III.1 Metamaterial structures classification

"Metamaterials are artificial materials engineered to have properties that may not be found in nature. They are assemblies of multiple individual elements fashioned from conventional microscopic materials such as metals or plastics, but the materials are usually arranged in periodic patterns". Considering this type of definition it occurs that the metamaterials can be classified according to their material, forms or aaccording to there working principles. The following four categories will be discussed:

- Arrays of metallic inclusions.
- Arrays of dielectric inclusions.
- Metamaterial based on loaded waveguides below cutoff.
- Transmission line based metamaterials.

III.1.1 Array of metallic inclusions

This class of metamaterial is based on the use of metallic structure implemented on dielectric substrate. However, all of them have different principle to achieve the negative refraction, depending on their structure and the way they are fabricated.

III.1.1.1 SRR-wire Structure

As already mentioned in the historic, the combination of two metal based mediums was the first reported metamaterial: the first medium consisted of combination of an array of magnetic resonators called split-ring resonators (SRRs), providing the negative permeability; while the negative permittivity is induced by the cut wires medium.

The first element of such medium known as "wire medium" exhibiting the negative permittivity consists of an array of thin wires, which can be implemented on parallel conducting wires or discontinuous wires [1,2,3]. In both cases, with the external

excitation with an electric field parallel to the wires, the whole system will act as an equivalent medium exhibiting: either plasma-like permittivity, thereby providing negative values below the plasma frequency for the parallel conducting wires. Or it will exhibit a resonant Lorentz-type permittivity, with possible negative values just above the resonant frequency for the discontinuous wires. Also, further investigations and analysis revealed that negative permittivity can be obtained by loading the wires with lumped elements [4], and indicated that the wire medium exhibits strong spatial dispersion [5].

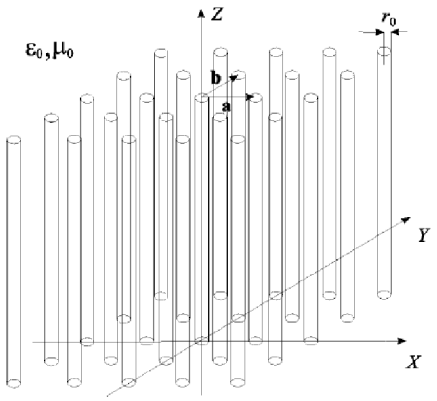

Figure III.1 : The geometry of wire media: A lattice of parallel ideally conducting thin wires [5].

The second element of this medium is called "split-ring resonator" (SRR), which is basically a subwavelength magnetic resonator made of inductive metallic ring loaded with capacitive gaps, as shown in Figure III.1(a). If the metal ring is penetrated by a magnetic flux, that will induce circulating current in the ring, which in turn give rise to a magnetic dipole moment, producing its own flux to enhance or oppose the incident field (depending on the SRR resonant properties); and therefore, providing a magnetic response without containing any magnetic material. As a consequence, an array of SRRs acts as an equivalent medium, exhibiting a Lorentz-like

permeability, with possible negative values just above the resonant frequency.

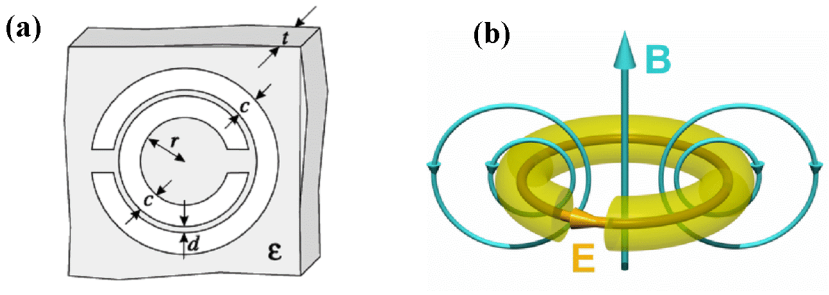

Figure III.2: circular SRR, a) Basic planar "edge-coupled" SRR[15] , b) magnetic field irradiation and circular current induction.

The first reported Metamaterial obtained by combining these two subsystems is shown in Figure III.3(a) [6]. This structure only exhibits a negative refraction (or left hand behavior) for one direction of propagation (1D left hand Material (LHM)) and for one polarization of the fields. Figure III.3 (b) shows an improved 2D isotropic version of this LHM [7], which allowed the first experimental verification of negative refraction [8]. Since these first investigations, SRR wire media have been extensively investigated and many variants have been reported.

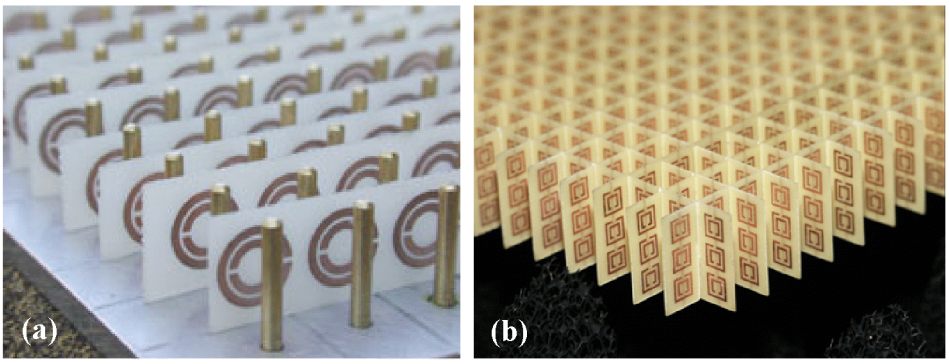

Figure III.3: Examples of SRR-wires metamaterials. a) 1D metamaterial, b) 2D metamaterial.

III.1.1.2. Metamaterial based on Ω-shape metallic patterns

The first time this type of structure was proposed in 2003 by CR. Simovski, it's based on Ω-shape metallic patterns [9]. The unit cell consists of a cube with a Ω pattern printed on each face, as shown in Figure III.4(a). From the shape we can notice that the Ω is a composed structure consisting of a sort of cut wires along a circle; which forms a combined electric-magnetic resonator. Indeed, an electric field parallel to the branches of the Ω gives rise to an electric resonance, whereas a magnetic field along the axis of the circle part, which represents some kind of SRR, induces a magnetic resonance. By adjusting the two resonant frequencies, simultaneous negative permittivity and permeability can be achieved.

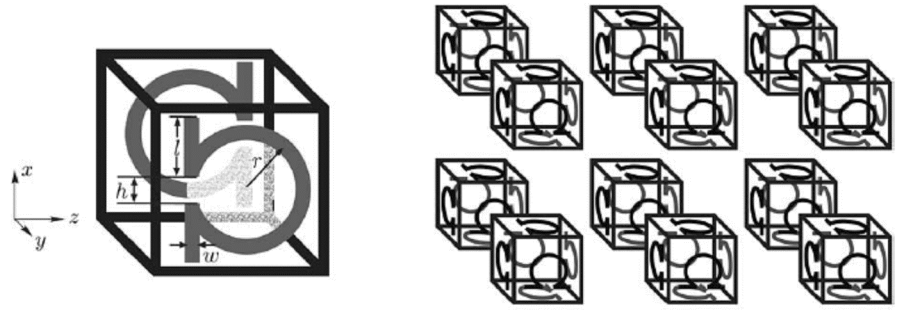

Figure III.4: Geometry for a cubic unit cell of Ω particles. a) 1 pair of Ω shaped perfectly conducting particles on 2 opposite faces of the cubic unit cell. (b) A rectangular lattice of isotropic cubic unit cells of Ω particles.

To avoid bianisotropic effects, pairs of opposite Ω patterns are used, as shown in Figure III.4(a). The final structure is obtained by printing, with appropriate orientation, three pairs of Ω patterns on the three pairs of opposite faces of a cube, as shown in Figure III.4(b).

III.1.1.3 Metamaterial based on S-shaped resonators

In general, in the classical type of SRR the negative permittivity frequency band (due to the electric resonance in the SRR at higher frequencies) does not ovelap with the negative permeability band.

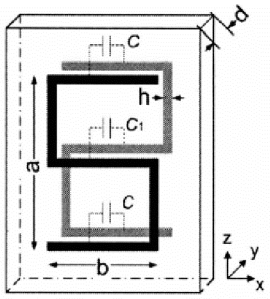

Figure III.5: S-shaped resonator [10]

The idea was to deform a classical SRR in order to shift the negative permittivity band to lower frequencies, allowing then the two negative bands to overlap. For that, H.Chen proposed an alternative implementation of the classical SRR; using an S shaped resonators (Figure III.5). Mainly, the unit cell consists of two metallic S-shaped, one on each face of the substrate. Simulation and experimental results on S-shaped metamaterial have been reported in [10,11].

III.1.1.4 Metamaterial based on the fishnet structure

Since Pendry's work on metamaterial, and the successful result he got using the SRRs and thin wire to create a negative refractive index medium, lot of researchers focused their work to find simplified structures derived from the SRR-wire medium, which can reproduce the same characteristics. One of those works leaded to a quit simplified structure which works better on higher frequencies and called fishnet structure. The idea behind this structure is to change the SRR on a conventional metamaterial by short wire pairs, which still provide a resonant magnetic response analogous to that of the SRRs, resulting from strong antiparallel currents in the two wires of

the pairs. This structure has been further modified by enlarging the short wires and merging them with the continuous wires.

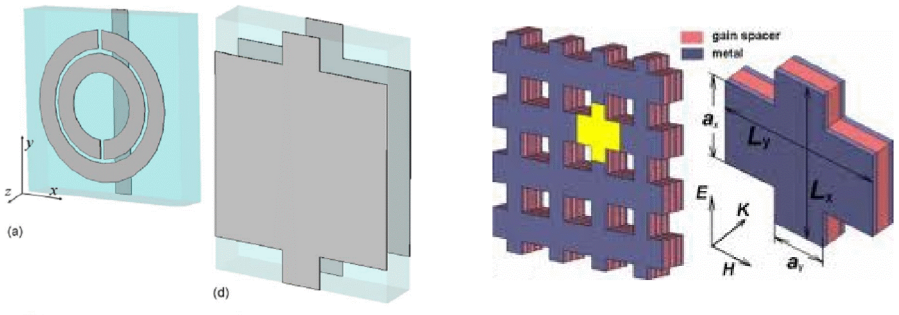

Figure III.6: Fishnet metamaterial, a) Analalogy between the SRR-wire media and fishnet. b) fishnet improved structure.

The resulting structure and its variations have been called fishnet structures [12]. The main advantage of these simplified structures resides in their planar topology, which facilitates their fabrication with conventional microfabrication techniques.

III.1.2 Purely dielectric structures

Metamaterial based on metallic patterns are well suited for microwave frequencies, but they become prohibitively lossy as the frequency is increased towards millimeter and submillimeter waves. To that respect, purely dielectric metamaterials represent an interesting alternative. Several groups have proposed various implementations of metamaterials consisting of arrays of dielectric inclusions, some of which are briefly described here:

• A metamaterial based on the combination of two lattices of high permittivity dielectric spherical particles has been proposed in [13]. The dielectric spheres support TE/TM resonant modes, from which it results equivalent magnetic/electric dipole moments. When the lattice constant is small compared to the wavelength, an homogenization procedure is possible, which leads to the definition of resonant equivalent permittivity and permeability, with possible negative values just above the resonant frequency. The idea is to

combine two lattices of dielectric spherical particles with different diameters, in such a way that both magnetic and electric resonances can be achieved at the same frequency, thereby leading to a narrow band with simultaneous negative permeability and permittivity.

• A very similar structure had been reported before in [14], where they used a single lattice of magnetodielectric spherical particles instead of a bilattice of purely dielectric ones. The main drawback of this structure is the requirement for a magnetodielectric material. • A LHM made of clustered dielectric cubes was further proposed in [98]. Interactions between the closely spaced dielectric cubes in the unit cell result in plasmonic artificial magnetic and electric dipole moments, which may lead to simultaneous negative permeability and permittivity. Such cubic inclusions are expected to be easier to fabricate than spheres. An advantage of these purely dielectric LHM over their metallic counterparts is that an isotropic response is achieved in a straightforward manner, due to the isotropy of the particles themselves. On the other hand, obtaining isotropy with metallic LHM appears to be a more challenging task. Although the purely dielectric LHM are expected to exhibit lower losses than the metallic ones, they remain rather narrowband since still relying on resonance phenomena. The aforementioned works showed proofs of concept through analytical and numerical investigations, but experimental validations remain to be done.

III.1.3 Metamaterial based on loaded waveguides below cutoff

Considering that a waveguide (WG) operated below the cutoff frequency of the first Transverse Electric (TE) mode can be seen as a guiding structure exhibiting a negative permittivity. For that, Left handed propagation can be achieved in WGs operated below cutoff when they are filled with an anisotropic uniaxial single negative metamaterial (i.e. a material for which the transversal permeability or permittivity is negative). This approach is expect to provide low loss structures compared to the SRR based approach, since wire

media do not rely on resonances. By that mean, practically the negative refraction can be achieved by:

- ✓ Loading such a WG with artificial negative permeability medium, such as an array of SRRs for instance. This principle of metamaterial was first suggested in [15]. where a negative refraction was achieved with a cutoff rectangular WG periodically loaded with SRRs for 1D propagation, while a parallel plate WG operated below the cutoff frequency of the first TE mode was used to perform a 2D isotropic metamaterial, with the advantage of being fully planar.
- ✓ With the underlying theory of the equivalence between evanescent WG modes and artificial plasmas, it come out that magnetic plasma responses can also be simulated in a WG by means of evanescent Transverse Magnetic (TM) modes. As a result, It is also possible to obtain a metamaterial by periodically loading a cutoff WG with a negative permittivity medium medium, such as the wire medium. The resulting structure is therefore the dual of the SRR loaded cutoff WG mentioned above.
- ✓ The third way consists of loading a parallel plate WG operated below the cutoff of TE modes with cylindrical dielectric resonators. Negative permeability is provided by a collective effect of the dielectric resonators under their fundamental TE resonance.

III.1.4 Transmission line based metamaterial

The basic idea behind Transmission lines (TL) based metamaterials consists in implementing a TL with a capacitive element in the series branch and an inductive element in the shunt branch, i.e. the dual topology of a conventional TL. Such an ideal continuous dual TL exhibits a left handed behavior at all frequencies. As fully

distributed, dual TLs cannot be realized, practical implementations of TL-based Metamaterial consist of a host TL periodically loaded with lumped series capacitances and shunt inductances. A LH response is achieved at frequencies where the loading L-C elements dominate the overall response. At higher frequencies, the response is mainly governed by the natural (right handed, RH) propagation along the host TL sections. For applications where both the Left Handed (LH) and RH bands are exploited, the general term Composite right/left handed (CRLH) TL has been introduced [16]. An interesting property of the CRLH TL is the possibility to obtain a seamless transition between the LH and RH bands by a proper choice of the design parameters, in which case the structure is called a balanced CRLH TL. It can be noted that a (balanced) CRLH response can also be achieved with the other types of left handed materials (LHM) previously presented, but this concept is introduced here because it has mainly been considered in the frame of TL-based LHM and related applications.

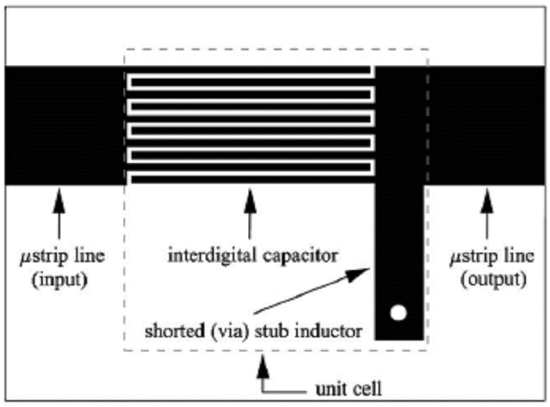

Figure III.7: Examples of TL-based LHM in microstrip technology. (a) Unit cell of a 1D LHM (taken from [17]),

In contrary to the other types of LHM, TL-based LHM do not rely on any resonance phenomena, thereby leading to low loss and wideband behavior compared to their resonant counterparts. In that context, a TL analysis of the SRR-wire medium showed that the SRR resonance

was not necessary to obtain an effective negative permeability [18]. Several implementations of TL based LHM have been reported in the literature, based on different host TLs (microstrip, coplanar waveguide, coplanar stripling e. . .), using different types of lumped L-C elements and with different physical dimensionality (1D, 2D or 3D). Figure III.7 shows example of 1D unit cell CRLH TL implemented in microstrip technology [19, 17]. The series capacitance is implemented by an interdigital capacitor, and a shorted stub is used for the shunt inductance.

III.2 Metamaterial tunability

The use of metamaterials, on an appropriate form such a Split Ring Resonators (SRR), could find applications for the development of novel devices operating in various frequency regions and aimed at filtering, modulating, and switching the electromagnetic signal. Since the first extensive studies on metamaterials, the attention of most researchers has been focused on the linear properties of these composite structures. Most of the early electronic devices involved active and, possibly, nonlinear processes, with the word active meaning that some extrinsic, or intrinsic, action is being added to an original passive design. The actions can include an intrinsic energy source, or an interrogation of the device with an external source of energy, such as a laser beam. In addition, many forms of control can be accessed by putting the device under an externally applied influence, such as a constant electric or magnetic fields, by incorporating into the device a feature that permits significant control over its resonant behavior. Having a controllable device is always of interest, as it makes its response more adaptive to the range of applications they are made for and more interactive with its environment. For that, and in order to achieve the full potential of the unique characteristics of metamaterials, the ability to dynamically control the material properties or tune them in real

time, through either direct external tuning or nonlinear response is required. By definition, A tunable metamaterial is a metamaterial which has the capability to arbitrarily adjust changes in the magnetic response of the medium, or the response of the refractive index, this includes remotely controlling how an incident electromagnetic wave EM interacts with a metamaterial. This means the capability to determine whether the EM wave is transmitted, reflected, or absorbed. In general, the lattice structure of the tunable metamaterial is adjustable in real time, making it possible to reconfigure a metamaterial device during operation.

III.2.1 Tunability Mechanisms

In order to tune or dynamically control a metamaterial, there is a variety of tuning mechanism depending on the tunining principle, with can be based either on changing the material properties, changing the metamaterial lattice, inserting new features inside it, or to change the medium properties of the metamaterial environment.

III.2.1.1 New features insertion tuning system

This tunability mechanism as the name indicates, is based on the insertion of new features inside the metamaterial itself, or in its sensitive regions.

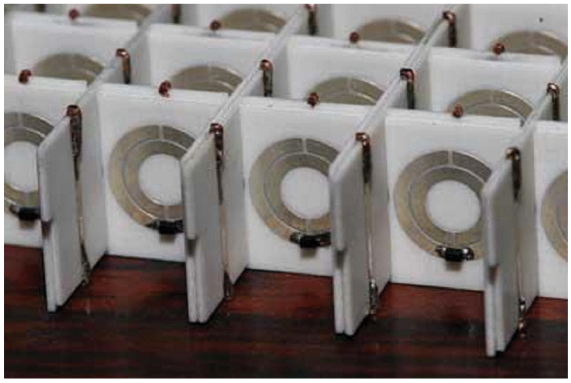

Figure III.8: Varicap metamaterials tuning based system

With an external control of this new feature we can change the metamaterial response. An example of this tunabity system is built on SRR metamaterial with gaps (sensitive area) where a voltage-controlled capacitors (Varactors) are inserted, the latter can be controlled using a voltage source, and by that mean tuning the whole system. Figure III.8 shows tuning mechanism based on varicaps.

Another example of this type of tuning, is built on RF MEMS switch, which can be inserted in the ring, and by activated the switch, we can turn ON/OFF the RF current generated in the loop, of the SRR as shown in Figure III.9.

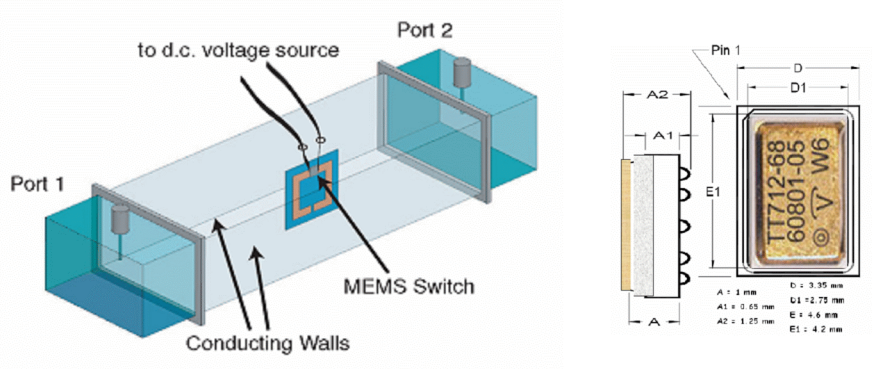

Figure III.9: metamaterial tunable system based on the insertion of an RF switch to control the circulation current on the ring.

III.2.1.2 Changing the material properties tuning system

In general the metamaterial structures are built on substrates, if we could change the intrinsic properties of those substrates; we can control the metamaterial response. The most common example of this tuning mechanism is semiconductors based system. As know, making changes on the metamaterial active areas, such as the gaps, will affect the metamaterial response. This technique has been recently used as tuning mechanism for the THz region. It shows a good overall performance and offers a variety of methods which can be used to realize the change in the substrate conductivity. The first one [7] is based on the implantation of a silicon layer in the gap

region. Changing its conductivity σ in the region near the surface by laser exposure, one can control the frequency shift using the laser energy variation.

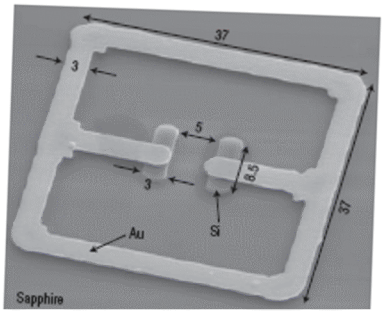

Figure III.10: Semiconductor tuning system, the conductivity σ in the region near the surface is changed laser exposure.

An alternative method uses the Schottky diode principle in order to change the substrate conductivity by creation of a depletion region in the active area of the unit cell [4]. In this case the tuning mechanism is given by a dc or slowly varying bias electric field. Figure III.11.

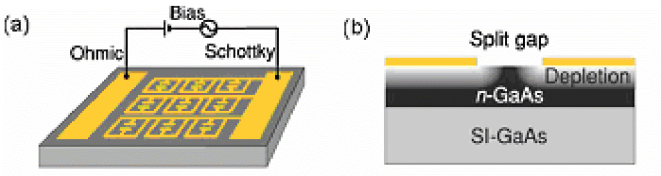

Figure III.11: Semi conductor based system; the conductivity of the material is changed using a Schottky diode principle.

III.2.1.3 MEMS based tuning system

The third tuning system is based on Micro-Electro- Mechanical Systems (MEMS). In this case, the frequency tuning can be performed using two different principles: the first one consist on a actual deposition of a MEMS element on the active area, in order to either change the split size or on the creation of new splits, as shown in Figure III.12 (a) and (b) respectively, which induces the variation

of the gap size and the increase of the overall capacitance of each unit cell. The split size modification can be based on the lateral movement of a MEMS comb drive implanted in the active area.

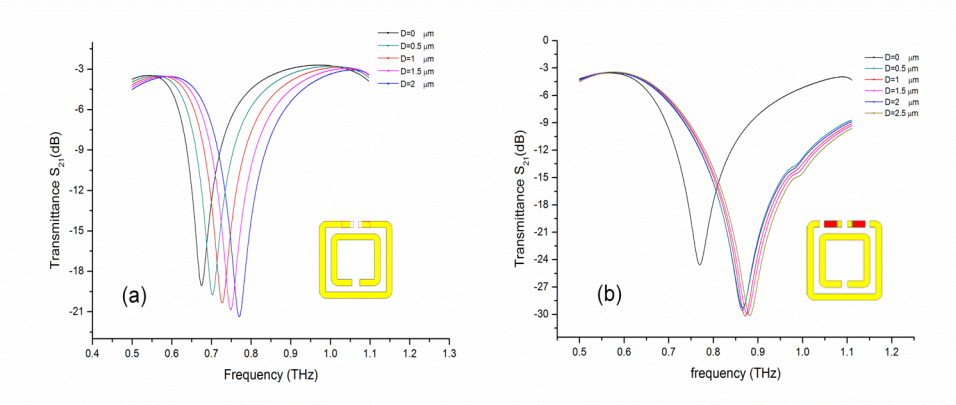

Figure III.12: MEMS based tunable mechanism fo double SRR: a) with gap size variation, b) creation of additional gaps

As for the second principle, it is well know that the metamaterial response is sensitive the incident angle of the radiated electromagnetic wave. There for, any change on the incident angle of the EM wave will tune the system response.

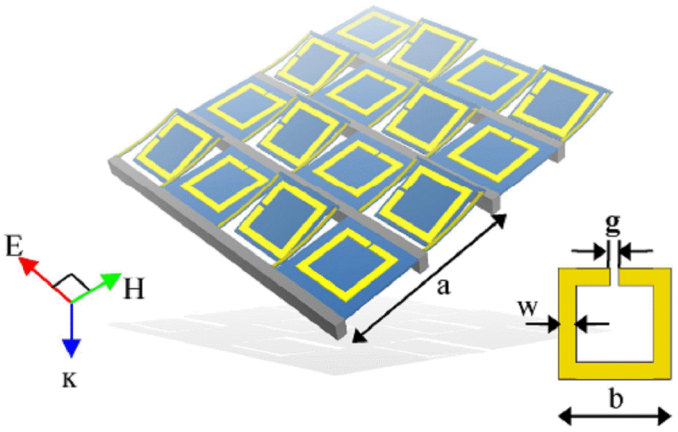

Figure III.13: MEMS embedded system, based on micro mirrors

Using MEMS, this can be easily arranged; by the implementation of the metamaterial on the top of MEMS mirror, for example we can change its orientation just by the variation of the mirror angle using a voltage control. Figure III.13 show a realization of such system.

III.2.1.4 Liquid crystal based tuning system

This tuning mechanism is of big interest for us. Therefore, and in order to understand properly how this mechanism works, we need to introduce first Liquid crystals, and how they works.

III.2.1.4.1 Liquid crystals

The notion "liquid crystal" (LC) suggests that it is an intermediate state of a matter, in between the liquid and the crystal. It must possess some typical properties of a liquid such as fluidity, inability to support shear, formation and coalescence of droplets. As well as some crystalline properties such as anisotropy in optical, electrical, and magnetic properties, periodic arrangement of molecules in one spatial direction, etc. The molecules in solids exhibit both positional and orientation order; such molecules are constrained to point only certain directions and to be only in certain positions with respect to each other. And, in liquids, the molecules do not have any positional or orientation order, thus the direction of the molecules point and their positions are random. However, in matters at liquid crystals phase, the molecules do not exhibit any positional order, but they do possess a certain degree of orientation order, these molecules do not all point the same direction all the time. They merely tend to point more in one direction over time than other directions.

Not all substances can have a liquid crystal phase because of some specific propriety that exhibit molecules in such particular matter. Actually, the molecules that tend to be candidates for having the liquid crystal phase are long; they have a rigid central region and ends that are slightly flexible. Liquid crystals are essentially more like liquids than they are like solids. This is

evident from the "latent heat" of transition (the amount of energy needed for a phase transition to occur).

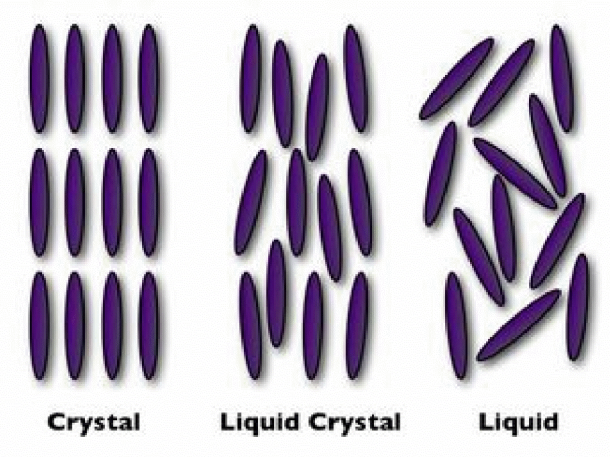

Figure III.14: different stat of matter, the molecules arrangement in each stat.

The liquid crystals have a number of particular and unique characteristics in which rise their exceptional suitability for use in displays. Most of these characteristics stem from the fact that liquid crystal is an anisotropic material. Anisotropic means that the properties of the material differ depending on what direction they are measured. The liquid crystal behaves differently depending on in which direction electric or magnetic fields are applied relatively to the director. Since light is an electromagnetic wave, what happens to light as it passes through the liquid crystal will also depend highly on the direction of its propagation and polarization with respect to the director of the crystal. There are many kinds of liquid crystal:

- ***Nematic LC***: This is a common type of LCs. The name comes from the Greek word for ``thread" because of the thread-like formations that defects in this kind of liquid crystal form which can be seen under a microscope. Optically a nematic behaves as a uniaxial material with a centre of symmetry.
- ***Chiral nematic (or cholesteric) LC***: exhibits a twisted structure. Literally, the director rotates about an axis as you move through the material. This helical structure is exploited in several ways in making modern flat-panel displays.

- ***Smectic LC***: which has a soapy texture and retains some positional order in that the molecules concentrate in planar layers.
- ***Lytropic LCs:*** which are mainaly a mixtures of the previous type of LCs. Quite often, mixing different kinds of liquid crystal can result in a material that has more useful properties. These lytropic LCs substances are extremely important in display applications.

Applying an electric field to a liquid crystal molecule with a permanent electric dipole will cause the dipole to align with the field. If the molecule did not originally have a dipole, then it is induced when the field is applied. Either of these situations has the ultimate effect of aligning the director of the liquid crystal with the electric field being applied. The order of the liquid crystal has not increased, so we have only achieved alignment of the director. Only a very weak electric field is needed to accomplish this in liquid crystal. In solids, applying an electric field has little effect because the molecules are held in place by their bonds to other molecules, and in liquids, the high kinetic energy of the molecules makes it impossible to orient them by simply applying an electric field. Since the electric dipole across liquid crystal molecules varies in degree along the length and the width of the molecule, some kinds of liquid crystal require less electric field and some require much more in order to align the director. The ratio of electric dipole per unit volume of crystal to the field strength is called the electric susceptibility and provides a measure of how easy it is to electrically polarize the material. These ideas are analogous when dealing with magnetic fields. Magnetic dipoles can be inherent, or more likely, they can be induced in the crystal by applying a magnetic field, and there is a corresponding magnetic susceptibility associated with the material.

Liquid crystal is birefringent structures, which means that it possesses two different indices of refraction. One index of refraction

corresponds to light polarized along the director of the liquid crystal, and the other is for light polarized perpendicular to the director. Light propagating along a certain direction has electric and magnetic field components perpendicular to that direction. Supposing that the director lies perpendicular to the direction of propagation of the light, we can think of each component as being made up of two more components, one parallel to the director of the crystal and one perpendicular. Essentially, what this birefringence property amounts to is that these two components of either the electric or the magnetic field will propagate through the liquid crystal at different speeds and, therefore, possibly be out of phase when they exit the crystal. Chiral nematic liquid crystal is birefringent in a different way. Supposing that the helical structure is aligned with the direction of propagation of the light, circularly polarized light will travel through the crystal at different speeds depending on whether it is right-circularly polarized or left-circularly polarized (referring to the direction the polarization rotates around the axis of propagation). This is called *circular birefringence*, and it is exhibited in chiral nematic liquid crystal because of the helical structure the molecules form. The circular birefringence is highly wavelength dependent, so light of different colors gets modified in different amounts. Circularly polarized light can be thought of containing two components, one of left- and one of right-circularly polarized light. If the light is linearly polarized, these components are equal. If we send linearly polarized light through chiral nematic liquid crystal, the component of circularly polarized light that matches the chirality of the crystal structure will travel faster than the other component, having the ultimate effect that its polarization will rotate faster with respect to the other component's polarization. When the two components emerge, their polarizations will again rotate at the same rate and the light will again be linearly polarized, but since one of the rotations got ahead of the other, the light will now be linearly polarized along a different angle. What the new angle is will depend on how far out

of ``circular phase" the two components were, which is directly dependent on thickness of the liquid crystal. This effect is called the *optical activity* it is a measure of the change in polarization angle per unit thickness, and it is heavily wavelength dependent.

III.2.1.4.2 Liquid crystals tuning mechanism

From the previous section, we know that the liquid crystal medium permittivity changes its value, depending on the orientation of the LC molecules. In general the permittivity ε varies value is related to the molecules orientation with the following equation:

$$\varepsilon_{LC} = \frac{\varepsilon_{\parallel}\varepsilon_{\perp}}{\varepsilon_{\parallel}\cos^2\theta + \varepsilon_{\perp}\sin^2\theta}$$

For that, its properties can be controlled reorienting the LC molecular director, described by the angle θ, in respect to the oscillating electric field direction. LC molecules reorientation can be done using a static or slowly varying electric field, by applying a magnetostatic field or even using thermal control. The LC tuning mechanism is based on the influence of the LC intrinsic parameters and its interaction with the metamaterial unit cell to achieve the tuning.

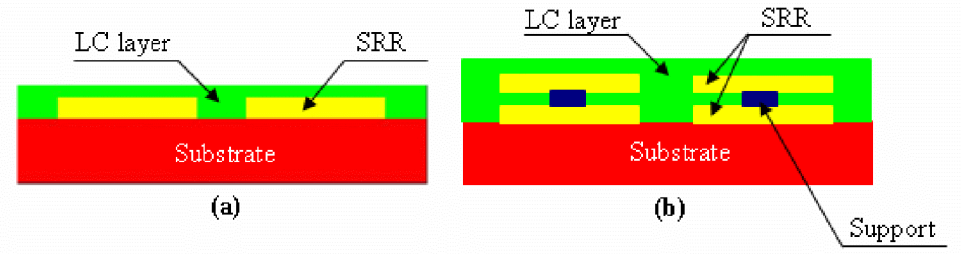

Figure III.15: LC configurations: (a) the LC top covers the metallic structure; (b) the LC is in between two metallic structures.

For this reason, two LC configurations can be identified: The first standard configuration implies the use of an appropriate amount of LC top layer covering the metamaterial (Figure III.15(a)); this will allow changing the permittivity of the environment surrounding the metamaterial, which obviously will induce a variation in the metamaterials response. Whereas the second one is based on the use of the LC in order to change some features properties inside the metamaterial itself. In such case, if we consider that the metamaterial has separated metallic parts, which will create a kind of capacitors inside the metamaterials with Air as dialectic. By infiltrating LC in between two metallic parts, we can change the permetivity of those capacitors by polarizing the LC, thing which lead to a metamaterial with two different responses, where the first one related to the first LC medium state, and the second is drived from the LC polarized state as shown in Figure III.15(b).

III.3 Microwave Applications of Metamaterial Concepts

The potential of metamaterials rise in their structures employed for the synthesis and design of new microwave devices and subsystems, where, high performances and novel functionalities are improved due to the unique and controllable electromagnetic properties of these structures, as well as device miniaturization (small electrical size of their constitutive elements). Here, several applications of metamaterials have been exhaustively analyzed in the area; mostly those oriented towards the resonant-type approach, in particular the metamaterial applications based on the dual transmission line concept.

It is well known that metamaterials are frequency-selective structures by nature of outstandingly controllable electrical characteristics. These particularities make them very suitable for the design of compact microwave filters and diplexers in a very simple way. Thus, designing microwave filters require resonant elements,

where the synthesis of filters and diplexers is based on one dimensional (1D) resonant-type metamaterials approach. It has been shown in several studies that SRRs and CSRRs metamaterial structures are useful particles for the synthesis of narrowband and wide-band-pass filters (also band-pass filters for ultra-wide-band UWB applications).

III.3.1 Filters and diplexers

The transmission lines simply loaded with SRRs or CSRRs have the power of inhibiting signal propagation in a narrow band in the vicinity of resonance [20,21]; due to the negative effective permeability or permittivity of such 1D artificial transmission media. They also can be modified to act as pass-band or stop-band filter, simply by introducing additional elements to the structures. In the following we introduce briefly some of them.

III.3.1.1 Stop-band Filters

Stop-band filters are typically of interest in microwave engineering for the suppression of undesired responses or for the elimination of interfering signals. Actually the single negative transmission lines based on SRRs or CSRRs are rejection band structures that produce reasonable suppression levels with small dimensions figure II.16. Due their electrically small elemental cells which are very effective in inhibiting signal propagation. Here, the multituning concept to SRR-loaded micro-strip lines (square-shaped SRRs) is also employed in order to enhance magnetic coupling between line and rings [22]. Whereas, CSRRs elements are expected to produce controllable stop-bands when etched in planar transmission lines and tuned at different frequencies [23].

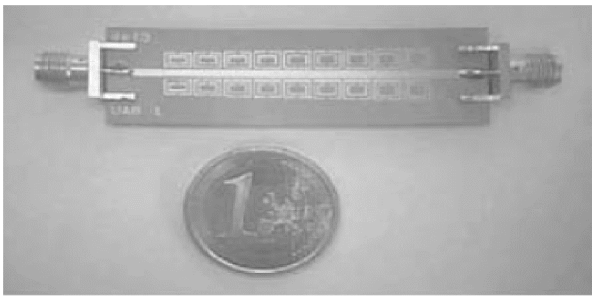

Figure III.16. Multi-tuned SRR-based micro-strip stop-band filter [22]

III.3.1.2 Planar Filters with Improved Stop-band

The implementation of microwave filters using distributed elements faces a very important limitation manifesting in the presence of spurious bands [24]. These undesired frequency bands can seriously degrade filter performance and may be critical in certain applications that require huge rejection bandwidths. Unfortunately, for most filter implementations the first spurious band is relatively close to the frequency region of interest. To overcome to this kind of limitation, design engineers used traditional techniques including the use of half-wavelength short-circuit stubs, chip capacitors or cascaded stop-band filters. However, these techniques are either narrow band, increase device area, or introduce significant insertion losses. Therefore, in coupled-line filters, several approaches based on modified structures [19], on the concept of EBGs [25,26] and on the use of SRRs or CSRRs, have been proposed to suppress harmonics in a wide variety of microwave circuits (passives and actives).

III.3.1.3 Narrow Bandpass Filter and Diplexer

It is known that, left-handed transmission lines consisting of a combination of SRRs with shunt-connected strips, or a CSRRs with series gaps, exhibit an abrupt transition band at the lower edge, with poor frequency selectivity at the upper edge of the band. A transmission zero present below and close to the left-handed allowed band explains the sudden change in the transmission coefficient

prior to this band. However, the upper band limit is determined by that frequency where the series impedance switches from capacitive to inductive behaviour (for SRR-based left-handed lines) or the shunt impedance switches from inductive to capacitive behaviour (for CSRRs lines). This change is gradual rather than abrupt and this is the reason for the soft transition that is typically measured above the passband. It is possible to improve frequency selectivity at the upper edge of the band by alternating left-handed transmission line sections with artificial right-handed sections, which consist of SRRs combined with gaps, or CSRRs combined with shunt-connected strips, to exhibit a transmission zero above the pass-band. As a result, by overlapping the pass-bands of both stages, it is potentially possible to achieve roughly symmetric and highly frequency-selective devices.

III.3.1.4 CSRR-Based Band-pass Filters with Controllable Characteristics

The design of band-bass filters with controllable characteristics in micro-strip technology is based on cascading filter stages consisting of a combination of CSRRs, series capacitive gaps, and grounded stubs to achieve the necessary flexibility in order to obtain simultaneously quite symmetric frequency responses, controllable bandwidths, and compact dimension. Generally the studied band-pass filters are usually described by a network consisting of a cascade of shunt resonators and admittance inverters. However, band-pass responses can also be synthesized by cascading series resonators and impedance inverters. As open split rings resonators modelled as series resonant tanks [27].

III.3.1.5 High-pass Filters and Ultra-wide Band-pass Filters

In microwave engineering the difference between a high-pass filter (HPF) and an ultra-wide band filter (UWBPF) is delicate. Precisely,

a microwave HPF implemented in planar technology does not exhibit an unlimited band above the cutoff frequency. Consequently, microwave HPFs are indeed band-pass filters with a very wide band and a controllable cutoff frequency at the lower band edge. This means that, the difference between an HPF and a UWBPF is simply the fact that in these UWBPF filters, both the upper and lower cutoff frequencies are controllable, and in HPFs the upper limit of the band is not considered to be specified. This is why balanced CRLH CSRR-based unit cells are useful for the synthesis of HPFs. Because they exhibit a huge transmission band above the cutoff frequency, good frequency selectivity and the presence of a transmission zero, where, the rejection below the cutoff frequency can be controlled by the number of stages of the structure. Such filters can be realised using CSRRs and CSRs structures [28, 29].

III.3.1.6 Tunable Filters on Varactor-Loaded Split Rings Resonators

Configurable or Tunable filters are usually based on electronically controllable components such as varactor diodes or RF-MEMS switches, among others, where a variable capacitance is used to tailor device characteristics. Varactor diodes and RF-MEMS are applied to the design tunable microwave components devices, such as filters and other, based on conventional configurations [30]. The possibility of designing tunable filters and resonators by means of active electromagnetic band-gaps (EBGs) based on varactor diodes has been reported in [31], where the tunable filters can be implemented by using resonant-type metamaterial transmission lines loaded with varactor diodes. However, due to varactor diode losses, the performance of such filters can be very limited. Thus, to synthesize tunable band-pass filters with good performance, low-loss tuning elements such as RF-MEMS are required to be used where the combination of these elements with SRRs or CSRR can be very promising area of working.

III.3.2 Metamaterial Antenna Applications

It is well known that small physical size, low cost, broad bandwidth, and good efficiency are desirable features for an integrated antenna. It is also well known that the quality factor Q and the radiation loss of the antennas are inversely related to the antenna size. Metamaterial-based small antennas are a class of antennas inspired by metamaterials to enhance their capability or to achieve novel functions and to provide them with a means to manipulate the dispersion relation and the near-field boundary conditions, which could result in antenna size miniaturization while maintaining a good radiation performance.

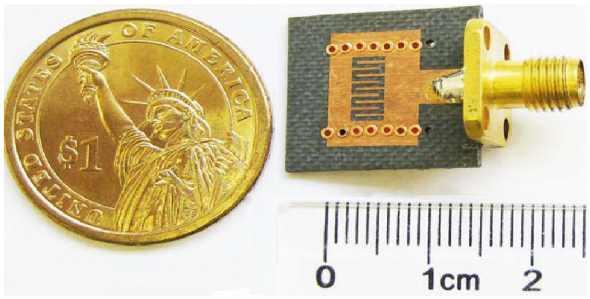

Figure III.17: Fabricated one-element CRLH SIW antenna. [33].

Metamaterial antennas open a way to overcome the restrictive efficiency-bandwidth limitation for small conventional antennas [32]. Figure III.17

III.4 Metamaterials for terahertz

III.4.1 Planar metamaterials

The resonator-based planar metamaterials are artificial electromagnetic structures, which is engineered to provide unusual features not readily found in nature. It generally consists of a regular

array of sub-wavelength ($\approx \lambda/10$) electric and/or magnetic elements in which they are placed on a dielectric substrate [34] [35].

Through the unprecedented properties of these synthetic structures, controlling the propagation of the electromagnetic waves became feasible. This led to numerous applications which made their principles of operation a ubiquitous concept in electromagnetic devices. In the microwave regime, periodic structures are able to exhibit properties such as electromagnetic bandgap [36] and negative refractive index [37]. In addition, incorporating perfect electric conductors (PEC) into the unit cell leads to metamaterials with strong resonances in the microwave domain. Frequency selective surfaces (FSS) [38, 39] and chiral metamaterials [40] are typical examples. Attempts to realize metamaterials have been mostly around planar structures because of their compatibility with well-developed fabrication techniques and the ease of integration in a planar platform [41]. In addition, recent advances in materials and fabrication techniques made it possible to fabricate multilayer planar structures with high complexity in geometry and in unit cell configuration. Currently, many studies focus on planar metamaterials that most often consist of structures with periodic symmetry in one (1D) or two dimensions (2D) and a layered or multilayer pattern in the other. Lamellar grating is an example of patterns with periodic symmetry only in one direction [42]. Two main groups of planar metamaterials with a two dimensional periodicity are photonic crystals (PC) slabs and Frequency selective surfaces FSS. Planar chiral metamaterials are known by their ability to affect the polarization states of light [43] which can lead to a whole new generation of optical devices and components with potential applications in optoelectronics, telecommunications and nanotechnology.

III.4.2 Terahertz Metamaterial

Terahertz metamaterials are new class artificial materials which interact at terahertz (THz) frequencies. The terahertz frequency range used in materials research is usually defined as 0.1 to 10 THz. In this bandwidth the waves are electromagnetic with frequencies in between microwaves and visible light (higher than microwaves but lower than infrared radiation and visible light). These characteristics mean that it is difficult to influence terahertz radiation via electronic means, as with microwaves [44].

The terahertz spectral band, bridging the worlds of electronics and optics, has been relatively unexplored and is referred to as the terahertz gap because of accessibility difficulties. It is only recently that terahertz technology has been developed to the point where the frequencies can be generated, detected, and manipulated routinely with tabletop equipment. Amongst many techniques [45], for instance, terahertz time-domain spectroscopy (THz-TDS) [46] utilizing a femto-second laser source is a potential candidate for generation and detection of broadband coherent terahertz radiation. The excitation of the emitter with ultra-short laser pulses results in a burst of sub-pico-second pulses with frequencies spanning from a few hundred gigahertz to a few terahertz. At the detector, a coherent detection scheme is capable of resolving the amplitude and phase of a terahertz pulse with an adequate SNR.

In this new wavelength, or frequency range applications, the terahertz metamaterial appears to be useful for security screening and medical imaging (in terahertz frequency range the radiation isnonionizing and hence favourable to applications seeking human exposure), for wireless communications systems, non-destructive evaluation, and chemical identification. As a non-ionizing radiation it does not have the risks inherent in X-ray screening.

III.4.3 Terahertz applications

Metamaterials play a potentially important role in creating necessary functional devices for THz applications. A variety of THz components/devices based on THz metamaterials have been presented. THz applications Includes perfect absorbers, THz amplitude/phase modulators, structurally reconfigurable THz MMs, and memory THz MMs. Here, we mention some of them.

III.4.3.1. Terahertz Metamaterial Absorbers

In metamaterials field, considerable effort has focused on the real parts of permittivity ε and permeability μ to create a negative refractive material. To create such structures, it is important to minimize losses (over the operating frequency range) associated with the imaginary portions of both ε and μ of the effective response functions. In the opposite side, for many applications, it would be desirable to maximize the loss; such in absorber devices (Figure III.18) which would be of particular importance at THz frequencies, where it is difficult to find naturally occurring materials with strong absorption coefficients that, further, would be compatible with standard micro-fabrication techniques.

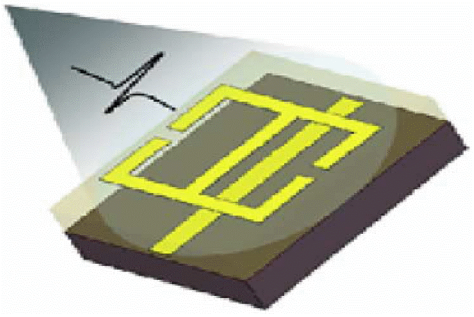

Figure III.18: Schematic of the Thz MM bsorber [47]

Tao et al. Studies in [48] and [48] have proved that, those metamaterial absorbers may find numerous applications ranging

from the active element in a thermal detector to THz stealth technology.

III.4.3.2. Terahertz Metamaterial Switches and Modulators

Metamaterials offer a promising alternative for the dynamic control and manipulation of THz radiation. Various THz metamaterial switches and modulators have been proposed through various modifications to the existing metamaterials. Functionalizing these metamaterial modulators is generally achieved via dynamic modification of the surrounding environment using external electrical, thermal, or optical stimuli, leading to a modulation of the resonance strength in the transmission amplitude. It has been reported in [50], that a THz metamaterial switch fabricated on GaAs substrates with the potential for creating dynamic metamaterial resonance responses. The electric resonance can be turned ON/OFF by photo-excitation of the free carriers in the GaAs substrate; to short or open the resonator gap, which leads to a modulation on the THz radiation transmission.

An other metamaterial switches/modulators based on SRR structures were fabricated on a thin n-type GaAs layer in [51], where the conductivity can be externally modified by applying a voltage bias through a group of metallic wires connecting those resonators to a voltage source. No resonance is observed, as the n-type GaAs substrate electrically shorts out the resonator gaps. The resonators serve as a Schottky contact with the substrate. However, when a reverse voltage bias depletes carriers in the capacitive regions, it causes the isolating of the metal from the doped substrate, resulting in the restoration of the resonance. This kind of devices can modulate the THz transmission by 50% at a few KHz, and an improved version with similar modulation mechanism can enable modulation at over 2 MHz [52]. It has also been demonstrated in [53] that the phase of THz radiation can be modulated by a THz metamaterial modulator

based on SRR structure, where the device achieves a voltage-controlled linear phase shift at 0.89 THz, with a modulation of around π/6 rad at 16 V.

This class of THz metamaterial switches/modulators reveal a promising approach toward promoting real-world applications such as THz communication and THz wave detections.

III.4.3.3. Terahertz Quarter Waveplates

Birefringent crystals have long been used as quarter wave-plates (QWPs) in optics for converting linear polarization to circular and vice versa. The meanderline polarizer is an artificial alternative to the crystal-based QWPs for use at millimetre wave and near-IR frequencies partly due to its low cost and ease of fabrication [54]–[56]. Recently, metamaterials and meanderlines have been investigated at microwave and THz frequencies [57]–[59], under the form of electric-split-ring resonator based QWP. According to Strikwerda et al [60], this form of metamaterials meanderline, presented good parameters and can be used for continuous wave sources (CW)

III.4.3.4. Structurally Reconfigurable Terahertz Metamaterials

It is known that the overall properties of a material are not only determined by the nature of the constituent atoms, but also depend significantly on the lattice structure. The same rule applies to metamaterials, and even better. Compared with natural materials, where the tunability of their properties through tuning, the crystal lattice is determined by the chemical bonding and nature of the atoms themselves, the range of tunability for metamaterials is more accessible, as the "lattice effects" can be made much stronger by an appropriate design [61]. It has been reported in [48] that structurally reconfigurable THz metamaterial with tunable electrically and magnetically resonant responses through mechanically reorienting

the microfabricated resonators within their unit cells [62], and the designed SRR structures (fabricated on bi-material cantilevers) bends out of plane in response to a thermal stimulus. Here, a 30% and 50% tunability of the electric and magnetic resonance in the transmission spectrum were experimentally observed at around 0.5 THz, respectively, this can be potentially used for reconfigurable filters, cloaks, and concentrators.

III.4.3.5. Terahertz Metamaterials with Memory Effects

Most metamaterials are designed to operate at a single resonant frequency; some progress has been done in developing frequency-agile metamaterials at THz frequencies that allow their resonant frequency to be tuned with certain stimulus. However, the tuning is lost when the stimulus is taken away. It has been reported in [63] that, a new THz metamaterial device can remember the new frequency of operation by incorporating vanadium dioxide (VO_2) into the conventional SRR structures. It is known that the metal-to-insulator phase transition of VO_2 can be controlled with external optical or electrical stimulus and exhibiting hysteresis enabling the programming of the metamaterials response [64], [65]. The resonant frequency of the SRRs depends on the VO_2's capacitive properties and is set until the phase changes back.

Bibliography

[1] J. B. Pendry, A. J. Holden, W. J. Stewart, and I. Youngs, "Extremely low frequency plasmons in metallic mesostructures," Physical Review Letters, vol. 76, no. 25, pp. 4773– 4776, 1996.

[2] J. B. Pendry, A. J. Holden, D. J. Robbins, and W. J. Stewart, "Low frequency plasmons in thin-wire structures," J. Phys.: Condens. Matter, vol. 10, pp. 4785 4809, 1998.

[3] S. I. Maslovski, S. A. Tretyakov, and P. A. Belov, "Wire media with negative effective permittivity: a quasi-static model," Microwave and Optical Technology Letters, vol. 35, no. 1, pp. 47–51, 2002.

[4] S. A. Tretyakov, S. I. Maslovski, and P. A. Belov, "An analytical model of metamaterials based on loaded wire dipoles," IEEE Transactions on Antennas and Propagation, vol. 41, no. 10, pp. 2652–2658, 2003.

[5] P. A. Belov, R. Marqués, S. I. Maslovski, I. S. Nefedov, M. Silveirinha, C. R. Simovski, and S. A. Tretyakov, "Strong spatial dispersion in wire media in the very large wavelength limit," Physical Review B, vol. 67, p. 113103, 2003

[6] D. R. Smith, W. J. Padilla, D. C. Vier, S. C. Nemat-Nasser, and S. Schultz, "Composite medium with simultaneously negative permeability and permittivity," Physical Review Letters, vol. 84, no. 18, pp. 4184–4187, 2000.

[7] R. A. Shelby, D. R. Smith, S. C. Nemat-Nasser, and S. Schultz, "Microwave transmission through a two-dimensional, isotropic, left-handed metamaterial," Applied Physics Letters, vol. 78, no. 4, pp. 489–491, 2001.

[8] R. A. Shelby, D. R. Smith, and S. Schultz, "Experimental verification of a negative index of refraction," Science, vol. 292, pp. 77–79, 2001.

[9] C. R. Simovski and S. He, "Frequency range and explicit expressions for negative permittivity and permeability for an isotropic medium formed by a lattice of perfectly conducting omega particles," Physics Letters A, vol. 311, pp. 254–263, 2003.

[10] H. Chen, L. Ran, J. Huangfu, X. Zhang, K. Chen, T. M. Grzegorczyk, and J. A. Kong, "Left-handed materials composed of only S-shaped resonators," Physical Review E, vol. 70, p. 057605, 2004.

[11] H. S. Chen, L. X. Ran, J. T. Huangfu, X. M. Zhang, K. S. Chen, T. M. Grzegorczyk, and J. A. Kong, "Magnetic properties of S-shaped split-ring resonators," progress In Electromagnetics Research, PIER, vol. 51, pp. 231–247, 2005.

[12] M. Kafesaki, I. Tsiapa, N. Katsarakis, T. Koschny, C. M. Soukoulis, and E. N. Economou, "Left-handed metamaterials: The fishnet structure and its variations," Physical Review B, vol. 75, p. 235114, June 2007.

[13] O. G. Vendik and M. S. Gashinova, "Artificial double negative (DNG) media composed by two different dielectric sphere lattices embedded in

a dielectric matrix," in European Microwave Conference (EuMC), Amsterdam, 2004, pp. 1209–1212.
[14] C. L. Holloway, E. F. Kuester, J. Baker-Jarvis, and P. Kabos, "A double negative (DNG) composite medium composed of magnetodielectric spherical particles embedded in a matrix," IEEE Transactions on Antennas and Propagation, vol. 51, no. 10, pp. 2596–2603, October 2003.
[15] R. Marqués, J. Martel, F. Mesa, and F. Medina, "Left-handed-media simulation and transmission of EM waves in subwavelength split-ring-resonator-loaded metallic waveguides," Physical Review Letters, vol. 89, no. 18, p. 183901, 2002.
[16] A. Lai, C. Caloz, and T. Itoh, "Composite right/left-handed transmission line metamaterials," IEEE Microwave Magazine, pp. 34–50, September 2004.
[17] C. Caloz and T. Itoh, "Transmission line approach of left-handed (LH) materials and microstrip implementation of an artificial LH transmission line," IEEE Transactions on Antennas and Propagation, vol. 52, no. 5, pp. 1159–1166, 2004.
[18] G. V. Eleftheriades, O. Siddiqui, and A. K. Iyer, "Transmission line models for negative refractive index media and associated implementations without excess resonators," IEEE Microwave and Wireless Components Letters, vol. 13, no. 2, pp. 51 53, 2003.
[19] A. Sanada, C. Caloz, and T. Itoh, "Characteristics of the composite right/left-handed transmission lines," IEEE Microwave and Wireless Components Letters, vol. 14, no. 2, pp. 68–70, 2004.
[20] F. Falcone, F. Martin, J. Bonache, R. Marque´s, and M. Sorolla "Coplanar waveguide structures loaded with split ring resonators." Microwave Opt. Tech. Lett., vol. 40, pp. 3–6, January 2004.
[21] F. Falcone, T. Lopetegi, J. D. Baena, R. Marque´s, F. Martı´n, and M. Sorolla "Effective negative-1 stop-band microstrip lines based on complementary split ring resonators." IEEE Microwave Wirel. Comp. Lett., vol. 14, pp. 280–282, June 2004.
[22] J. Garcı´a-Garcı´a, J. Bonache, I. Gil, F. Martı´n, R. Marque´s, F. Falcone, T. Lopetegi, M. A. G. Laso, and M. Sorolla "Comparison of electromagnetic bandgap and split rings resonator microstrip lines as stop band structures." Microwave Opt. Tech. Lett., vol. 44, pp. 376–379, February 2005.
[23] J. Garcı´a-Garcı´a, F. Martı´n, E. Amat, F. Falcone, J. Bonache, I. Gil, T. Lopetegi, Miguel A. G. Laso, A. Marcotegui, M. Sorolla, and R. Marque´s "Microwave filters with improved stop band based on sub-wavelength resonators." IEEE Trans. Microwave Theory Tech., vol. 53, pp. 1997–2006, June 2005.
[24] D. M. Pozar Microwave Engineering. Addison-Wesley, Reading, MA, 1990. 19. C. Person, A. Sheta, J. Ocupes, and S. Toutain "Design of high performance band pass filters by using multilayer thick film technology." Proc. 24th European Microwave Conf., Cannes, France, September 1994, vol. 1, pp. 446–471.

[25] J. D. Joannopoulos, R. D. Meade, and J. N. Winn Photonic Crystals: Molding the Flow of Light. Princeton University Press; Princeton, NJ, 1995.
[26] E. Yablonovitch "Photonic bandgap structures." J. Opt. Soc. Am. B, vol. 10, pp. 283–295, February 1993.
[27] J. Martel, R. Marque´s, F. Falcone, J. D. Baena, F. Medina F. Martı´n, and M. Sorolla "A new LC series element for compact band pass filter design." IEEE Microwave Wirel. Comp. Lett., vol. 14, pp. 210–212, May 2004.
[28] W. Menzel and P. Feil "Ultra-wide band (UWB) filter with WLAN notch." Proc. 36th European Microwave Conf., pp. 595–598, Manchester, UK, September 2006.
[29] K. Li, D. Kurita, and T. Matsui "UWB band pass filters with multi notched bands." Proc. 36th European Microwave Conf., pp. 591–594A, Manchester, UK, September 2006.
[30] G. Rebeiz, RF MEMS Theory, Design and Technology. Wiley, New York, 2003.
[31] I. Gil, J. Bonache, J. Garcı´a-Garcı´a, and F. Martı´n "Application of active electromagnetic bandgaps to the design of tunable resonators in CPW technology." Microwave Opt. Tech. Lett., vol. 45, pp. 229–232, May 2005.
[32] Yuandan Dong, Tatsuo Itoh, "Metamaterial-Based Antennas" Proceedings of the IEEE, Vol. 100, 0018-9219, 7 July 2012.
[33] Y. Dong and T. Itoh, "Miniaturized substrate integrated waveguide slot antennas based on negative order resonance", IEEE Trans. Antennas Propag., vol. 58, no. 12, pp. 3856–3864, Dec. 2010.
[34] K.V. Seshagiri Rao, P.V. Nikitin, and S.F. Lam, Antenna design for UHF RFID tags: A review and a practical application, IEEE Trans Antennas Propag 53 (2005), 3870–3876.
[35] H. Kwon and B. Lee, Compact slotted planar inverted-F RFID tag mountable on metallic objects, Electron Lett 41 (2005), 1308–1310.
[36] F.-R. Yang, K.-P. Ma, Y. Qian, and T. Itoh, "A uniplanar compact photonic-bandgap (UC-PBG) structure and its applications for microwave circuit," Microwave Theory and Techniques, IEEE Transactions on, vol. 47, no. 8, pp. 1509–1514, Aug. 1999.
[37] G. V. Eleftheriades, A. K. Iyer, and P. C. Kremer, "Planar negative refractive index media using periodically L-C loaded transmission lines," Microwave Theory and Techniques, IEEE Transactions on, vol. 50, no. 12, pp. 2702–2712, Dec. 2002.
[38] T. K. Wu, Ed., Frequency Selective Surface and Grid Array. New York, NY: John Wiley and Sons, 1995.
[39] B. A. Munk, Frequency Selective Surfaces Theory and Design. New York, NY: John Wiley and Sons, 2000.
[40] D. L. Jaggard, A. R. Mickelson, and C. H. Papas, "On electromagnetic waves in chiral media," Applied Physics A, vol. 18, no. 9, pp. 211–216, Feb. 1979.

[41] M. Loncar, T. Yoshie, J. Vuckovic, A. Scherer, H. Chen, D. Deppe, P. Gogna, Y. Qiu, D. Nedeljkovic, and T. Pearsall, "Nanophotonics based on planar photonic crystals," in Lasers and Electro-Optics Society, 2002. LEOS 2002. The 15th Annual Meeting of the IEEE, vol. 2, 2002, pp. 671–672 vol.2.

[42] L. C. Botten, M. S. Craig, R. C. McPhedran, J. L. Adams, and J. R. Andrewartha, "The dielectric lamellar diffraction grating," Journal of Modern Optics, vol. 28, no. 3, pp. 413–428, 1981.

[43] A. Potts , A. Papakostas , D.M. Bagnall, N.I. Zheludev, Planar chiral meta-materials for optical applications, Elsevier, Microelectronic Engineering 73–74 (2004) 367–371.

[44] Johnston, Hamish (Nov 29, 2006). "Metamaterial bridges the terahertz gap". physics world (Institute of Physics). http://physicsworld.com/cws/article/news/2006/nov/29/metamaterial-bridges-the-terahertz-gap. Retrieved 2012-07-29.

[45] B. Ferguson and X.-C. Zhang, BMaterials for terahertz science and technology,[Nat. Mater., vol. 1, no. 1, pp. 26–33, 2002.

[46] M. van Exter, C. Fattinger, and D. Grischkowsky, BHigh-brightness terahertz beams characterized with an ultrafast detector,[Appl. Phys. Lett., vol. 55, no. 4, pp. 337–339, Jul. 1989.

[47] Hu Tao, Willie J. Padilla, Xin Zhang, and Richard D. Averitt; " Recent Progress in Electromagnetic Metamaterial Devices for Terahertz Applications". IEEE JOURNAL OF SELECTED TOPICS IN QUANTUM ELECTRONICS, VOL. 17, NO. 1, JANUARY/FEBRUARY 2011.

[48] H. Tao, N. I. Landy, C. M. Bingham, X. Zhang, R. D. Averitt, and W. J. Padilla, "A metamaterial absorber for the terahertz regime: Design, fabrication and characterization," *Opt. Exp.*, vol. 16, pp. 7181–7188, May 2008.

[49] H. Tao, C. M. Bingham, A. C. Strikwerda, D. Pilon, D. Shrekenhamer, N. I. Landy, K. Fan, X. Zhang, W. J. Padilla, and R. D. Averitt, "Highly flexiblewide angle of incidence terahertz metamaterial absorber: Design, fabrication, and characterization," *Phys. Rev. B*, vol. 78, pp. 241103R-1–241103R-4, Dec. 2008.

[50] W. J. Padilla, A. J. Taylor, C. Highstrete, M. Lee, and R. D. Averitt, "Dynamical electric and magnetic metamaterial response at terahertz frequencies," *Phys. Rev. Lett.*, vol. 96, pp. 107401-1–107401-4, Mar. 2006.

[51] H. T. Chen,W. J. Padilla, J. M. O. Zide, A. C. Gossard, A. J. Taylor, and R. D. Averitt, "Active terahertz metamaterial devices," *Nature*, vol. 444, pp. 597–600, Nov. 2006.

[52] H. T. Chen, S. Palit, T. Tyler, C. M. Bingham, J. M. O. Zide, J. F. O'Hara, D. R. Smith, A. C. Gossard, R. D. Averitt, W. J. Padilla, N. M. Jokerst, and A. J. Taylor, "Hybrid metamaterials enable fast electrical modulation of freely propagating terahertz waves," *Appl. Phys. Lett.*, vol. 93, pp. 091117-1–091117-3, Sep. 2008.

[53] H. T. Chen,W. J. Padilla, M. J. Cich, A. K. Azad, R. D. Averitt, and A. J. Taylor, "A metamaterial solid-state terahertz phase modulator," *Nature Photon.*, vol. 3, pp. 148–151, Mar. 2009.

[54] A. K. Bhattacharyya and T. J. Chwalek, "Analysis of multilayered meander line polarizer," *Int. J. Microw. Millimeter-Wave Comput.-Aided Eng.*, vol. 7, pp. 442–454, Nov. 1997.

[55] T. K. Wu, "Meander-line polarizer for arbitrary rotation of linearpolarization," *IEEE Microw. Guided Wave Lett.*, vol. 4, no. 6, pp. 199–201, Jun. 1994.

[56] L. Young, L. A. Robinson, and C. A. Hacking, "Meander-line polarizer," *IEEE Trans. Antennas Propag.*, vol. AP21, no. 1, pp. 376–378, Jan. 1973.

[57] J. Y. Chin, J. N. Gollub, J. J. Mock, R. Liu, C. Harrison, D. R. Smith, and T. J. Cui, "An efficient broadband metamaterial wave retarder," *Opt. Exp.*, vol. 17, pp. 7640–7647, 2009.

[59] P. Weis, O. Paul, C. Imhof, R. Beigang, and M. Rahm, "Strongly birefringent metamaterials as negative index wave plates," *Appl. Phys. Lett.*, vol. 95, pp. 171104-1–171104-3, 2009.

[60] A. C. Strikwerda, K. Fan, H. Tao, D. V. Pilon, X. Zhang, and R. D. Averitt, "Comparison of birefringent electric split-ring resonator and meanderline structures as quarter-wave plates at terahertz frequencies," *Opt. Exp.*, vol. 17, pp. 136–149, Jan. 2009.

[61] M. Lapine, D. Powell, M. Gorkunov, I. Shadrivov, R. Marqu´es, and Y. Kivshar, "Structural tunability in metamaterials," *Appl. Phys. Lett.*, vol. 95, pp. 084105-1–084105-3, Aug. 2009.

[62] H. Tao, A. C. Strikwerda, K. Fan, W. J. Padilla, X. Zhang, and R. D.Averitt, "Reconfigurable terahertz metamaterials," *Phys. Rev. Lett.*, vol. 103, pp. 147401-1–147401-4, Oct. 2009.

[63] T. Driscoll, H. T. Kim, B. G. Chae, B. J. Kim, Y. W. Lee, N. Marie Jokerst, S. Palit, D. R. Smith, M. Di Ventra, and D. N. Basov, "Memory metamaterials," *Science*, vol. 325, pp. 1518–1521, Sep. 2009.

[64] B. G. Chae, H. T. Kim, D. H. Youn, and K. Y. Kang, "Abrupt metalinsulator transition observed in VO2 thin films induced by a switching voltage pulse," *Physica B, Conds.Matt.*, vol. 369, pp. 76–80, Dec. 2005.

[65] A. Zylbersztejn and N. F. Mott, "Metal-insulator transition in vanadium dioxide," *Phys. Rev. B*, vol. 11, pp. 4383–4395, 1975.

Chapter IV:

Proposed Microwave and terahertz structures

IV Proposed Microwave and terahertz structures

IV.1 Tunability mechanisms computational investigation

We first present a computational investigation of different tunability mechanisms, where a consistent theoretical study was carried out in order to define the most effective ones and understand their working principles. This study used several simulations with CST microwave studio, which were performed targeting two aims: the first was to get familiarized with the software, and inspecting its capabilities in order to adapt them to metamaterial based simulations. Whereas the second one was to achieve the concrete validation of the metamaterials responses through their simulation curves, consisting of the S-parameters and fields distributions.

IV.1.1 MEMS tuning system simulation

For the simulation of this type of tuning mechanism, a double SRR unit cell was considered, with a single gap in the inner and outer rings (Figure IV.1).

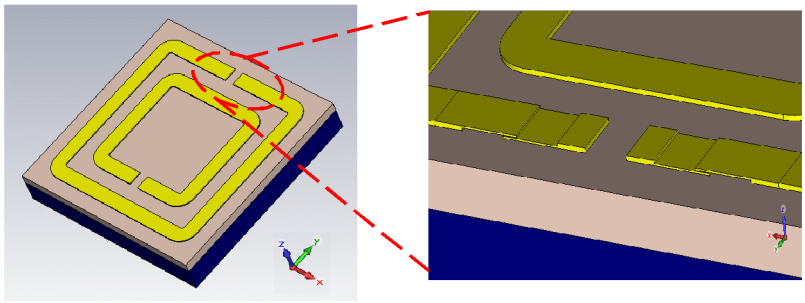

Figure IV.1: Double SRR unit cell used to simulate the MEMS tuning system, with a close up on the sliding system

The simulated tuning mechanism consists in the insertion of a MEMS element in the active area, to either change the split size or to create new splits. In order to simulate the MEMS element, a sliding system was inserted in the SRR gap regions, with variable values D and D1 (distances in μm), which were used to simulate the

gap size change and the sliding system movement respectively, as shown in Figure IV.2 (a) and (b),

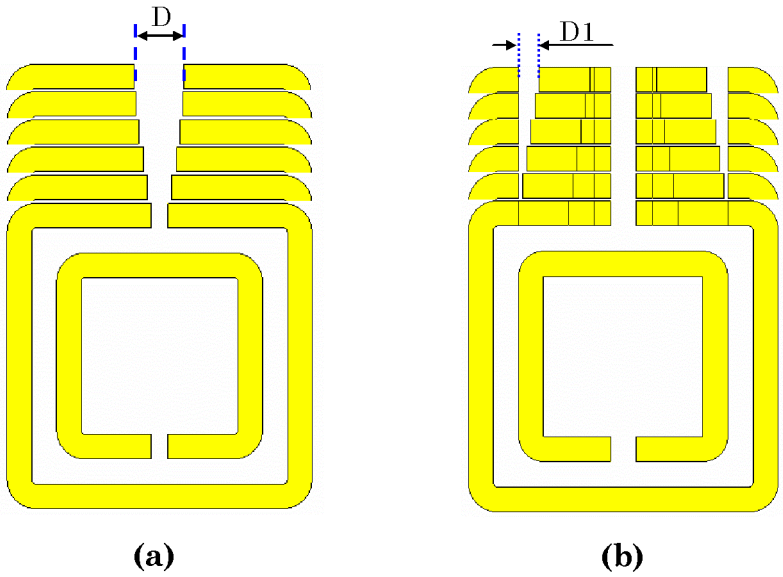

Figure IV.2: MEMS based configurations for a tunable SRR

The metamaterial structure was implemented on a silicon substrate with 200 nm Gold layer; the outer ring is 37 µm square size with 3 µm width, while the inner one is 25 µm square size.

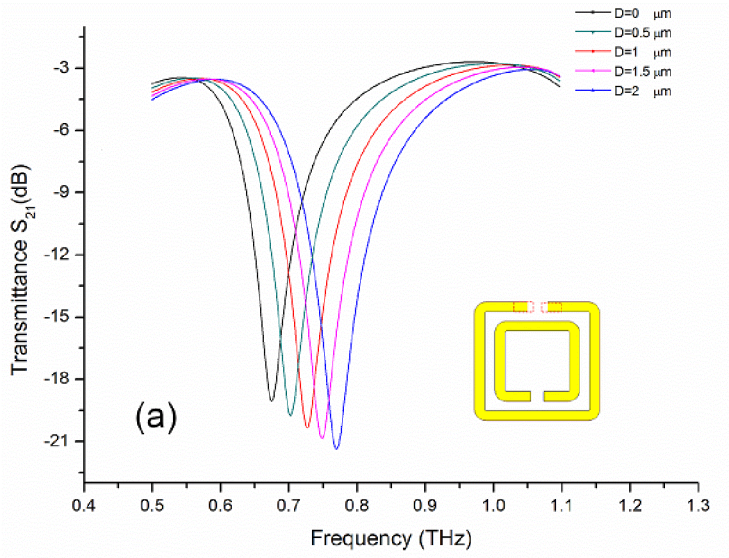

Figure IV.3: simulation result for MEMS mechanism based on the variation of the gap size

As for the simulation, the S-parameters for each system were calculated for the different values of D and D1 starting from the "0" configuration.

The Figure IV.3 shows the graph of the first simulated mechanism, where one can observe the metamaterial response (transmittance curve S_{21}) for different values of the variable D (the gap size increase), starting from 0 to 2 µm with a 0.5 µm step. The results show that as far as we increase the gap size we get a uniform frequency shift from 0.67 THz (initial gap) to 0.77 THz, obtaining therefore around 15 % frequency shift, with a 0.03 THz bandwidth (defined as the FWHM at -3dB), that is around 4% bandwidth.
The results for the second mechanism are shown in Figure IV.4. Again, the metamaterial response (transmittance curve S_{21}) was calculated for different values of the variable D1 (the gap size increase), starting from 0 to 2.5 µm with a 0.5 µm step.

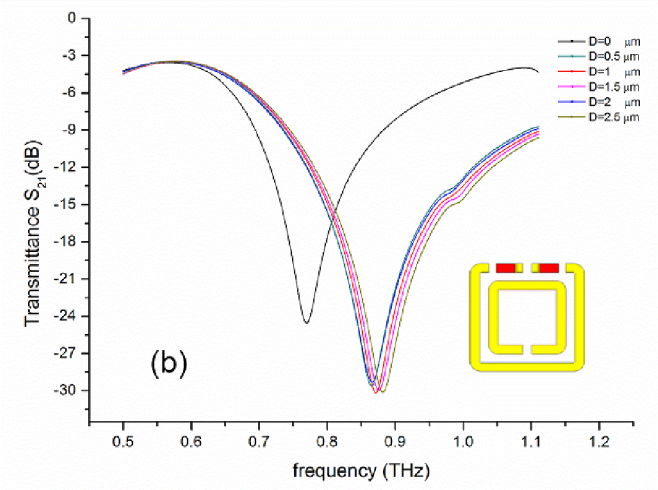

Figure IV.4: simulation result for MEMS mechanism based on the creation of new gaps and changing their size

From the graph, we can notice that the central frequency shifted from 0.76 THz (initial structure) to 0.86 THz (with the creation of two new gaps), which means around 13% frequency shift. We can also observe a small uniform shift for the other D1 values with a maximum of 0.88 THz (16%).

IV.1.2 Semiconductor tuning system simulation

The simulation for this tuning system was based on the use of Schottky diode principle, so that to change the substrate conductivity by creation of a depletion region in the active area of the unit cell. In this case the tuning mechanism is given by a dc or slowly varying bias electric field. For this mechanism we used a different geometry based on a kind of so-called "omega shape! structure (Figure IV.5).

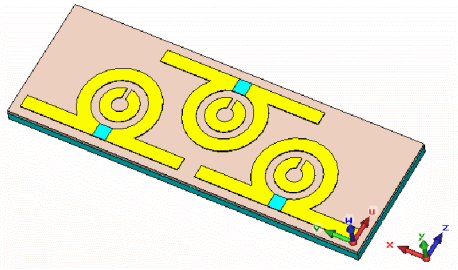

Figure IV.5: Double SRR Omega shape structure, to simulate the semiconductor tuning system, using Schottky diode principle

From the graph we observe a blue shift close to 7% relatively to the central resonant frequency.

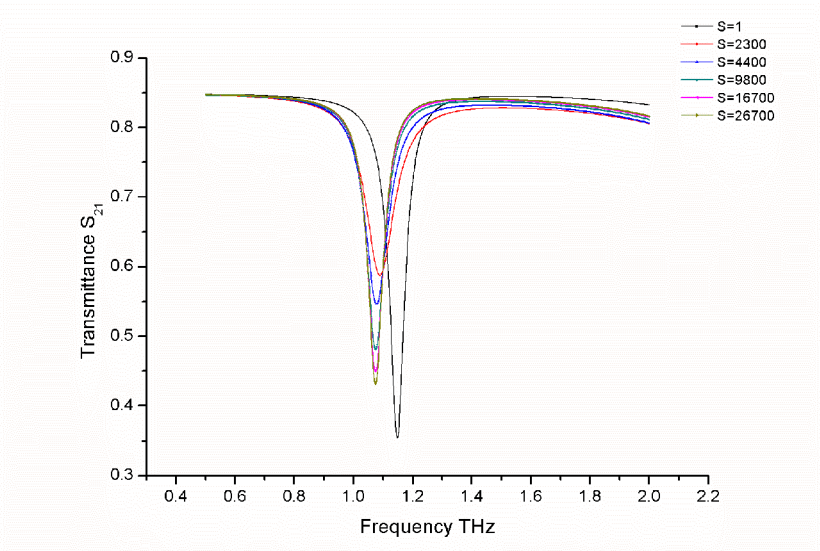

Figure IV.6: Simulation results for the tuning system based on the substrate conductivity change

IV.1.3 Liquid Crystal tuning system simulation

A third approach on the study of metamaterials tuning mechanisms was based on the use of liquid crystals. We recall that the control of the LC system is based on the reorientation of the LC molecular director, described by the angle θ, with respect to the oscillating electric field direction. LC molecules reorientation can be done using a static or slowly-varying electric field, applying a magneto static field or even using thermal control.

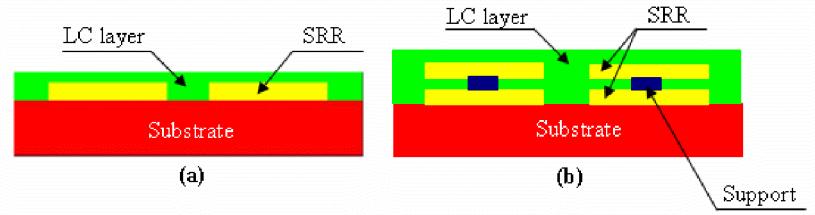

Figure VI.7: LC configurations: (a) the LC top covers the metallic structure; (b) the LC is in between two metallic structures

In this case, two configurations were identified. The first standard configuration implies the use of an appropriate amount of LC top layer covering the SRR (Figure IV.7 (a)) whereas the second one is based on the use of the LC in between two metallic structures (SRRs). In such a case, a first SRR, the LC layer and then a second SRR are combined to give a sandwich configuration, inducing a capacitor with a permittivity medium (i.e. capacitance value) controlled by the LC polarization, as shown in Figure IV.7 (b).

The whole mechanism was built around the control of the LC properties; therefore, a proper LC modeling was necessary. As we know, the LC is an anisotropic material, represented in the e.m. simulations as an anisotropic medium with different values of permittivity along the 3 different axes, with an ordinary optical index *no* = 1:51, an extraordinary optical index *ne* = 1:84, and thus a birefringence of 0.33. Therefore, in our simulations the LC layer permittivity is considered as [3.3856, 2.2801, 2.2801] and [2.2801, 3.3856, 2.2801] respectively for two orientations: θ = 0◦ and 90◦. We

also used a variable parameter "S" representing the difference between the ordinary and the extraordinary permittivity, so that the LC layer is treated as [ε_x −s, ε_x +s, ε_z]. Loss tangent values were set as tandδ_o = 0:020 for no and tandδ_e = 0.016 for ne. Two different SRRs geometries were used, namely: Circular SRR, Double Squared SRR.

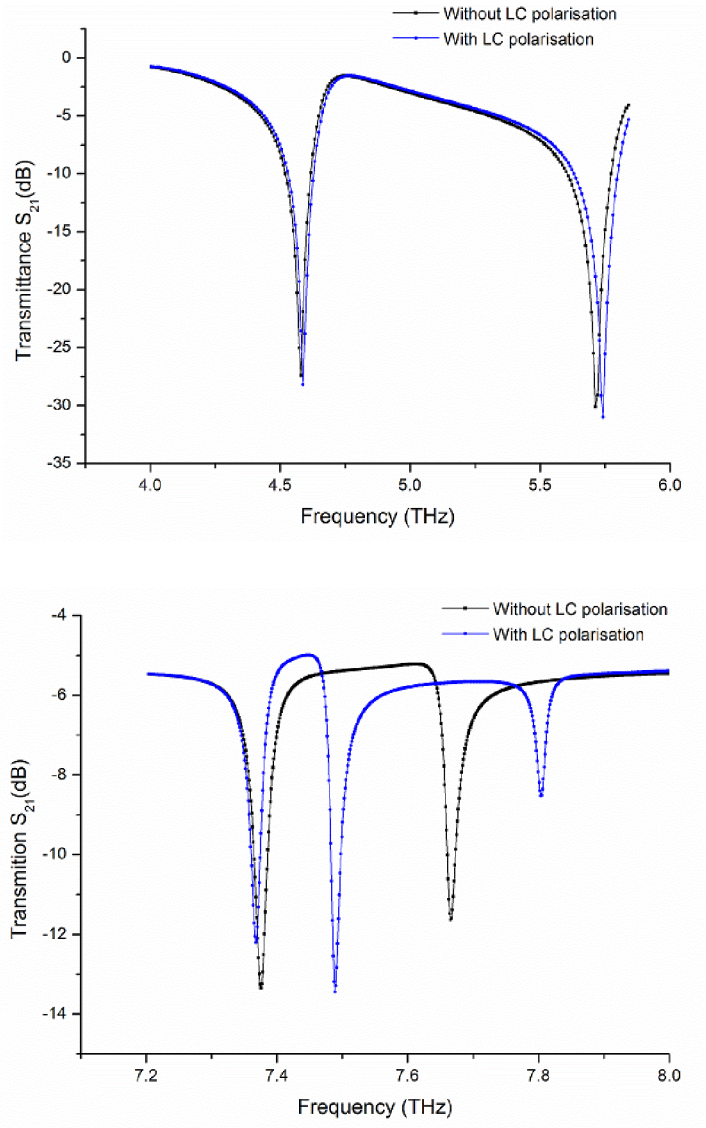

Figure IV.8: Simulation results for the double SRR with large internal gap and LC tuning system: a) top LC layer configuration, b) sandwich LC configuration

Several simulations were performed using CST, in order to see the device response in the required frequency region. Figure IV.8 shows the scattering parameter S_{21} vs frequency graph for the double SRR with internal large gap geometry. The resonance frequencies depend on the chosen geometry and are located within the range between 4 and 8 THz for the same SRR dimensions. A much larger shift is observed in the "sandwich" configuration compared to the "top layer" one with a significant difference in the modulation of the response (2.3% and 0.5 % respectively).

IV.1.4 Discussion

A number of mechanisms have been proposed and studied, all of them allowing a significant variation of the electromagnetic response of metamaterials operating in the THz region and based on resonant metallic substructures. Presently, the most promising ones seem those based on micro-electro-mechanical systems or on semiconducting substrates, both electrically controlled; however, they usually produce also a large change in the shape of the response curve. On the contrary, the mechanism based on the use of liquid crystals, even if producing a less effective frequency modulation of the metamaterials compared to the other mechanisms under study, it is however characterized by a "rigid" frequency shift of the electromagnetic signal, without modifying its overall profile, and it is also more "flexible" with the nature of the external control (that can be electric, magnetic, thermal). Therefore, an improved frequency modulation will make this type of system of large interest, and open the path to a large variety of applications.

IV.2 Microwave first experiment

In the following, we focus our attention to the tuning mechanisms based on liquid crystals. From the previous results, we observed that the sandwich configuration is the most efficient in terms of tunability. We started adapting the structure reported in [1] shown in Figure IV.9.

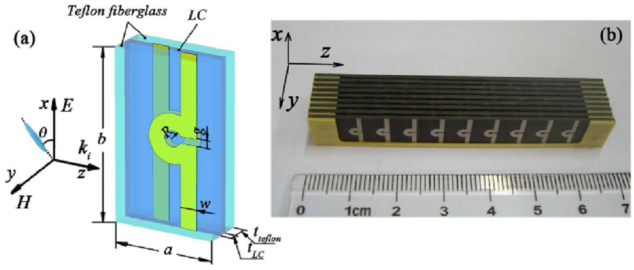

Figure IV.9: Structure reported in [1], a) Schematic of the basic unit cell of the tunable metamaterial. b) Close-up view of the structure.

IV.2.1 Simulation

The first step was to try and reproduce the structure response. For that we used CST to model the Ω-shape metamaterial structure, which consists of inter-layered Rogers slabs with a copper clad, where the Ω-shape structure were patterned on each side.

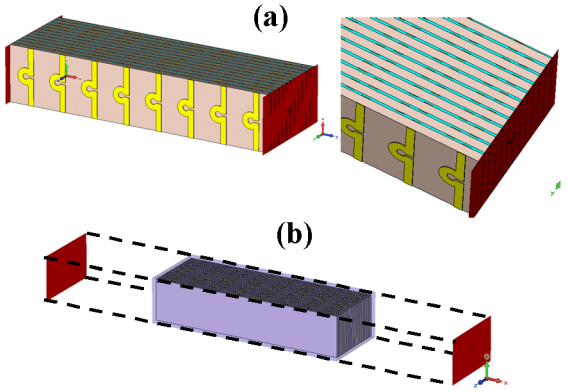

Figure IV.10: Omega shape structure used to simulation the LC tuning mechanism

The gaps between the slabs were filled with the LC (Figure IV.10 (a)). As we were planning to use a liquid, a Plexiglas container was

designed to prevent the LC from leaking and keep the inter slabs distance fixed. The whole structure was inserted inside an X-band waveguide for the microwave measurements. The simulation was performed with the appropriate boundary conditions, using the following parameters:

- ✓ Rogers substrate + D/sided 70µm clad. $\varepsilon \approx 3$
- ✓ 300 µm spacing.
- ✓ LC {2.0994, 1.9044,1.9044} ≈ 5CB

As for the LC, it was modeled as described in section IV.1.3. The simulation results show a clear resonance curve occurring at 9.74 GHz. (This matches the results reported in [1]).

IV.2.2 Fabrication

After the simulation, we proceeded towards the fabrication process. The first step was to realize the metamaterial patterning on the Rogers slabs, which was performed using a standard PCB service. The slabs had 8 Ω structures on each side (10 x 48 mm slab) Figure IV.11 (a).

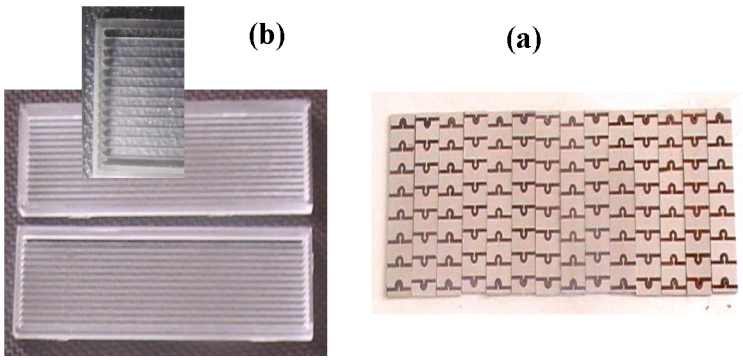

Figure IV.11: Ω structure fabrication, a) slabs patterning, b) LC box fabrication.

In the final structure, the dielectric slabs needed to be aligned, separated from each other by 300 µm spacing, and filled with liquid

crystal. At this aim, we fabricated a "LC box" shown in Figure IV.11 (b), made from Plexiglas, which was machined using a CAD controlled tool machine. As mentioned in section III.2.1.4, the LC needed to be aligned before the polarisation in order to have the maximum tuning effect. To test the alignment, we realised single unit cell with LC infiltrated on it and checked that the alignment was very accurate (Figure IV.12 (a)). The last fabrication part was devoted to the final assembly of the structure, in which the slabs were arranged inside the LC box (sealed using the epoxy glue), and filled with the LC from a small aperture left for that purpose. Figure IV.12 (b) shows the final structure.

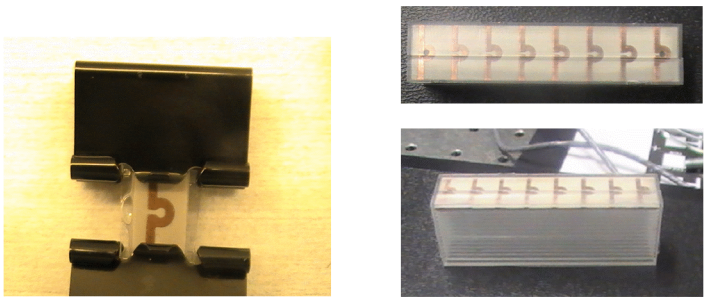

(a) **(b)**

Figure IV.12: LC structure, a) single unit cell, b) final structure.

IV.2.3 Microwave measurements

Measurements were performed immediately after the LC was infiltrated inside the structure, in order to avoid leakage and contamination. Figure IV.13 shows the measurements setup used for this experiment. The metamaterial structure was placed inside an X-band waveguide, that was inserted in a high magnetic field (superconductor based) remotely controlled system. The waveguide (with the structure inside) was connected to a vector network analyzer (VNA), linked to a PC for data acquisition.

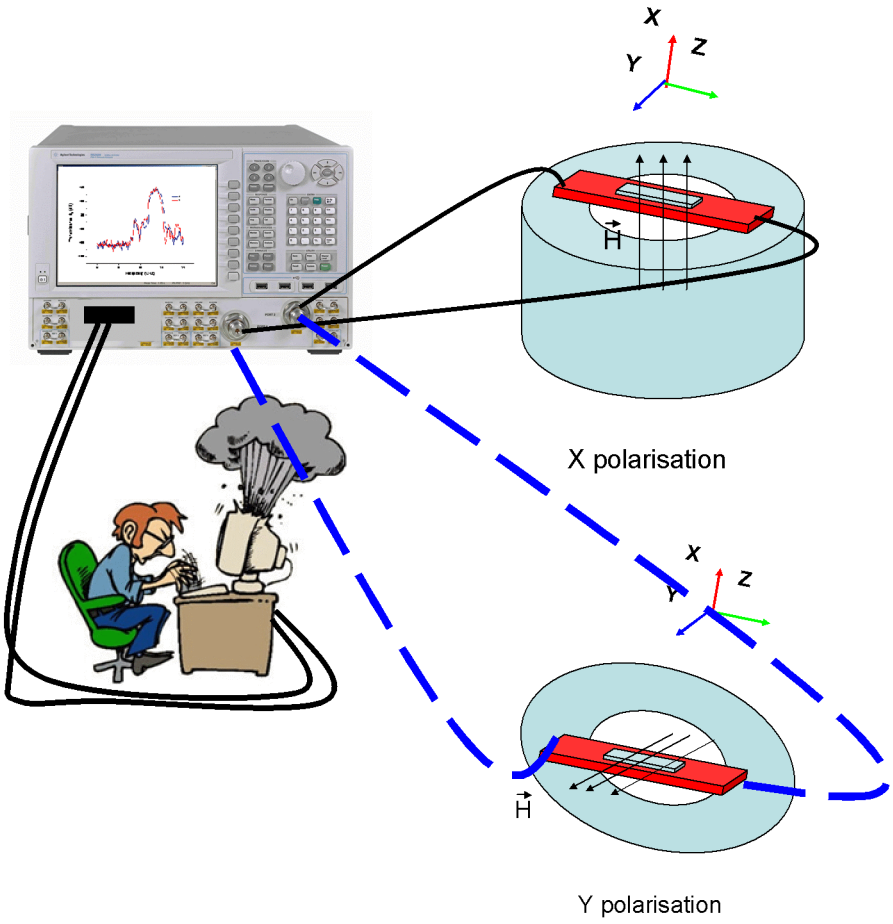

Figure IV.13: the proposed experimental setup

The measurements were carried out following these steps:

- ✓ Magnet switched on in the X direction, starting from 0 to 5 Tesla with a 0.5 Tesla step, in order to determine the required field intensity and get the metamaterial response with the LC molecules oriented trough the X direction.
- ✓ The VNA sends the e.m. signal to the waveguide (structure) and detect the output signal from it.
- ✓ The S-parameters were acquired and registered using a customized Labview program.
- ✓ The Magnet is set back to zero, and rotated 90° to the Y direction, without rotating the waveguide.

✓ The first 3 steps were reproduced, in order to get the metamaterial response with the LC molecules reoriented trough the Y direction.

The results in Figure IV.14 show that we do observe a resonance as expected, however with a small frequency shift, close to 1.3 %.

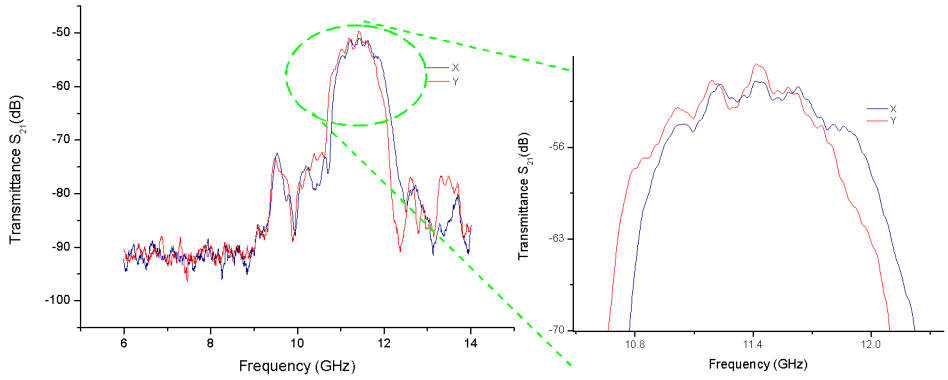

Figure IV.14: The measured tunable metamaterial response, based on the LC tuning system

IV.2.4 Discussion

Results show therefore the presence of a resonance, similar to the one reported in the simulation section, but with a different central frequency, a bandwidth larger and a frequency modulation smaller than expected. We believe that the observed discrepancy is mainly due to the slabs fabrication and the assembly process. First, the Ω-shape structures on each slab were designed to have a gap of 0.4mm, however that was difficult to realize in a controlled way using a simple PCB process, that is unable to control the chemical etching on that scale. Also, the LC box separator could not guarantee a uniform spacing between the slabs. Then, the small modulation in the metamaterial response was likely caused by leaking and contamination of the LC. In fact, the LC box was composed of two parts bonded with epoxy glue. Since sealing was not perfect, this produced the LC leaking. Also, the contact of the epoxy glue with the LC contaminated the latter one, rendering its polarization less effective.

IV.3 Modified Ω-shape structure

From the results of the first experiment based on the Ω structure, several problems were identified. We then started a new design in order to cope with these problems and build a better structure with higher performances.

IV.3.1 Design and simulation

From the previous experience, it appears that the tuning mechanism is more effective if we can maximize the internal capacitance inside the metamaterial itself and then change it using the LC.

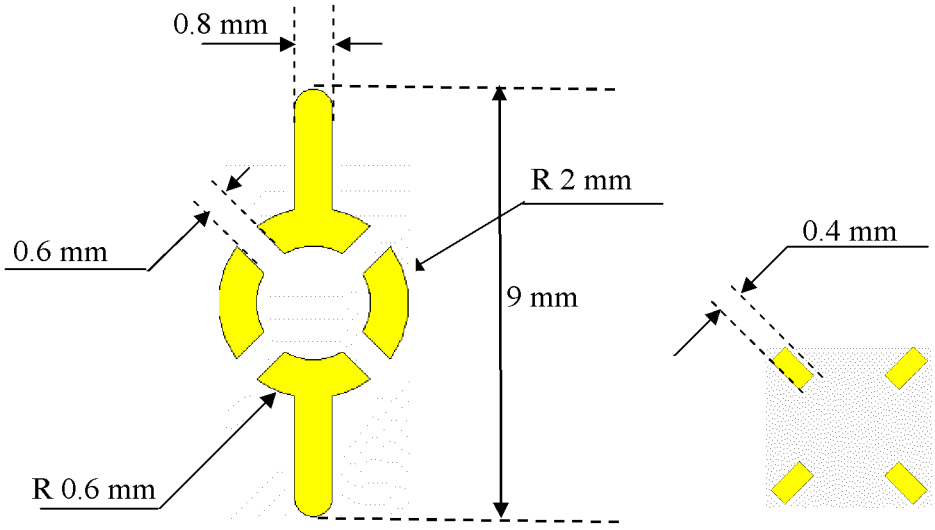

Figure IV.15: the new modified Ω-shape structure, with the optimized dimensions

Therefore, we designed modified Ω-shape geometry in order to increase the gap regions inside the metamaterial. The new structure is shown in Figure IV.15, and the whole metamaterial and unit cell assembly on Figure IV.19. Simulations were performed with the appropriate boundary conditions, using the following parameters:

- ✓ FR-4 + D/sided 70µm clad.
- ✓ 20 µm spacing.

✓ LC {3.6, 2.97, 2.97} ≈ ITC

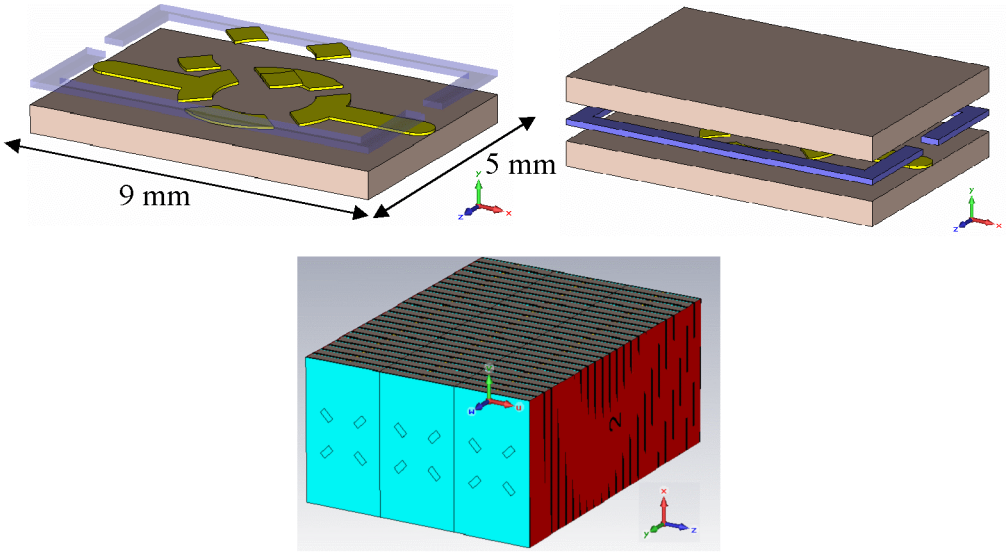

Figure IV.16: the modified Ω-shape unit cell structure

As for the LC, it was modeled as described in section IV.1.3.

In order to define the optimized structure we realized a series of simulations in order to define the optimal spacing between the slabs.

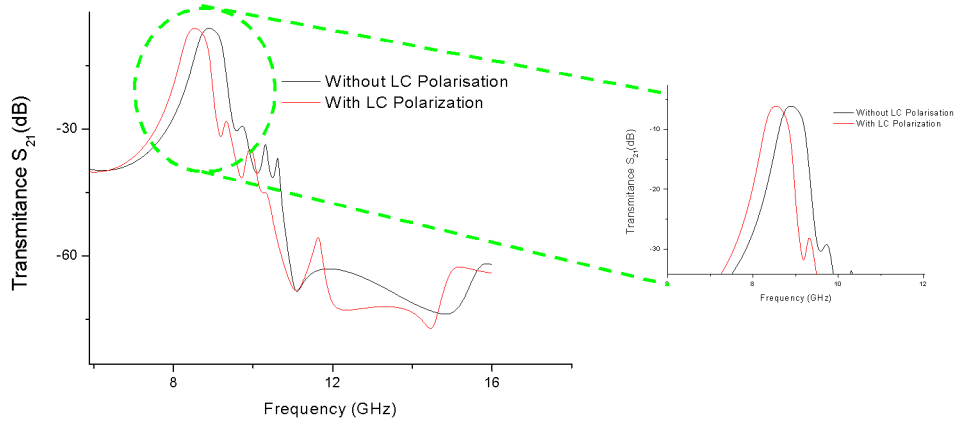

Figure IV.17: the simulation results of the modified Ω-shape structure.

From the simulation results we can see a clear resonance at f1=9.34 GHz and a rigid shift to f2=8.62 GHz, with Δf=0.72 GHz and 8% shift whereas the bandwidth (defined at -3dB) is around 5%. The curve in Figure IV.17 shows the metamaterial response and its frequency modulation using the LC system.

The graph in Figure IV.18 shows in detail the frequency shift dependence on the LC layer thickness. From the data, the smaller is the spacing the larger is the shift, as expected. 20 µm spacing between the metals corresponds to 160 µm slab-to-slab interdistance, taking into account the metal thickness.

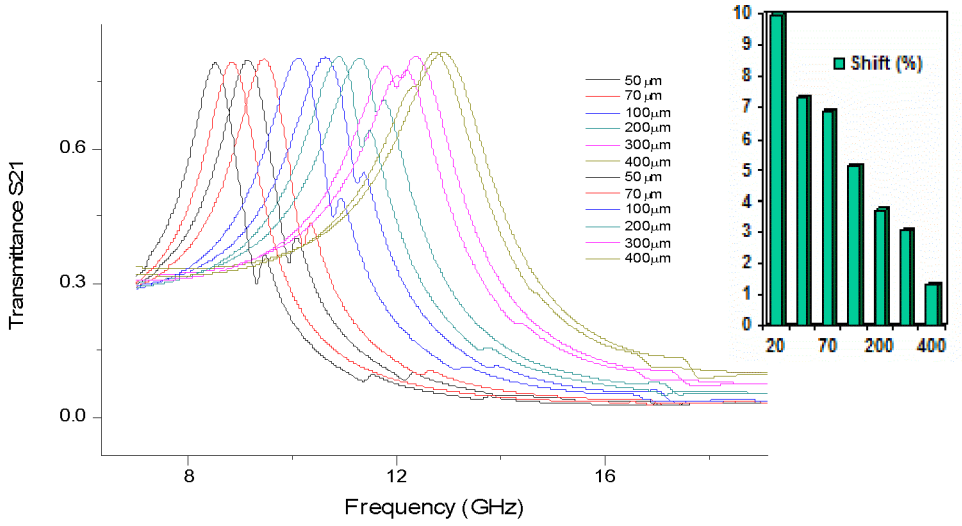

FigureIV.18: the influence of the spacing between the Ω-shape and the metal strips on the frequency modulation.

After the promising simulation results, and before proceeding with the fabrication process, we wanted to check that the designed structure was exhibiting a real left handed behavior. For that we decided to retrieve the metamaterial parameters, by using the technique described by Smith in 2002, which consists on the use of the scattering parameters to calculate the electromagnetic properties of the designer structure.

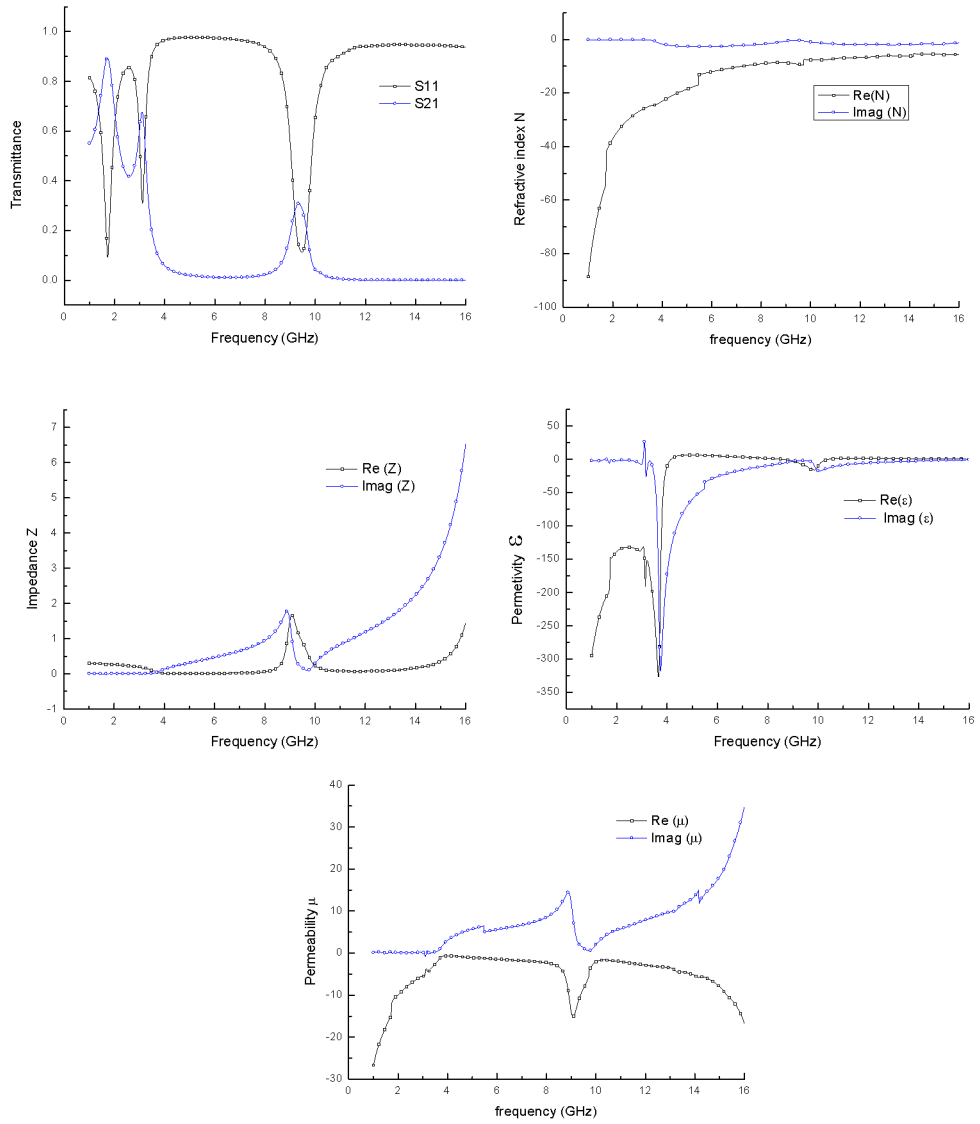

Figure IV.19: Retrieval parameters plots, a) metamaterial transmittance S_{21} and S_{11}, b) refractive index real and imaginary parts, c) impedance Z, medium permittivity and f) medium permeability

For that, a small Matlab source code was used to calculate and plot the Refractive index N, impedance Z, permittivity ε, and the permeability μ. As shown in Figure IV.19.

The whole electromagnetic parameters are gathered in Figure IV.20 (a), with a close up on the frequency region where there is a resonance on Figure IV.20 (b). The graph shows an actual left

handed behavior in that frequency window, with negative values of permittivity, permeability and refractive index at the same time.

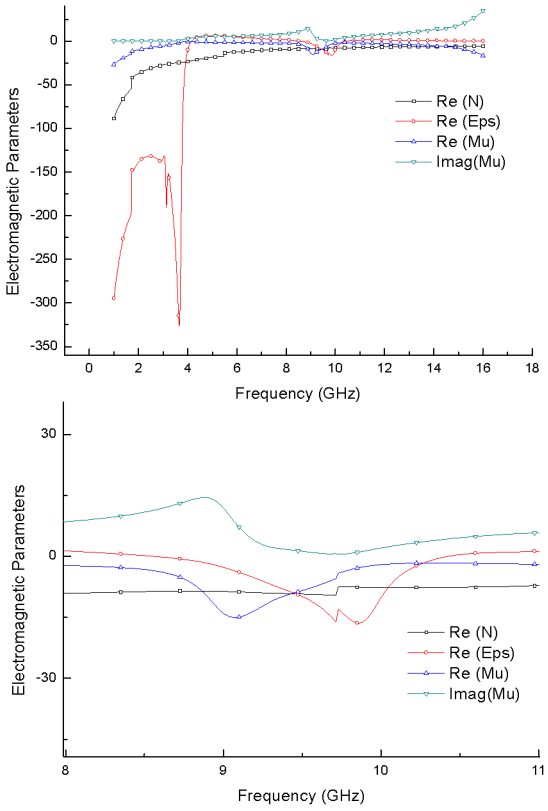

Figure IV. 20: retrieved electromagnetic parameters, that show the left handed behavior

IV.3.2 Fabrication

The whole metamaterial consists of an assembly of 23 slabs, each having an area of 9x15 mm^2 and a thickness of around 0.8 mm, and aligned with 160 µm spacing. The structure was fabricated using double sided PCB slab, with 2 **oz/ft² copper** coated on a FR4 slab. For each slab, the modified omega shapes with four splits have been patterned on one side and the four strips which fit the omega gaps on the other side. The designed metamaterial has three critical parameters, the first one is the dimension of the split gaps, the second one is related to the alignment of the strips facing the splits, and the third one is the spacing between the strips and the splits.

Therefore, the metamaterial fabrication was divided in three main steps:

Slabs fabrication: in this step, the designed structure was patterned on the PCB slabs using mechanical and chemical etching. The dimensions of the metamaterial are quite small and need high precision, for that, a vacuum holder was realised in order to keep the PCB slabs during both the mechanical etching and the cutting process, which were performed using a tool machine controlled using a CAD program with a 100 μm as lateral precision and 10 μm for the vertical one. It would have been better if we were able to pattern the metamaterial using only the mechanical etching, but that would have caused lose of the vertical reference, which is very important to keep the correct inter-slab spacing. For that, this type of etching was used only to pattern the critical areas with high precision and cut the slabs (each one containing three unit cells, as shown in figure IV.16). As for the copper left on the surface, it was removed using standard PCB process, with a double layer of photo-resist applied on the top of the modified omega shape in one side and the strips on the other one, in order to protect the copper parts that define the metamaterial geometry.

Structure assembly: this step is the most critical in the whole fabrication process, because of the pair strip/split alignment, the slab spacing, and the liquid crystal contamination, that was the main problem we faced during the metamaterial fabrication process. Therefore, all the slabs were first mechanically polished in order to remove all the residuals caused by the etching and cutting process, after that treated with standard acetone and methanol for a final cleaning procedure before entering them in the clean room. From this stage all the assembly process was performed in a clean room environment specifically designed for the liquid crystal research activity at the CNR - Lycril Lab (University of Calabria in Cosenza). In the clean room slabs were rinsed again with acetone and distillate water and then thermally treated under vacuum in order to

evaporate all the chemicals used in the cleaning process. After that, removable supports were fabricated and used to hold the slabs during the alignment process on the lateral and vertical directions.

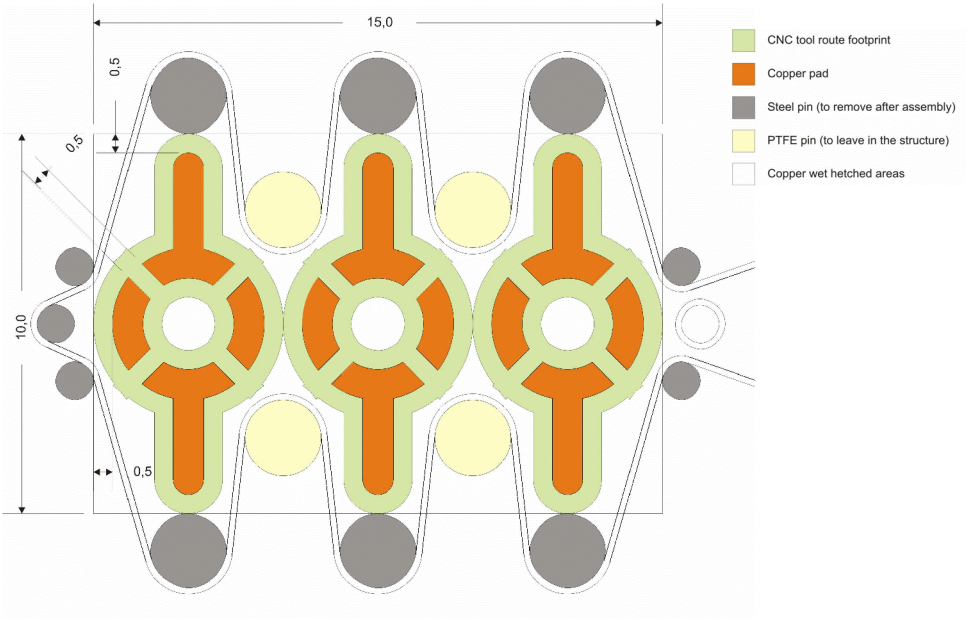

Figure IV.21: Slabs and assembly process of the metamaterial structure

The spacing between the slabs was realized using plastic wires having the required thickness of 160 μm (Figure IV.21). The final result was a "sandwich" consisting of the metamaterial slabs interlayered with plastic wires. The whole structure was then mechanically pressed to keep the required inter-slab spacing and bonded using epoxy glue. A second epoxy glue layer was finally applied to ensure a proper sealing in order to avoid the LC leaking.

Liquid crystal filling: this action consists in infiltrating the LC inside the structure, in order to realise the LC layers in between the metamaterial slabs. There were two problems that rose at this stage, the LC contamination and the thickness of the inter-slab spacing. In the previous structure, the contact between the LC and the glue might have caused the LC contamination. Therefore, a small thin cap made from FR4 slabs with two holes on it was attached to the

structure and sealed using the epoxy glue. As for the LC filling, we used a vacuum chamber with a support for our structure equipped with a small syringe with LC inside. In this way, all the air was evacuated from the structure and the LC was infiltrated from the top with the help of gravity and Capillary forces. To make sure that the structure was completely filled, a small recipient filled with LC was realized on the top of the structure, kept under vacuum for 24 hours. The final structure is shown in Figure IV.22.

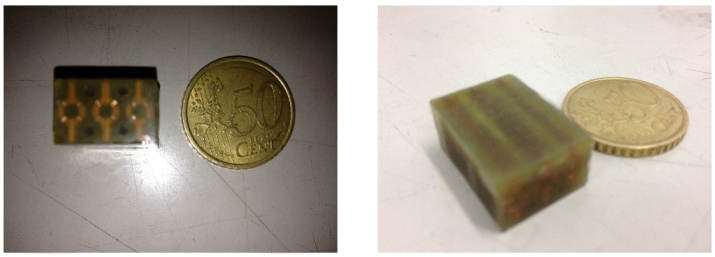

Figure IV.22: the modified Ω-shape metamaterial structure used for LC tenability system.

IV.3.3 Microwave measurements

The experimental setup used to perform these measurements is identical to the one used in the first experiment (Figure IV.13).

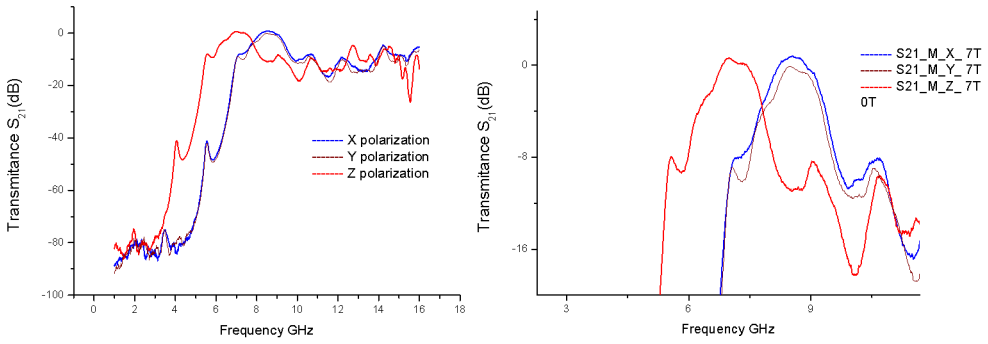

Figure IV.23: Measured metamaterial response with the LC tuning mechanism

The metamaterial structure was inserted inside an X-band waveguide, which was placed in the superconductor based magnetic system. The waveguide was again connected to a VNA linked to a PC for data acquisition. Measurements followed the same steps already described in section IV.2.3.

The measurement results are plotted in the graph of Figure IV.23, from which we can observe a clear shift of around 7%, with central frequency of 8.53 GHz.

IV.4 Terahertz metamaterial

In this last part, we will present the result of computational studies and fabrication steps on planar hybrid tunable THz split ring resonators metamaterials that can achieve a high frequency shift using liquid crystal (LC) as tuning mechanism.

IV.4.1 Design and Simulation

At first stage, our attention was devoted to design a similar tuning system based on a THz planar structure operating at around 1 THz and composed of arrays of SRR unit cells covered with liquid crystal Figure IV.24. Each unit cell consists of a normal square ring with bended edges of 40 μm lateral sides, 5μm width, 0.2 μm thickness and a 7 μm gap in each side, connected to the adjacent ones using conducting strips aimed at ensuring the voltage bias necessary for the LC polarization. Our idea was based on the creation of different capacitors over the ring gaps (as they cover the most sensitive area) and use of the LC to change the overall permittivity.

Therefore, a suspended metallic cap was made in order to have cantilevers which overlap each side of the ring gaps, after the infiltration of the LC.

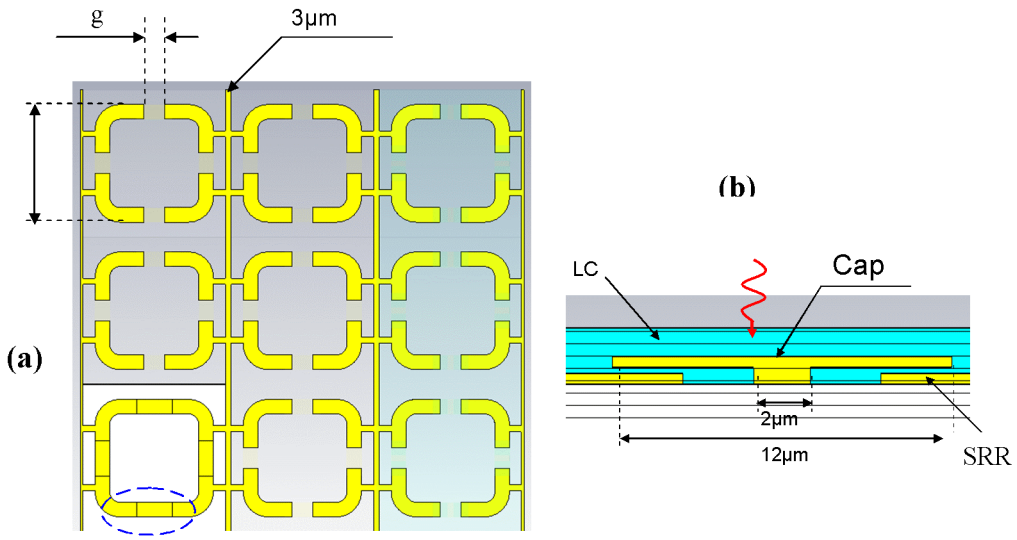

Figure IV.24: Hybrid metamaterial-liquid crystal based structure. a) metamaterial array based on SRR unit cells with l = 40 µm, w = 5 µm, and g = 7 µm, with 3 µm connection wire; b) plan cut of the unit cell where the gap is present, showing the LC interaction with the SRR.

Each gap side will form a capacitor with cantilever on the top using LC as dielectric medium. In order to use the electric field to polarize the LC, we designed metallic connections between the different part of the SRRs, and in this configuration an ITO glass was put on the top of the structure to cover the LC and connect the caps to each other. Several simulations were performed using CST, where the LC under evaluation is represented as an anisotropic materials with an ordinary optical index n_o = 1.62, an extraordinary optical index n_e = 1.83, and thus a birefringence of 0.21. Therefore, in our simulations the LC layer permittivity is considered as [3.3489, 2.6244, 2.6244] and [2.6244, 3.3489, 2.6244] respectively for two orientations: $\theta = 0°$ and 90°. The results show that the metamaterials response shifts from f_1 = 1.04 THz to f_2 = 0.96 THz with Δf = 0.08 THz. This translates in a high frequency shift up to 8% around the central frequency, compared to less than 4 % bandwidth as shown in Figure IV.25.

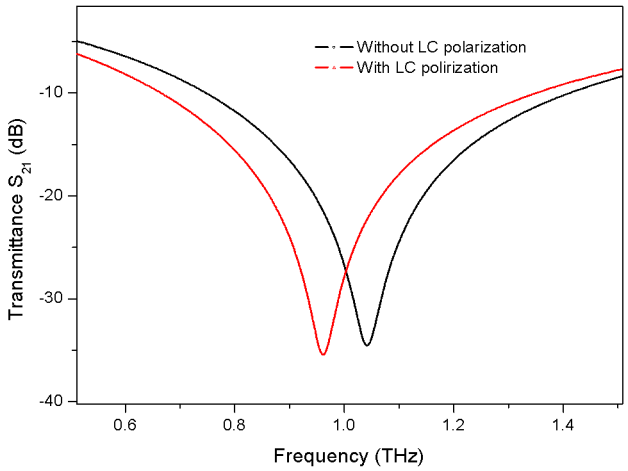

Figure IV.25: Simulation results of the hybrid metamaterial-liquid crystal based structure. The transmittance S_{21} response to the THz radiation when the LC is oriented on the $\theta = 0°$ direction is shown in the black curve. The red curve shows instead the metamaterial response when the LC is reoriented to $\theta = 90°$. A red shift of around 8% is observed in this configuration

IV.4.2 Fabrication: first results

The fabrication of the designed metamaterial operating at THz frequencies was realised exploiting a standard well-developed lithography planar technology. Figure IV.24 shows a small area of the designed structure consisting of arrays of SRR unit cells with metallic connections. The fabricated structure was implemented on a area of 3 x 3 mm^2 on 1 cm^2 Si substrate. Basically the process was divided in three steps, in each one a standard fabrication process was applied, namely: mask fabrication, spinning, patterning, deposition, and etching.

First layer fabrication

This layer basically consists of the arrays of SRRs spread on a Si substrate with metallic connection designed for the LC polarizations shown in Figure IV.24 (a). To fabricate this layer, first we made the mask to be used to pattern the designed first layer structure. It was a Cr mask on glass fabricated using a laser writing machine as light exposure tool, followed by a standard development and etching

process. We then started a series of lithography process calibration using different photo resists, in order to get the right lithography parameters which are:

- ✓ Photo resist: S1813.
- ✓ Spinning: 4000 rpm for 30 sec.
- ✓ Soft bake: 88 C° for 5mn using oven.
- ✓ Exposure: 15 sec using the mask aligner.
- ✓ Development: 10 sec150 ml (1:1).
- ✓ Hard bake: 118 C° 50 sec on hotplate
- ✓ Etching at 50C° for 45sec.

This was the optimal recipe for the etching process made after the deposition of a thin aluminum layer on the Si substrate.
Lift-off process for the first layer was developed using the photo resist S1805, following the same previous steps with different parameters. After the lift-off a thickness measurement of the Al layer was performed using a Profilometer. The Figure IV.26 shows the fabricated structure.

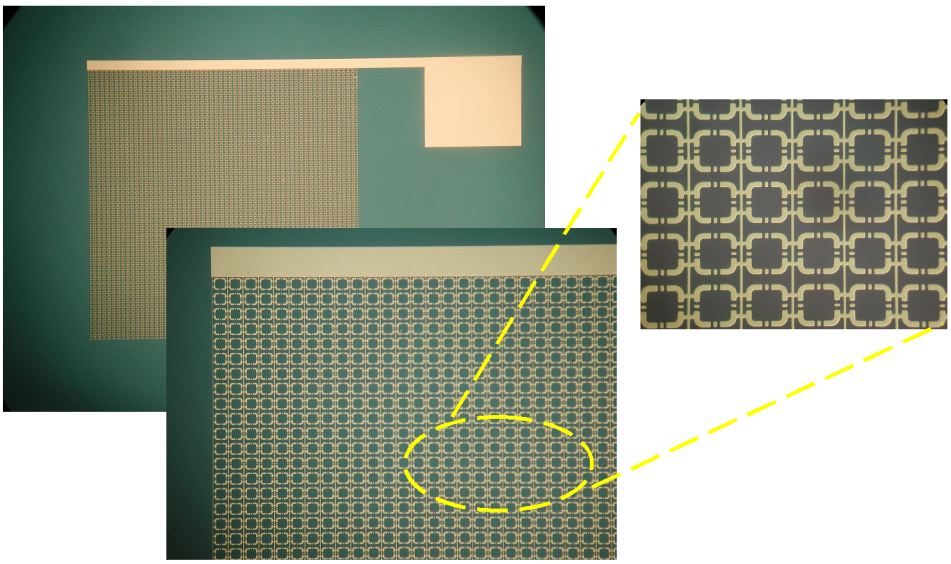

Figure IV.26: Microscope image of the first layer

Bibliography

[1] F. Zhang, L. Kang, Q. Zhao, J.Zhou,3 X.Zhao and D. Lippens, "Magnetically tunable left handed metamaterials by liquid crystal orientation", Opt Exp, Vol. 17, No. 6, 4360, 2009.

Conclusions

Conclusions

The main aim of this work was to design, fabricate and characterize metamaterials (mainly based on SRRs) that can be used to build and develop novel devices operating in various frequency regions to mold, filter, modulate and switch the electromagnetic signal. In order to accomplish this task, an intensive study related to the metamaterials design and fabrication was carried out: different structures have been investigated in different frequency ranges using CST microwave studio; allowing a better understanding of the metamaterials functioning principle and modeling constraints. As we were targeting practical applications of our designer, a particular interest was devoted to the mechanisms of tunability in metamaterials.

As a result of this study, we came out with a new tunable metamaterial structure, based on a modified "Ω-shape" structure; designed to operate in the microwave area. The simulated structure shows resonant device characteristics at around 9.5 GHz with 4% bandwidth. To make this metamaterial more flexible in terms of frequency modulation, we introduced a tuning mechanism, based on the use of liquid crystals to dynamically control the metamaterials response. The liquid crystal properties could be controlled reorienting the LC molecular director, described by the angle θ, in respect to the oscillating electric field direction using an external magnetic field. The measurements showed a resonance response in agreement with simulations, with a clear observed shift of around 7%, with central frequency of 8.53 GHz, confirming the efficiency of the designed tuning mechanism. The successful results obtained on the fabricated hybrid structure operating in the microwave region encouraged us to try and reproduce a similar structure for use in the terahertz domain. Therefore, design and simulation of a new structure operating at around 1.04 THz was performed. The

simulation results show that the metamaterials response shifts from $f_1 = 1.04$ THz to $f_2 = 0.96$ THz with $\Delta f = 0.08$ THz. This translates in a large frequency shift up to 8% around the central frequency, compared to less than 4 % bandwidth. Future actions will consist in the accomplishment of the fabrication steps for the terahertz region, with a full characterization of the final device using a terahertz time domain spectroscopic technique.